New statistical methods in risk assessment by probability bounds

Victoria Montgomery

A thesis presented for the degree of

Doctor of Philosophy

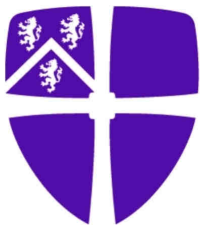

Department of Mathematical Sciences

Durham University

UK

February 2009

Dedication

To Willem for his love and support

New statistical methods in risk assessment by probability bounds

Victoria Montgomery

Abstract

In recent years, we have seen a diverse range of crises and controversies concerning food safety, animal health and environmental risks including foot and mouth disease, dioxins in seafood, GM crops and more recently the safety of Irish pork. This has led to the recognition that the handling of uncertainty in risk assessments needs to be more rigorous and transparent. This would mean that decision makers and the public could be better informed on the limitations of scientific advice. The expression of the uncertainty may be qualitative or quantitative but it must be well documented. Various approaches to quantifying uncertainty exist, but none are yet generally accepted amongst mathematicians, statisticians, natural scientists and regulatory authorities.

In this thesis we discuss the current risk assessment guidelines which describe the deterministic methods that are mainly used for risk assessments. However, probabilistic methods have many advantages, and we review some probabilistic methods that have been proposed for risk assessment. We then develop our own methods to overcome some problems with the current methods. We consider including various uncertainties and looking at robustness to the prior distribution for Bayesian methods. We compare nonparametric methods with parametric methods and we combine a nonparametric method with a Bayesian method to investigate the effect of using different assumptions for different random quantities in a model. These new methods provide alternatives for risk analysts to use in the future.

Declaration

I declare that the research presented in this thesis is, to the best of my knowledge, original. Where other work is quoted, due reference has been made.

Acknowledgements

Firstly I would like to thank Professor Frank Coolen for being an excellent supervisor. His enthusiasm, untiring support and calm advice throughout this project made this research much more productive and enjoyable. I would also like to acknowledge the help I received from Dr. Peter Craig and Professor Michael Goldstein. I am grateful for their interest in my research.

My thanks also go to the members of the risk analysis team at CSL, York. In particular Dr. Andy Hart, who gave unfailing support and advice throughout the project.

Thank you to the members of Durham Probability and Statistics Department for being there and helping when asked.

However the greatest thanks is reserved for my family and partner: Willem for his enduring love and support throughout the highs and lows of my research, my gran for her love, support and never-ending chocolate supply, my sister for listening to me stressing for hours on end, my dad for providing endless cups of tea and my mum for her constant editing and unwavering belief in me.

Contents

Chapter 1

Introduction

This chapter offers an explanation of the motivation for this thesis and introduces the particular areas of risk assessment that are discussed later in the thesis. It also provides an outline of the focus of subsequent chapters and introduces the collaborators for the project.

1.1 Motivation

Recent years have seen a diverse range of crises and controversies concerning food safety, animal health and environmental risks, e.g. the safety of Irish pork, dioxins in seafood, foot and mouth disease and GM crops. These crises have led to increased recognition of the need for improvement in risk assessment, risk management and risk communication. It is important to improve the handling of uncertainty in risk assessment, so that decision makers and the public are better informed on the limitations of scientific advice. Codex, which is the international forum for food safety issues, annually adopts new working principles for risk analysis. These include, "*Constraints, uncertainties and assumptions having an impact on the risk assessment should be explicitly considered at each step in the risk assessment and documented in a transparent manner. Expression of uncertainty or variability in risk estimates may be qualitative or quantitative, but should be quantified to the extent that is scientifically achievable.*" (Codex, 2007). Various approaches to quantifying uncertainty exist, but none of them are yet generally accepted amongst mathemati-

cians, statisticians, natural scientists and regulatory authorities.

In this thesis we introduce new methods for two specific areas of risk assessment. One is ecotoxicological risk assessment (e.g. protection of ecosystems from pesticides) and the other is food safety risk assessment (e.g. protection of humans from food additives and contaminants). We discuss current guidelines for risk assessment for ecosystems and for human dietary exposure. Both are based on deterministic approaches in which a conservative exposure estimate is compared with a threshold value. Deterministic methods are methods where point values are used to represent random quantities, rather than probabilistic methods which assume a distribution for each random quantity. The difficulty with probabilistic methods is that decision makers may not fully understand the results and the effect of assumptions made in the methods may not be clear. Probabilistic methods present results as a distribution or as bounds on distributions. They may produce results where the majority of the distribution or the bounds on the distribution fall below a safe threshold. This can make it difficult to determine if the chemical is safe enough to be licensed. There are also many uncertainties in risk assessments that are ignored because it is not easy to include them in an analysis, for example, because appropriate methodology has not yet been developed or because there is not enough information available to choose distributions.

There are many agencies working in the area of pesticides and food safety risk assessment. These include regulatory bodies and research agencies who consider which methods should be used and how reliable current methods are. As we are in the UK, we focus on the EU legislation and on the guidance provided by the UK Chemicals Regulation Directorate (CRD). On behalf of the UK government, the CRD of the Health and Safety Executive (HSE) implements European and National schemes to assess the risks associated with biocides, pesticides and plant protection products. These schemes are used to ensure that potential risks to people and the environment from these substances are properly controlled. The CRD are the UK Competent Authority (CA) regulating chemicals, pesticides, biocides and detergents and are authorised to act on behalf of ministers. As the CA for the UK, they are authorised to carry out work under programmes such as the Biocidal

Products Directive (BPD)[1], the REACH (Registration, Evaluation, Authorisation and Restriction of Chemicals) regulation and Plant Protection Products directives and regulations. They also have ongoing regulatory responsibilities under the UK Control of Pesticides Regulations (CoPR). Each European Union Member State has the responsibility of establishing their own CA and is responsible for implementing the Directives into their national legislation. In UK law this is through the Biocidal Products Regulations 2001 (BPR)[2] and the Biocidal Products Regulations (Northern Ireland) 2001[3] and corresponding legislation for pesticides. The CRD is responsible for representing the UK and making recommendations at the Commission of the European Communities (CEC's) and Standing Committee on Biocides (SCB) and the Standing Committee on Plant Health (SCPH) as well as examining the recommendations proposed by other EU Member States. The CRD works closely with the Department of the Environment, Food and Rural Affairs (Defra). Defra is responsible for strategic policy for pesticides, chemicals and detergents. Further information can be found on the CRD website (www.pesticides.gov.uk) or the biocides area of the HSE website (http://www.hse.gov.uk/biocides/about.htm).

There are also advisory groups such as the European Food Safety Agency (EFSA). They work in collaboration with national authorities and stakeholders to provide objective and independent scientific advice and clear communication on various risks based on the most up-to-date scientific information and knowledge available. EFSA was set up in January 2002, following a series of food crises in the late 1990s, to provide an independent source of scientific advice and communication for risks in several areas including food safety, animal health and welfare and plant protection. Their aim is to improve EU food safety, to ensure that consumers are protected and to try to restore and then maintain confidence in the EU food supply. EFSA is responsible for producing scientific opinions and advice to direct EU policies and legislation and to support the European Commission, European Parliament and EU member states in taking effective risk management decisions.

[1] http://eurlex.europa.eu/LexUriServ/LexUriServ.do?uri=CELEX:31998L0008:EN:NOT
[2] http://www.opsi.gov.uk/si/si2001/20010880.htm
[3] http://www.opsi.gov.uk/sr/sr2001/20010422.htm

Currently the deterministic methods used in risk assessment use safety or uncertainty factors to include uncertainty in the risk assessment. Frequently these factors are used for various uncertain extrapolation steps and it is often difficult to assess which factor is used for which extrapolation. For example, when using rat data to predict toxicity for humans, the current method would divide the toxicity value by an overall factor of 1000 which should account for several extrapolation steps, e.g. species-to-species extrapolation, within species extrapolation and short-term exposure to long-term exposure. Often the overall extrapolation factor is interpreted as the product of these three extrapolation steps, hence the assumption that a factor of 10 is used for each of them. However, this assumption cannot be justified based on the literature. Other factors may be applied if there are other uncertainties, for example, lab-to-field extrapolation. Unfortunately it is not clear whether these factors of 10 are too conservative or not conservative enough. A discussion of the deterministic method is given by Renwick (2002). The factors are not transparent in the sense that it is not clear which uncertainties they represent and the uncertainties included vary between assessments. Probabilistic methods that take variability and uncertainty (explained in Section 2.6.1) into account will provide more information on the distribution of risk. Therefore they can be a better representation of the risk distribution than the point estimate from a deterministic risk assessment.

The aim of this research is to provide new methods which quantify uncertainty to provide decision makers with a more transparent and realistic description of the risks to individuals or populations. To do this, we consider a new method that can include various uncertainties, Bayesian probability boxes (p-boxes), and a method that does not require strong distributional assumptions, nonparametric predictive inference (NPI). We also provide a method that allows analysts to mix Bayesian methods with NPI.

Bayesian probability boxes, presented in Chapter 3, were developed because of the advantages of the probability bounds analysis framework. These advantages include easily interpreted output, methodology that allows us to assume nothing about dependence between random quantities and methodology for sensitivity analysis. Currently p-boxes for distributions with more than one parameter fail to

take parameter dependence into account. Therefore we developed a Bayesian p-box method because Bayesian methods can include parameter dependence.

In Chapter 4, we look at nonparametric predictive inference (NPI) as this method has not been implemented in exposure risk assessment before. It has useful characteristics, such as only making Hill's assumption and not having to assume a distribution. In contrast, Bayesian methods require the choice of a prior distribution and a distribution for the data.

In Chapter 5, we present a new hybrid method that allows us to combine random quantities modelled by NPI with random quantities modelled by Bayesian methods. This is useful when we have different levels of information about each random quantity in the model. We show that NPI can be combined with the Bayesian posterior predictive distribution and Bayesian two-dimensional Monte Carlo Simulation (2D MCS).

In this thesis we make several contributions to knowledge. These include developing the Bayesian p-box to represent variability and uncertainty for random quantities for ecotoxicological risk assessment. Bayesian p-boxes are useful as they can use tools from the general probability bounds framework. These tools include combining random quantities without making assumptions about dependence and sensitivity analysis by pinching p-boxes to a single distribution and seeing how this affects the output. We illustrate how NPI can be used for exposure assessment for food safety risk assessment as it has not been implemented in this field before and it has the advantage of not having to assume a parametric distribution. We propose a method that combines Bayesian methods with NPI as they have not been combined in a model before. This allows analysts to make different levels of assumptions about random quantities in the model. For example, analysts may only be prepared to assume Hill's assumption, $A_{(n)}$, which is weaker than a parametric distributional assumption. These methods have been developed or implemented specifically for the ecotoxicological or food safety risk assessments. However they may be applicable in many other types of risk assessment. For example, p-boxes are currently used in the fields of reliability and engineering and NPI has applications in areas such as survival analysis.

1.2 Outline of Thesis

In this thesis we aim to add to the methods available for risk assessment. We begin in Chapter 2 by discussing the current state of risk assessment and the various uncertainties that need to be considered, when appropriate, in risk assessment. We explain why methods that model variability and uncertainty separately are used when answering questions about population risk. We provide an overview of several methods that are currently available. We look both at methods that model variability and uncertainty separately and those that do not. We explain the advantages and disadvantages of several of the methods and provide a simple exposure model (Section 2.2) which we focus on throughout the thesis. The use of this model allows us to illustrate methods clearly.

One of our main contributions to the literature is a new method called Bayesian p-boxes, which models variability and uncertainty separately to look at the risk to populations including parameter uncertainty. We present this in Chapter 3, and provide an illustration of how it works for two different distributions. We look at two different classes of prior distributions to include robustness to the prior distribution in the analysis and show how fixed measurement uncertainty can be incorporated in the analysis. We compare Bayesian p-boxes to other methods and show that a Bayesian p-box produces bounds that take parameter uncertainty and the dependence between parameters into account. We also illustrate the results of combining Bayesian p-boxes using the method by Williamson and Downs (1990), which allows us to make no assumptions about dependence between random quantities. The majority of this research will appear as Montgomery et al. (In press).

In Chapter 4, we illustrate how nonparametric predictive inference (NPI) can be used for exposure assessment by forming NPI lower and upper cumulative distribution functions (cdfs) for exposure. NPI can incorporate left-censored data in the analysis which is useful because left-censoring is a common occurrence with concentration data sets. We investigate how NPI lower and upper cdfs are affected by strongly and weakly correlated data sets and how known measurement uncertainty can be included in an NPI analysis. We compare NPI with another predictive method, the Bayesian posterior predictive distribution, where NPI compares

favourably because it includes interval uncertainty and makes no distributional assumptions. Then we consider an ad hoc method to form robust NPI lower and upper cdfs.

In Chapter 5 we develop a hybrid method that allows us to combine random quantities modelled by NPI and random quantities modelled by Bayesian posterior predictive distributions. We illustrate this method and investigate the effect of sampling variation and sample size using a simple exposure model. A robust hybrid method is presented where we include robustness for each random quantity in the model. We also illustrate a method of combining 2D Monte Carlo Simulation with NPI. Papers based on Chapters 4 and 5 and aimed at both the risk assessment and statistics literatures are in preparation.

In Chapter 6 we sum up the results of this thesis and the contribution we have made to the area of risk assessment. We also suggest some areas that we think would be useful for future research, including combining random quantities using uncertain correlations, forming Bayesian p-boxes for other distributions, and developing the methods we have considered for more realistic models.

Appendix A contains the specific parameterisations for all the distributions used in this thesis. All computations were performed using Matlab (Release 2006b, The Mathworks).

1.3 Collaborators

This thesis is the result of a collaboration between Durham University and the Risk Analysis team at Central Science Laboratory in York. Central Science Laboratory is a government agency that is dedicated to applying science for food safety and environmental health. The Risk Analysis team specialises in quantitative risk assessment for environment, agriculture and food safety. Their main work is to develop and implement probabilistic approaches for risk assessment. They also undertake consultancy work and contribute to international expert committees.

Chapter 2

Statistical methods for risk assessment

2.1 Introduction

In this chapter we introduce two different types of risk assessment, food safety and ecotoxicological (pesticide) risk assessment and statistical methods that are currently used for different parts of a risk assessment. We have investigated these due to the recognised need, by policy makers and analysts, that the handling of uncertainty in risk assessment must be improved. This is a consequence of previous health scares (e.g. dioxins in seafood, GM crops, etc). It is also important to communicate the limitations of scientific advice to decision makers and the public in a transparent way. There are difficulties with terminology in risk assessment, as users and analysts often interchange the use of the terms 'random quantities', 'variables' and 'parameters' and frequentist confidence intervals are often interpreted as Bayesian credible intervals. Therefore it is important to communicate exactly what the results from a particular approach show and which uncertainties have been taken into account to arrive at those results.

We begin by explaining the different parts of a risk assessment for chemicals (Section 2.2) and introduce a specific exposure model that we will use throughout the thesis to illustrate various methods. In Section 2.3, we discuss the current EU guidance for plant protection products and food safety risk assessment and describe

some of the data sets that are available for effects assessment and exposure assessment (both assessments are explained in Section 2.2). In exposure assessment, there is the added difficulty of left-censored data sets for concentration, which is discussed in Section 2.4. For the effects assessment for ecotoxicological risk assessment, we consider species sensitivity distributions (Section 2.5) to describe the variation between different species' sensitivities to various chemicals.

When a risk manager wants to make a decision about a population, an important concept is the separate modelling of variability and uncertainty (both defined in Section 2.6.1). A population is defined as the group of individuals or entities to which a distribution refers. We discuss some important types of uncertainty and provide an example that explains why analysts and risk managers want to model variability and uncertainty separately when considering a population.

In Sections 2.7 - 2.12, several methods for risk assessment are briefly explained, all of which are implemented in the thesis. These include Bayesian methods, non-parametric predictive inference (NPI), probability bounds analysis and methods for dealing with dependence between random quantities. Some of these methods model variability and uncertainty separately and would thus be useful for questions about populations, while others, e.g. NPI and the Bayesian posterior predictive distribution, do not model variability and uncertainty separately. These methods are important for decision making if the interest is in an individual randomly selected from the population. In Section 2.13, we also look at some alternative methods which have been used in risk assessment but not in the research reported in this thesis.

2.2 Risk assessment of chemicals

Chemicals are tested to assess their risk to a population or to an individual. If risk managers deem the risk to be small enough, the chemical will be licensed and can be used. Risk assessments are performed in different ways depending on their intended purpose and other factors such as available data and resources. Van Leeuwen and Hermens (1995) define risk assessment as a process which entails the following

elements: hazard identification, effects assessment, exposure assessment and risk characterisation.

Hazard identification is the process of determining if a substance can cause adverse health effects in organisms. It also includes investigating what those effects might be. It involves evaluating data on the types of possible health effects and looking at how much exposure will lead to environmental damage or diseases. Data may be available from laboratory or field studies.

Effects Assessment is the determination of the relationship between the magnitude of exposure to a substance and the severity or frequency of occurrence, or both, of associated adverse health effects. One chemical may produce more than one type of dose-response relationship, for example, a high dose over a short time period may be fatal, but a low dose over a long time period may lead to effects such as cancer. The data available are usually laboratory data. Extrapolation factors are sometimes used when only surrogate data sets are available, e.g. if we want to look at the effect of a particular exposure on humans but we only have data for tests done on rats. In human risk assessment, the variations in exposure routes (e.g. dermal absorption, inhalation or ingestion) and variation in the sensitivity of different individuals to substances may be considered. A discussion of species-to-species extrapolation and other research needs in environmental health risk assessment is provided by Aitio (2008).

Exposure Assessment is the evaluation of the likely intake of substances. It involves the prediction of concentrations or doses of substances to which the population of interest may be exposed. Exposure can be assessed by considering the possible exposure pathways and the rate of movement and degradation of a substance. A simple exposure model that we consider throughout the thesis is:

$$\text{Exposure} = \frac{\text{Concentration} \times \text{Intake}}{\text{Bodyweight}} \tag{2.1}$$

where exposure is measured in μg/kg bw/day, concentration in μg/kg, intake in

kg/day and bodyweight in kg. As stated by Crocker (2005), in the context of birds' exposure to pesticides, if we assume that the only exposure pathway is through food, the simplest estimated theoretical exposure is the food intake rate multiplied by concentration of the pesticide and divided by the bodyweight of the bird. There are several other factors affecting birds, such as the proportion of food items obtained from a field that has been sprayed with pesticide, and these can be incorporated to make a more detailed model. Similarly for human risk assessment there are complicated exposure models available, where analysts are trying to combine different exposure pathways, for an example see Brand et al. (2007). However, as our aim in this thesis is to explore different methodologies, we restrict attention to the simple model (2.1), where we only consider the exposure pathway from food or drink via the random quantity Intake. From here on we will refer to model (2.1) as the Exposure Model.

Risk Characterisation is the assessment of the probability of occurrence of known or potential adverse health effects in a population, together with their effects, due to an actual or predicted exposure to a substance. It is based on hazard identification, effects assessment and exposure assessment and aims to include variability and uncertainty.

2.3 Current EU guidance

The above steps for risk assessment for chemicals have been implemented at the EU level. Currently under EU legislation, risk assessments for plant protection products are mainly deterministic. Probabilistic methods are mentioned as a refinement option in the current EU guidance documents on assessing environmental risks of pesticides (European Commission, 2002a,c). These documents recognise the potential usefulness of probabilistic methods, but they also express reservations about the lack of reliable information for specifying distributions of random quantities, about the validity of assumptions, and about the lack of officially endorsed statistical methods.

In deterministic modelling for exposure assessment, point estimates, either mean values or worst-case values chosen by experts, are used for each different random quantity in an exposure model. The resulting point estimate is assumed to be a conservative estimate of exposure. The endpoint of the risk assessment for birds, wild mammals, aquatic organisms and earthworms is the Toxicity-Exposure-Ratio (TER), which is the ratio of the measure of effects and an exposure value. The measure of effects is the toxicity value that is relevant for the assessment. This may, for example, be an LD_{50}, which is the concentration at which a chemical kills 50% of the individuals in the tested population. Alternatively it may be a no-effect level, which is the highest concentration at which the chemical causes no toxicological effects. The exposure value is the value calculated using the deterministic values mentioned previously. The risk is considered acceptable if the TER is greater than a chosen threshold value. If this is not the case, the pesticide is not acceptable *unless* it can be shown by higher tier risk assessment, e.g. probabilistic risk assessment or field studies, that the substance is likely to have a low risk.

For food safety risk assessment a similar framework is used where a conservative deterministic exposure assessment is carried out and compared to a threshold toxicity value. However approaches used in the EU to assess exposure vary in detail between different types of chemicals and foods which are controlled by different parts of legislation. An overview of the approaches used in different areas is given by EFSA (2005).

For exposure assessments in both types of risk assessment, it is common to use conservative point estimates as inputs to an exposure model, as the aim is to protect the whole population including the individuals most at risk. However, when conservative assumptions are made for several random quantities, the compounding effect is frequently not quantitatively understood (Frey, 1993). These assumptions may lead to so-called hyperconservativism, where several conservative assumptions are made and compound each other to create a level of conservatism that is extreme (Ferson, 2002).

2.4 Data sets for risk assessment

In ecotoxicological effects assessment, we may be faced with data sets containing as few as one or two observations for toxicity, or there may only be surrogate data available. When modelling these data, the small sample size leads to several of the uncertainties that will be discussed in Subsection 2.6.2. These uncertainties include uncertainty about the distribution that the data have come from, extrapolation uncertainty and measurement uncertainty.

One of the main databases of toxicity data is the ECOTOX database[1], provided by the US environmental protection agency (USEPA). Another is the e-toxbase[2], provided by the Netherlands National Institute of Public Health and the Environment (RIVM). These provide chemical toxicity information for both aquatic and terrestrial species. They contain toxicity values for test endpoints, which include the concentration at which half of the tested population experiences an effect such as behavioural changes, effects on growth, mortality etc. and the highest measured concentration at which no effects are observed (NOEC). The records contain specific information such as the chemical name, toxic mode of action, species name and test endpoint. There are generally very few observations available for new chemicals that are tested in order to be licensed and there are generally more data available for aquatic species than for terrestrial species.

Consider the number of observations available in the AQUIRE database (the aquatic section of the ECOTOX database) for various chemicals for aquatic species. There are 4127 chemicals, of which 1742 have only been tested on one species, 185 have been tested on more than 25 species, and of these, 71 have been tested on more than 50 species.

In food safety risk assessment there tends to be more data available as data are collected for every day of a short (e.g. between 1 and 4 days) or long (e.g. around 7 days) survey on the intake of food for hundreds or thousands of people. However, there are often problems with the data including measurement uncertainty

[1] http://cfpub.epa.gov/ecotox/
[2] http://www.e-toxbase.com/default.aspx

and missing values, where e.g. some intakes of food are not recorded. The relatively short length of the food surveys leads to issues with extrapolation for predictions for individuals over longer time spans. An example of a dietary database is the UK Data Archive Study No. 3481 − National Diet, Nutrition and Dental Survey of Children Aged 1.5 − 4.5 years, 1992 − 1993[3]. This is a 4 day survey for 1717 individuals giving information such as their age, sex, weight, height and their consumption of different types of food and drink.

For the exposure assessment for a food safety risk assessment there is concentration data available about chemicals in different food types. A problem that often occurs with concentration data is that there are observations that are only recorded as less than a specific limit. When the concentration of a chemical is measured, there is often a positive limit of detection (LOD) below which the equipment cannot measure. The measured concentrations of the chemical which fall below the LOD will be recorded as less than the LOD. Some methods can easily incorporate left-censored data including Bayesian methods (Section 2.7), NPI (Section 2.9) and bootstrap methods (Subsection 2.13.1).

2.5 Species sensitivity distributions

Species sensitivity distributions (SSDs) are used in effects assessment to describe the distribution of the variation in toxicity of a compound between species. There are biological differences between living organisms and these mean that different species will respond in different ways to compounds at varying concentrations. We can model these differences using an SSD. The SSD is formed from a sample of toxicity data for different species, for example, the No Observed Effect Concentrations (NOEC). An SSD is often represented by the cumulative distribution function (cdf) of a distribution that is fitted to the data. This may be a parametric distribution or the empirical distribution function for the data. For a detailed account of the theory and application of SSDs, see Posthuma et al. (2002).

As toxicity data sets tend to be small there is a lot of uncertainty about the

[3]http://www.esds.ac.uk/findingdata/snDescription.asp?sn=3481&key=coding

distribution that is fitted to the data. However, in some cases other information may be available to suggest a particular distribution. When parametric distributions are fitted to the data sample, there may also be uncertainty about the parameters of the SSD. In practice, uncertainty about the parameters of the chosen distribution can be included in the analysis to provide lower and upper bounds on the SSD. To include parameter uncertainty, the SSD may be formed in many ways including the use of a Bayesian p-box (Chapter 3), the Bayesian pointwise method (Subsection 2.7.7) or a nonparametric p-box (Subsection 2.10.1).

2.6 Variability and uncertainty

In this section variability and uncertainty that may be present in a risk assessment are explained and discussed. In Subsection 2.6.4, we illustrate with an example, why variability and uncertainty need to be modelled separately when the population is of interest.

2.6.1 Description of variability and uncertainty

The definitions below are taken from Burmaster and Wilson (1996).

Variability represents heterogeneity or diversity in a well-characterised population which is usually not reducible through further measurement or study. For example, different people in a population have different body weights, no matter how carefully we weigh them.

Uncertainty represents ignorance about a poorly characterised phenomenon which is sometimes reducible through further measurement or study. For example, the analyst may be able to reduce his or her uncertainty about the volume of wine consumed in a week by different people through a survey of the population.

It is possible to reduce variability in some situations. For example, if government advice is to eat 500g of fish a week and people follow that advice, the variability in the amount of fish consumed in a week may reduce.

2.6.2 Types of uncertainty

There are many uncertainties that may need to be accounted for in a risk assessment. A selection of uncertainties relevant to the problems addressed in this thesis is explained here.

Parameter uncertainty refers to the uncertainty about parameters of input distributions for a model. For every random quantity in the model for which we assume a parametric distribution, we must choose values or a distribution for the parameter(s). Common statistical methods for fitting distributions to data include the maximum likelihood method or the method of moments (Rice, 1995). However, these choose a single parameter value for the distribution and ignore any uncertainty about that value. Bayesian methods (Section 2.7) and parametric p-boxes (Subsection 2.10.2) can be used to express parameter uncertainty.

Uncertainty about dependence may refer to dependence between observable random quantities or dependence between parameters of a distribution. In many risk analyses there is no information available about the relationships between all the random quantities in the model and therefore many analyses assume independence between random quantities, e.g. Fan et al. (2005); Havelaar et al. (2000). This assumption may lead to some uncertainty not being captured in the results of the analysis. This is discussed and illustrated in Section 3.7. If analysts have enough information about dependence, they can incorporate it into the analysis using methods such as copulas (Subsection 2.11.1). Dependence between the parameters of a distribution can be included in a Bayesian framework whereas it is not included in methods such as parametric p-boxes. The importance of including dependence between parameters is discussed in Section 3.6.

Data uncertainty can arise from measurement errors, censoring (see Section 2.4) or extrapolation uncertainty (explained in Effects Assessment in Section 2.2), or all three. Measurement errors include human error and inaccuracy of measuring equipment and may be presented as an interval within which the datapoint falls. We consider measurement errors in Subsection 3.5.5 and Section 4.7.

Model uncertainty refers to the fact that the models that we use to analyse phenomena do not fully describe the real world. Two different models may explain observed behaviour equally well, yet may produce significantly different predictions. The performance of models can be tested by comparing the results with observations from laboratory experiments or field studies. Model uncertainty may refer to choosing the distribution of a random quantity. This can be difficult, because if the data set is small, almost any distribution will fit, and if the data set is large, often no standard distributions, such as the Normal, Gamma or Exponential distributions, will fit.

2.6.3 Modelling variability and uncertainty

In the literature it is stated that variability and uncertainty should be considered separately (Burmaster and Wilson, 1996; Frey, 1993; Vose, 2001). The motivation for this appears to be that decision makers and analysts want to see which has more influence on the results. Also, they may find it more useful to have estimates of the proportion or number of people that will be affected, together with a measure of the uncertainty of that estimate, rather than an estimate of the probability that a random individual is affected. Modelling variability and uncertainty separately provides a clearer picture of how much uncertainty surrounds the output for a population. These methods, which we refer to as 2D methods, can be used to identify important random quantities with large uncertainty or variability or both, which may have a large effect on the overall risk. A case study providing motivation for modelling variability and uncertainty separately in exposure risk assessments is given by Frey (1993). Modelling variability and uncertainty separately helps to identify further data collection needs, as uncertainty can usually be reduced by more data collection

whereas variability cannot. However, gathering more information may be useful in quantifying the variability correctly. The separate modelling of variability and uncertainty helps the risk manager in deciding whether it is better to collect more data on the risk or act immediately to reduce it.

Modelling variability and uncertainty separately is important when risk managers want to make a decision about a population. When dealing with a population, if variability and uncertainty are not modelled separately it can lead to assessments where sensitive individuals may be put at risk. We illustrate this in the next section by implementing a one-dimensional method which mixes variability and uncertainty and comparing it to a two-dimensional method that models variability and uncertainty separately.

2.6.4 Example

We explore the use of two Bayesian methods, one which mixes variability and uncertainty, which we call method A, and one which models variability and uncertainty separately, which we call method B. These methods allow us to illustrate the need to model variability and uncertainty separately for a population.

Assume that we have the following data $\{1, 1, 1, 2, 3, 4, 5, 5, 10, 23\}$ in μg/kg for concentration of benzene in different cans of soft drink. We assume that the concentrations follow a Lognormal distribution. We use the same non-informative $p(\mu, \sigma) = \frac{1}{\sigma}$ prior for both method A and method B, where μ and σ are the parameters for the Normal distribution assumed for the $\log_{10}$ of the data.

Using method A we can predict a concentration value for a random can from the population of cans by integrating over the posterior distribution. This leads to a Student t-distribution with location parameter $\overline{y}$, scale parameter $\left(1 + \frac{1}{n}\right)^{\frac{1}{2}} s$ and $n-1$ degrees of freedom (Gelman et al., 1995). We can plot the cdf for this Student t-distribution after transforming the values back to the original scale. This is shown in red in Figure 2.1.

In method B we first need to look at what is variable and what is uncertain. Each can of drink has a different concentration of benzene in it due to the natural variability in the concentration of benzene between cans. We do not know the

parameters of the Lognormal distribution, so these are treated as uncertain. We model this parameter uncertainty by sampling 1,000 values for the parameters σ and $\mu|\sigma$, so we have $(\mu_i, \sigma_i), i = 1, ..., 1,000$. The cdfs for each (μ_i, σ_i) pair can be plotted. Then if we want e.g. 95% limits on the concentration, we calculate 2.5th and 97.5th percentiles pointwise at 1,000 values between 0 and 1 (i.e. by taking horizontal slices through the 1,000 cdfs). This then provides the 95% pointwise bounds shown in Figure 2.1.

Figure 2.1: Method A (red) and 95% pointwise bounds from method B (black)

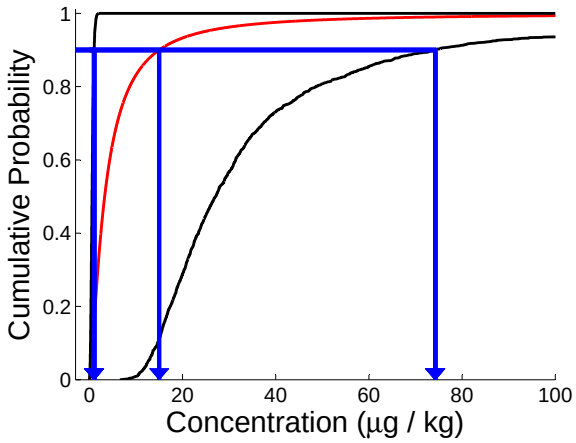

As indicated by the arrows in Figure 2.1, we can see that the 90th percentile when using method A is 14.97 μg/kg, whereas for method B the 90th percentile is between 1.00 and 74.22 μg/kg with 95% probability. So method B shows that the concentration in the can of drink can be as high as 74.22 μg/kg at the 90th percentile given the 95% limits on the 90th percentile. A concentration of 14.97 μg/kg may be relatively safe, leading a risk manager to declare the cans of drink safe for consumption without being aware that the 90th percentile could be as high as 74.22 μg/kg, which may be high enough to be of concern. Therefore, to make sure that we are protecting a population and in particular, the sensitive individuals in the population, it is important to model variability and uncertainty separately. We consider the 90th percentile and the 95% level of credibility for method B. The choice of percentile to consider, i.e. the level of protection required, and the level of confidence or credibility about that percentile are risk management decisions.

These decisions may involve social, economic, ethical, political and legal considerations that are outside the scope of the scientific estimation of risk.

2.7 Bayesian methods

In this section we discuss Bayesian methods and introduce some concepts that are important for later chapters in this thesis. A basic introduction to Bayesian statistics is given by Lee (2004), while a guide to Bayesian data analysis is given by Gelman et al. (1995). Bayesian methods are very versatile and can be used in many applications, such as in meat quality analysis (Blasco, 2005) and cost-effectiveness analysis from clinical trial data (O'Hagan and Stevens, 2001). An overview of Bayesian methodology and applications is presented by Berger (2000) and O'Hagan and Forster (2004). Two case studies illustrating Bayesian inference in practice are given by O'Hagan and Forster (2004) and many applications of Bayesian statistics are illustrated by Congdon (2001).

Bayesian methods involve choosing a parametric model, $M(X|\theta)$, where M represents the model, X is the random quantity of interest and θ represents the parameters. Then a prior distribution, $p(\theta)$, needs to be selected for each parameter. The likelihood function, $L(\theta|x)$, is $p(x|\theta)$ where $p(x|\theta)$ is a function of θ for given X. We then use Bayes Theorem to multiply the prior distribution(s) with the likelihood function for the chosen model to give a posterior distribution. This allows any prior information that we have about a random quantity to be included in the analysis via the prior distribution. It also naturally models the joint distribution of the parameters. An advantage of Bayesian methods is that additional observations can be used to update the output. Once a joint probability distribution for all observable and unobservable quantities has been chosen, posterior distributions and Bayesian posterior predictive distributions (see Subsection 2.7.4) can be calculated. The Bayesian posterior predictive distributions for Normal and Lognormal distributions are well known for specific priors (Gelman et al., 1995). When distributions do not have closed-form solutions, Markov Chain Monte Carlo (MCMC) methods

can be implemented using software like WinBUGS (1990), so we can make inferences by sampling from the posterior distribution.

2.7.1 Credible or posterior intervals and regions

A $100(1-\alpha)\%$ Bayesian credible or posterior interval for a random quantity X is the interval that has the posterior probability $(1-\alpha)$ that X lies in the interval (Gelman et al., 1995). There are different types of credible interval, including a central interval of posterior probability which for a $100(1-\alpha)\%$ interval is the range of values between the $\frac{\alpha}{2}$ and $\frac{1-\alpha}{2}$ percentiles. Another way of summarising the posterior distribution is by considering the highest posterior density (hpd) interval (or hpd region in higher dimensions). This set contains $100(1-\alpha)\%$ of the posterior probability, and the posterior density within the interval is never lower than the density outside the interval. The central posterior interval is identical to the hpd interval if the posterior distribution is unimodal and symmetric. If the posterior distribution is multimodal, the central posterior interval may contain areas of low pdf values whereas the hpd region will consist of several intervals. When the posterior distribution is integrated over these intervals, they will contain $100(1-\alpha)\%$ of the probability. Therefore the hpd intervals provide more information about the posterior distribution than the credible interval as they indicate that the posterior distribution is multimodal which the credible interval does not. If Θ represents multiple parameters, then the hpd space is a subset of the joint posterior parameter space for all parameters in Θ. Next we show an example of an hpd region for the Normal distribution.

2.7.2 Example of hpd region for the Normal distribution

To find the hpd region for a Normal distribution with parameters μ and σ we can follow the steps by Box and Tiao (1973). We start with the non-informative prior, $p(\mu, \sigma) = \frac{1}{\sigma}$, and find the posterior distribution for μ and σ. Each contour $p(\mu, \sigma|\text{data}) = c$ is a curve in the (μ, σ) plane, where $c > 0$ is a suitable constant.

The density contour is given by

$$-(n+1)\ln(\sigma) - \frac{((n-1)s^2 + n(\mu - \overline{y})^2)}{2\sigma^2} = d \tag{2.2}$$

where n is the sample size, $\overline{y}$ is the sample mean, s is the sample standard deviation and d is a function of c. The posterior probability contained in this contour can be calculated by integrating the posterior pdf over the contour. An example of an hpd region for the Lognormal distribution is illustrated in Subsection 3.3.3. For large samples a χ^2 approximation can be used to approximate the hpd region (see Box and Tiao (1973) for more details). This approximation is needed to form Bayesian p-boxes for large n, as discussed in Section 3.6.2.

2.7.3 Prior distributions

Bayesian analyses are often criticised because a prior distribution has to be chosen and may lead to biased posterior distributions that do not produce results consistent with the data. If information is available about the random quantity of interest then it is useful to try and incorporate this into the prior distribution. However, it is often the case that analysts assume a non-informative prior to try and avoid biasing the analysis.

One choice of prior distribution is a conjugate prior distribution. These have the advantage that they lead to a posterior distribution with the same distribution family as the prior distribution. For example, the Normal distribution is conjugate to itself for μ when σ^2 is known, so combining a Normal prior distribution with the Normal likelihood function leads to a Normal posterior distribution. Similarly the Gamma distribution is the conjugate prior for one parameterisation of the Exponential distribution (see Appendix A). The advantages of conjugate families are discussed by Gelman et al. (1995). These advantages include that they can often be put in analytic form and they simplify computations. There are infinitely many subjective prior distributions and a selection are discussed by O'Hagan and Forster (2004). Distributions that integrate to 1 are called proper distributions whereas those that do not are called improper distributions. However if the data dominates

the analysis, it is possible that an improper prior can lead to a proper posterior distribution (Gelman et al., 1995).

There are also objective priors such as reference priors and Jeffrey's prior which are discussed by O'Hagan and Forster (2004). A review of methods for constructing 'default' priors is given by Kass and Wasserman (1996). Default priors are intended to make the prior choice as automatic as possible. Box and Tiao (1973) discuss non-informative priors and how to check if prior distributions are non-informative in different scenarios.

It is also possible to choose a prior distribution using expert elicitation. There is much discussion about how best to elicit distributions from experts and the pitfalls that face analysts trying to get such information (O'Hagan, 1998; Kadane and Wolfson, 1998). Difficulties may arise when experts disagree and their opinions need to be combined in some way. Some applications of expert elicitation in risk assessment are given by Krayer von Krauss et al. (2004), Walker et al. (2001) and Walker et al. (2003).

2.7.4 Bayesian posterior predictive distribution

The Bayesian posterior predictive distribution for a future observation $\hat{y}$ is given by:

$$p(\hat{y}|\text{data}) = \int_{\theta} p(\hat{y}|\theta, \text{data}) p(\theta|\text{data}) \; d\theta \tag{2.3}$$

where θ represents the parameters of the distribution and the data are assumed to be independent and identically distributed. For the Normal distribution, with a non-informative prior, $p(\mu, \sigma) = \frac{1}{\sigma}$, the Bayesian posterior predictive distribution can be shown to be a Student t-distribution with location parameter $\overline{y}$, scale parameter $\left(1 + \frac{1}{n}\right)^{\frac{1}{2}} s$ and $n - 1$ degrees of freedom (Gelman et al., 1995). Therefore we can sample from this distribution to produce predictions for a random individual in a population. The posterior predictive distribution can also be used to predict for any number of future observations.

The Bayesian posterior predictive distribution can also be used to check that the chosen distribution for the data set is a plausible model. We can do this by taking a sample from the Bayesian posterior predictive distribution and comparing it with the observed data set. If the sample does not resemble the observed data then we would know that the model (here, choice of distribution) or the prior distribution is not appropriate (Gelman et al., 1995). We would then need to investigate why this was the case, for example, it may be due to some surprising features of the data or due to a lack of knowledge about the random quantity.

2.7.5 Robustness to the prior distribution

Robustness to the prior distribution can be achieved by using classes of prior distributions to see how sensitive the results of an analysis are to the prior distributions that are used. There are several classes of prior distributions available and some are discussed by Berger (1990). These include the conjugate class, classes with approximately specified moments, neighbourhood classes and density ratio classes. The class of all distributions is not useful because this produces vacuous posterior distributions. Berger (1985) introduces the ϵ-contamination class and Berger and Berliner (1986) recommend using this class when investigating posterior robustness for several reasons. Firstly, it is natural to specify an initial prior and then adjust it by ϵ after more thought or discovering new information. Therefore we should include the priors that differ by ϵ in the analysis. Secondly, this class is easy to work with and flexible through the choice of the class of contaminations (Berger and Berliner, 1986). Robust Bayesian analysis involves minimising and maximising over the class of prior distributions. As explained by Berger (1990), often we need to find a low dimensional subclass of prior distributions which contains the minimising or maximising prior distribution. Optimisation can then be carried out numerically over this smaller subclass. Examples for different criteria are given by Berger (1990).

Robust Bayesian analysis has been conducted in many areas, such as on the linear regression model by Chaturvedi (1996). In this model an ϵ-contamination class of priors is used, where the starting prior is a g-prior distribution with specific parameters. The g-prior distribution is a form of conjugate prior distribution for

the parameters in a linear regression model developed by Zellner (1986). Bayesian robustness of mixture classes of priors was investigated by Bose (1994). Clearly, robust Bayesian analysis can be useful in risk assessment as it would provide an indication of how sensitive the output is to the prior distributions and therefore may show how robust a decision based on the results can be. Robustness and choices for the class of prior distributions are also discussed by O'Hagan and Forster (2004).

2.7.6 Bayesian methods for left-censored data

In a Bayesian framework censored data can be accounted for via the likelihood function. Where this is a closed form solution, we can sample from the relevant distribution. However if this is not the case or we want to model variability and uncertainty separately, censoring can be dealt with using data augmentation (Tanner and Wong, 1987). To use the method for a Lognormal distribution, we take the log of the data and then assume initial values for the parameters of a Normal distribution. There are two steps. First we sample k values from the tail below the LOD, where k is the number of censored values. Secondly, we sample a value for μ and a value for σ from the joint posterior distribution based on the original data above the LOD and the data we sampled in the first step. Both these steps can be repeated several times to obtain samples of the posterior distribution of the parameters.

2.7.7 Bayesian pointwise method

Aldenberg and Jaworska (2000) devised a method for dealing with uncertainty about specific percentiles of a (Log)Normal distribution, we will refer to this as the Bayesian pointwise method. The Bayesian pointwise method is used to describe posterior uncertainty around percentiles of a (Log)Normal distribution and uses pointwise bounds on cdfs to represent uncertainty. The width of the bounds at each percentile depends only on the shape of a non-central t-distribution with $(n-1)$ degrees of freedom scaled by $\frac{1}{\sqrt{n}}$ (Aldenberg and Jaworska, 2000). When n is small this distribution is very skewed, so wide intervals are observed at high and low percentiles.

At the median, there are narrower credible intervals. As n increases, the skewness in the non-central t-distribution quickly reduces, producing narrower bounds. This method can only be used for (Log)Normal distributions. For more complex models with several random quantities, distributions other than (Log)Normal distributions and non closed-form posterior distributions, two-dimensional Monte Carlo Simulation (see Subsection 2.12.2) could be used. Aldenberg and Jaworska (2000) also display the median distribution which is found by calculating the 50th percentile of the possible cdfs horizontally at several percentiles. An example of the Bayesian pointwise output with the median distribution and credible intervals for each percentile is given in Section 3.6.

2.8 Frequentist confidence methods

The frequentist alternative to a p% credible region is a p% confidence region. This has the interpretation that in a large number of repeated trials m, $(m \to \infty)$, the true values of the parameters would fall in the p% confidence region $\frac{mp}{100}$ times. As with the Bayesian methods, visualising and plotting confidence regions is difficult when working with more then three parameters. In Burmaster and Thompson (1998), maximum likelihood estimation is used to fit parametric distributions to data. Point estimates of parameters are obtained and used to produce joint confidence regions using standard methods (e.g. Mood et al. (1974); Cox and Snell (1989)). Both a χ^2 approximation and the standard Taylor series approximation are used to illustrate approximate confidence regions. The confidence regions differ depending on which approximation is used but as $n \to \infty$, where n is the sample size, the confidence regions will converge. This is similar to the Bayesian credible region which will differ depending on the prior distribution that is chosen for the parameters. As $n \to \infty$, generally the likelihood function of the data will dominate and the prior distribution will have less influence. The maximum likelihood method is illustrated for both the Normal and Beta distributions in Burmaster and Thompson (1998) and an assumption that the parameters of both the Normal distribution and the Beta distribution are distributed according to a Multivariate Normal distribution is made.

The Bayesian framework allows the choice of other distributions for the parameters via the prior distribution and the likelihood function. There are other methods available such as given by Bryan et al. (2007), who construct confidence regions of expected optimal size, and Evans et al. (2003) who consider a hybrid Bayesian-frequentist confidence region with the frequentist coverage properties. The Bayesian framework allows more flexibility as it can include prior information using the prior distribution which the frequentist methods cannot. The frequentist method however has the advantage that there is no need to choose a prior distribution if there is no information available a priori. In this thesis, for illustration, we use Bayesian credible regions and thus illustrate the Bayesian p-box. However different p-boxes could be constructed in the same way as for the Bayesian p-box by using different regions such as the ones illustrated by Burmaster and Thompson (1998), Evans et al. (2003) and Bryan et al. (2007). These would produce frequentist p-boxes with the interpretation that p% of the time, where p is some chosen confidence level, the true distribution would fall within the p-box.

2.9 Nonparametric Predictive Inference (NPI)

Nonparametric Predictive Inference (NPI) is a method that provides lower and upper probabilities for the predicted value(s) of one or more future observation(s) of random quantities. NPI is based on Hill's assumption $A_{(n)}$, explained in Subsection 2.9.1, and uses interval probability to quantify uncertainty (Coolen, 2006). It is an alternative to robust Bayes-like imprecise probability methods (Walley, 1991). NPI has been presented for many applications including comparison of proportions (Coolen and Coolen-Schrijner, 2007), adaptive age replacement strategies (Coolen-Schrijner et al., 2006) and right-censored data (Coolen and Yan, 2004). Due to its use of $A_{(n)}$ in deriving the lower and upper probabilities, NPI fits into a frequentist framework of statistics, but can also be interpreted from a Bayesian perspective (Hill, 1988; 1993). Other advantages of NPI include that it is consistent within interval probability theory (Augustin and Coolen, 2004), in agreement with empirical probabilities, exactly calibrated in the sense of Lawless and Fredette (2005), and it

allows the analyst to study the effect of distribution assumptions in other methods. NPI makes only few assumptions, one of which is that the data are exchangeable, so inferences do not depend on the ordering of the data. There is also an underlying assumption that there is a uniform distribution of the intervals between the data points but without further specification on how the probabilities are distributed within these intervals. NPI has never been implemented before in the area of exposure assessment but as it can provide predictive probability bounds for the exposure of an individual without making an assumption about the distribution that the data have come from, it seems useful to implement it. Therefore we present an NPI analysis for exposure assessment on the simple Exposure Model (Section 2.2) in Chapter 4, to explain how it can be implemented and to illustrate the advantages of using a nonparametric method.

2.9.1 Hill's $A_{(n)}$

Nonparametric Predictive Inference (Section 2.9) is based on the assumption $A_{(n)}$, proposed by Hill (1968) for prediction when there is very vague prior knowledge about the form of the underlying distribution of a random quantity. Let $x_{(1)}, ..., x_{(n)}$ be the order statistics of data $x_1, ..., x_n$, and let X_i be the corresponding random quantities prior to obtaining the data, so that the data consist of the realised values $X_i = x_i,\ i = 1, ..., n$. Then the assumption $A_{(n)}$ is defined as follows (Hill, 1993):

1. The observable random quantities X_1, ... , X_n are exchangeable.

2. Ties have probability 0, so $\mathrm{p}(x_i = x_j) = 0, \forall\ i \neq j$

3. Given data $x_i, i = 1, .., n$, the probability that the next observation, X_{n+1} falls in the open interval $I_j = (x_{(j-1)}, x_j)$ is $\frac{1}{n+1}$, for each $j = 1, ..., n+1$, where we define $x_{(0)} = -\infty$ and $x_{(n+1)} = \infty$

For nonnegative random quantities, we define $x_{(0)} = 0$ instead and similarly if other bounds for the values are known. Hill's $A_{(n)}$ can be adjusted to include ties (Hill, 1988) by assigning the probability $\frac{c-1}{n+1}$ to the tied data point, where c is the number of times the value is present in the data set and n is the sample size. In the

NPI framework, a repeated value can be regarded as a limiting situation where the interval between the repeated observations is infinitesimally small, but can still be considered as an interval to which we can assign the probability $\frac{1}{n+1}$.

2.9.2 Lower and Upper probabilities

As explained in Augustin and Coolen (2004), we can find lower and upper bounds for the probability of $X_{n+1} \in B$ given the intervals I_1, ..., I_{n+1} and the assumption $A_{(n)}$, where B is an element of $\mathscr{B}$ and $\mathscr{B}$ is the Borel σ-field over $\mathbb{R}$. The Borel σ-field is the set consisting of all sets of intervals on the real line. The lower bound is then $L(X_{n+1} \in B) = \frac{1}{n+1}|\{j : I_j \subseteq B\}|$ and the upper bound is $U(X_{n+1} \in B) = \frac{1}{n+1}|\{j : I_j \cap B \neq \emptyset\}|$, where $|\cdot|$ denote absolute values. The lower bound only takes into account the probability mass that must be in B, which only occurs with probability mass $\frac{1}{n+1}$ per interval I_j when the interval I_j is completely contained within B. The upper bound takes into account any probability mass that could be in B, which occurs with probability mass $\frac{1}{n+1}$ per interval I_j if the intersection of the interval I_j and B is nonempty. The NPI lower and upper cdfs for X_{n+1} can then be calculated by taking $B = (-\infty, x]$, where $x \in (x_{(0)}, x_{(n+1)})$. Subsection 4.2.3 explains how we can form NPI lower and upper cdfs for left-censored data.

2.9.3 M function

One useful tool for representing the probability mass on intervals for NPI is an M function which is a Dempster-Shafer structure. A Dempster-Shafer structure can represent the partial specification of a probability distribution on intervals with no restrictions as to where the probability mass falls in the interval. For example, instead of a discrete probability mass function over the real-line with probabilities for each point, a Dempster-Shafer structure might give a probability mass that corresponds to an interval rather than a point value (Ferson et al., 2004). The masses must sum to one and the sets containing non-zero mass are called focal elements. This structure can be represented using the notation of the M function for a random quantity, say X. The probability mass assigned for a random quantity

X to an interval (a, b) can be denoted by $M_X(a, b)$. It is important to note that the intervals to which positive M function values are assigned can overlap.

2.10 Probability Boxes (p-boxes)

In ecotoxicological risk assessment there is often a lack of information available to quantify random quantities and the uncertainty around them. Probability bounds analysis incorporates established results on bounding distributions and random quantities by, e.g. Chebyshev (1874) and Markov (1886), with modern computational methods to solve two common problems: (1) not knowing the exact input distributions, and (2) not knowing dependencies between the inputs. The idea of p-boxes is that the output p-box will contain all possible output distributions that could result from the input distributions, assuming the distributions of the random quantities actually lie in their respective p-boxes (Ferson and Tucker, 2003). They may be nonparametric or parametric as discussed next.

2.10.1 Nonparametric p-boxes

Some p-boxes do not need a large amount of information, for example some types can be constructed based on the minimum, maximum, mean or variance of the data or a combination of these. Nonparametric p-boxes may have confidence levels associated with them, such as the 95% Kolmogorov-Smirnov (KS) confidence limits introduced below, or they may be formed assuming 100% confidence. For more information on nonparametric p-boxes see Ferson et al. (2003).

Methods based on the maximum and minimum values do not model sampling uncertainty separately, where sampling uncertainty is the uncertainty that arises from only having one small sample from a larger population. For example, if a second sample was taken the empirical distribution for the first sample would not be the same as for the second sample. It is similar to parameter uncertainty (see Subsection 2.6.2), but it is termed sampling uncertainty here because we have no specific distribution and no parameters. Kolmogorov-Smirnov (KS) confidence limits (Kolmogorov, 1941; Smirnov, 1939), can be used to include sampling uncertainty.

These bounds rely on the calculation of the one-sample Kolmogorov-Smirnov critical statistic $D(\alpha, n)$ for confidence level $100(1-\alpha)\%$ and sample size n. Kolmogorov proved that these confidence limits can be used for entire distributions and Smirnov produced a formula to calculate $D(\alpha, n)$. KS confidence limits are distribution-free bounds for the empirical cdf, so they are bounds on a probability distribution as a whole. Miller (1956) improved the formulation for $D(\alpha, n)$ and provided extensive tables of $D(\alpha, n)$ values. The KS confidence limits are frequentist bounds that have the interpretation that they will totally enclose the true empirical distribution function in 95% of a given number of trials. An example to illustrate KS confidence limits for a random sample including and excluding measurement uncertainty is given by Ferson et al. (2003). In theory, the left tails of the KS limits continue to negative infinity and the right tails of the KS limits continue to positive infinity. In practice these may be truncated at reasonable values that depend on the data or any other available information.

An example of KS confidence limits is shown in Section 3.6. The advantage of KS confidence limits is that no distribution has to be assumed. A disadvantage of the KS confidence limits, which it shares with other nonparametric methods, is that for small n, the bounds are often too wide to be of practical use. However if there is no other information available then these infinite tails are useful because they express this lack of knowledge to risk managers.

2.10.2 Parametric p-boxes

For parametric models where the distribution is specified, but the parameter estimates are only described by intervals, probability bounds can be calculated (Ferson et al., 2003). This works well for single parameter distributions, assuming there is some justification for the choice of interval for the parameter. However for distributions with more than one parameter, the method proposed by Ferson et al. (2003) does not include the dependence between the parameters. For example, if we assume that a random quantity X has a Normal distribution, to create a parametric p-box for X we need to choose intervals for μ and σ. Assume we choose the intervals $\mu \in [\mu_l, \mu_u]$ and $\sigma \in [\sigma_l, \sigma_u]$, then the Normal p-box is constructed by taking the

envelope of the four Normal distributions, $N(\mu_l, \sigma_l^2), N(\mu_l, \sigma_u^2), N(\mu_u, \sigma_l^2), N(\mu_u, \sigma_u^2)$. This leads to a Normal p-box as shown in Figure 2.2.

Figure 2.2: Normal p-box

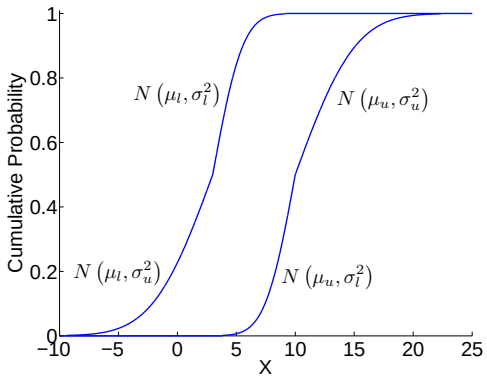

In Section 3.6 we use 95% frequentist confidence intervals to form the Normal p-box as is done by Aughenbaugh and Paredis (2006). Therefore we will call this the frequentist Normal p-box to distinguish between the Bayesian p-boxes introduced in Chapter 3 and this type of p-box that is formed using frequentist confidence intervals. As a consequence of ignoring the dependency between parameters, the frequentist parametric p-boxes may lead to wider or narrower bounds than necessary at some percentiles, although this depends on how the intervals for the parameters are chosen. This is discussed in Subsection 3.6.1 where we compare the Bayesian Normal p-box, developed in Chapter 3, which does include parameter dependence with the frequentist Normal p-box. In Subsection 3.6.1 we briefly mention some frequentist approximations which could be used to improve the frequentist Normal p-box by including parameter dependence.

2.10.3 Discussion

There are some problems with both nonparametric and frequentist parametric p-boxes, such as where to truncate the p-box and not knowing the probability of any of the distributions within the p-box. Advantages of p-boxes are that there is a method for combining p-boxes for different random quantities without assuming anything about the dependence between random quantities (explained in Section 2.11) and they are useful tools for sensitivity analysis as explained further by Ferson and

Tucker (2006), who consider pinching the p-boxes for each random quantity in the model to single distributions and then looking at the effect on the output. They also compare combining the p-boxes for the random quantities assuming independence with p-boxes based on no assumptions about dependence. Numerical examples of the use of p-boxes for ecotoxicological risk assessment, effects assessments, and discussion of issues such as truncation, are given by Ferson (2002) and Ferson and Tucker (2003). P-boxes have been used for species sensitivity distributions (Dixon, 2007a) and for uncertainty propagation for salinity risk models (Dixon, 2007b).

2.11 Dependence between random quantities

In this section we discuss dependence between random quantities and how this can be included in a risk assessment. We first look at copulas which are used to include known correlations between random quantities and we then look at the case where we make no assumption about dependence. It is common in risk assessments to assume independence between random quantities, e.g. Fan et al. (2005); Havelaar et al. (2000) and Chow et al. (2005). We include the explanation of copulas to aid the understanding of Fréchet bounds which are important for the method developed by Williamson and Downs (1990). This method enables the derivation of bounds for the combination of random quantities whilst making no assumptions about the dependence between them. It is useful to consider these bounds and then compare them with the bounds formed under the assumption of independence, to see how much the assumption of independence influences the results. Ferson et al. (2004) discuss dependence in probabilistic modelling including copulas, Fréchet bounds and the method developed by Williamson and Downs. We briefly explain these methods here.

2.11.1 Copulas

Copulas are used as a general way of representing various types of dependence in models. For an introduction to copulas see Nelsen (2002), while an introduction to copulas in risk assessment is given by Haas (1999). Sklar's Theorem (Sklar, 1959)

underlies most applications of copulas. The theorem states that if we have a joint distribution function F for n random quantities then there exists a copula C which joins the marginal distributions of the random quantities to form the joint distribution function. For example, for any bivariate distribution, $F(x, y)$, let $G(x)$ and $H(y)$ be the marginal probability distributions. Then there exists a copula C such that $F(x, y) = C(G(x), H(y))$. Also, if the marginal distributions are continuous, the copula function is unique.

There are many families of copulas available, such as Normal (Gaussian) copulas which are derived from the bivariate Normal distribution using Sklar's Theorem and can cover the entire range of correlation from -1 to 1. The family of bivariate Gaussian copulas is parameterised by the linear correlation matrix $\left(\begin{smallmatrix} 1 & \rho \\ \rho & 1 \end{smallmatrix}\right)$, where ρ is the rank correlation. As we only use the Gaussian copula in this thesis, we do not elaborate on the other families here.

2.11.2 Dependency bounds

When we have very little or no information about dependencies between the random quantities in a model, it may be useful to compute bounds on the results of an analysis without making an assumption about any of the dependencies. If we have two marginal cdfs, F and G with finite positive variances and we have the set $\Pi \equiv \Pi(F, G)$ of all cdfs H on R^2, then contained within Π are two cdfs that correspond to the maximum and minimum correlation (Whitt, 1976). This was discovered by Fréchet (1951) and Hoeffding (1940) who showed that the lower bound for all copulas is $W(u, v) = \max(u + v - 1, 0)$ for two random quantities U and V and the upper bound for all copulas for two random quantities is $\min(u, v)$. These are often referred to as Fréchet bounds or Fréchet-Hoeffding limits.

Williamson and Downs (1990) explain how Fréchet bounds can be used to combine probability boxes with no assumption about dependence. Ferson et al. (2004) state that if the p-box for a random quantity X is $[\underline{F}_X, \overline{F}_X]$ and the p-box for a random quantity Y is $[\underline{F}_Y, \overline{F}_Y]$, where $\underline{F}$ represents the lower cdf and $\overline{F}$ represents the upper cdf, then the p-box for $X+Y$, without any assumptions about dependence between X and Y, can be written as:

$$\underline{F}_{X+Y}(z) = \sup_{z=x+y} \max(\underline{F}_X(x) + \underline{F}_Y(y) - 1, 0)$$

$$\overline{F}_{X+Y}(z) = \inf_{z=x+y} \min(\overline{F}_X(x) + \overline{F}_Y(y), 1)$$

There are similar formulas for subtraction, multiplication and division, given by Ferson et al. (2004). Williamson and Downs (1990) provide algorithms for efficient calculation of these limits. This method can be used for any type of p-box and is implemented in Section 3.7 to combine Bayesian p-boxes with no assumptions about dependence. It can also be used to combine other types of bounds, such as those produced in the Bayesian pointwise method or in a 2D Monte Carlo Simulation (Section 2.12.2). This allows a comparison between making no assumption about dependence and assuming independence which may provide useful information to decision makers. However, they contain all possible dependencies and cannot exclude dependencies so they may not be useful if, for example, it is known that there is no negative correlation between the two random quantities.

Ferson et al. (2004) show the Fréchet bounds on conjunctions of events. For example, using the Fréchet inequality, $\max(0, a + b - 1) \leq \mathrm{P}(A \cap B) \leq \min(a, b)$, where $a = \mathrm{P}(A)$ and $b = \mathrm{P}(B)$, we can calculate the interval of probability that A and B occur. This can be generalised to the multivariate case, giving $\max(0, a_1 + a_2 + ... + a_n - (n-1)) \leq \mathrm{P}(A_1 \cap A_2 \cap ... \cap A_3) \leq \min(a_1, a_2, ...a_n)$. We use this result to combine p-boxes in Section 3.7.

2.12 Monte Carlo Simulation

Monte Carlo simulation (MCS) is one of several techniques currently employed to carry out risk assessments. In the 1940s MCS, originated at Los Alamos from the work of Ulam, von Neumann and Fermi, as a random sampling technique for solving difficult deterministic equations (Ulam, 1976; Cullen and Frey, 1999). An overview of the history of Monte Carlo Simulation is given by Rugen and Callahan (1996). Since then Monte Carlo methods have continued to evolve and due to advances in

computing they can now be used in many applications. Two-dimensional Monte Carlo simulation (2D MCS) is used in a wide range of applications including human health risk assessment, (Burmaster and Wilson, 1996; Glorennec, 2006; Pouillot et al., 2007), avian risk assessment, (Hart et al., 2007), environmental flood risk assessment, (Lindenschmidt et al., 2008) and microbial risk assessment (Miconnet et al., 2005; Vicari et al., 2007).

2.12.1 One-Dimensional Monte Carlo Simulation

One-Dimensional Monte Carlo simulation (1D MCS) is a method which provides predictive results for a random individual from a population. There are different implementations of one-dimensional Monte Carlo Simulation (1D MCS) of which one is given by Frey (1993), who states that each input random quantity is assigned a distribution based on observed data values. Assigning a distribution is usually done by using maximum likelihood methods or the method of moments. The model is then run for many iterations using sampled values from the input distributions for each random quantity. Typically anything from 100 to 10,000 iterations are made giving a set of sample values for a random quantity of interest. The number of iterations used is generally determined by the analyst using trial and error by looking at the output after each run and checking it is consistent with all the previous runs. If it is, then the number of iterations is considered sufficient. The number of iterations required will depend on the complexity of the model and the sampling technique used.

2.12.2 Two-Dimensional Monte Carlo Simulation

Two-dimensional Monte Carlo simulation (2D MCS) is an extension of Monte Carlo simulation. In 2D MCS there are two loops (as opposed to just one in MCS) allowing variability and uncertainty to be modelled separately. The variability is modelled in the inner loop and the uncertainty in the outer loop. An introduction to modelling variability and uncertainty separately and for setting up a 2D MCS in a classical

framework is given by Burmaster and Wilson (1996).

2D MCS can be implemented in a Bayesian framework because it assumes that the distribution parameters are uncertain. However, the advantage of a Bayesian 2D MCS has not always been recognised and non-Bayesian versions have been implemented. In these non-Bayesian versions, distributions for the parameters are selected by analysts and dependencies between the parameters are often ignored. In the Bayesian framework, prior distributions are assigned for parameters of the random quantities and then updated using the data. This accounts for parameter uncertainty and the dependencies between parameters, so we only describe a Bayesian 2D MCS in this thesis.

Bayesian 2D MCS can produce bounds on the output of a particular model at any credible level and it takes into account parameter uncertainty for each random quantity in the model. Some advantages of Monte Carlo methods are listed by Vose (2001). These include the availability of software to implement the procedure and that it can be used as a sensitivity analysis by making adjustments to the model and then comparing the results from each adjustment to see the effect of changes. Model uncertainty (Subsection 2.6.2) can also be included by setting up different models and comparing or enveloping the results from each of them. Also, 2D MCS can be implemented with copulas (explained in Subsection 2.11.1) to take account of any known correlations between the random quantities in the model. Problems with 2D MCS have been described by Ferson (1996), including difficulties with assigning input distributions and dealing with unknown correlations.

2.13 Alternative methods

In this section we provide a brief overview of some methods that have been used for risk assessment but are not used further in this thesis.

2.13.1 Bootstrapping

Introductions to bootstrapping are presented by Davison and Hinkley (1997), Efron and Tibshirani (1993), Vose (2001) and many others. Bootstrapping is a compu-

tationally intensive approach to statistical inference. It is commonly used to find confidence intervals for particular parameters, such as the mean, when sampling from an approximate distribution such as the commonly used empirical distribution of the data set. Generally one can sample many times with replacement from the observed data set to get new data sets of the same size and then calculate the statistic of interest for each sample. We can sample with or without replacement and we can sample smaller or larger size data sets from the whole data set if desired.

Bootstrapping is a useful alternative to parametric methods which require strong assumptions about the distribution of the data. However, in exposure risk assessment we are often interested in the tails of distributions and resampling from the data set that we have can never provide information on more extreme values than those observed. To deal with this, a parametric model can be fitted to the data and then random samples can be drawn from this distribution, but this does not account for uncertainty about the parameter values themselves. Bootstrap methods can also be used to deal with censored data as illustrated by Zhao and Frey (2004).

Bootstrapping has also been used for species sensitivity distributions (SSDs) (Section 2.5) as illustrated by Grist et al. (2002) and Verdonck et al. (2001). Grist et al. (2002) illustrate their method of a bootstrap regression for estimation of SSDs for the aquatic environment. They use the empirical distribution function (edf) so each observation has a probability of $\frac{1}{n}$. They point out that with their choice of edf, at least $n = 20$ is necessary for a 5th percentile to exist as the minimum percentile of the edf is $\frac{100}{n}$. Therefore, with data sets less than 20, which is a common situation for toxicity in birds and mammals, no 5th percentile can be calculated. Even with a sample of 20, bootstrapping may not capture the 5th percentile in the confidence limits. Therefore, it appears that bootstrapping should not be used on small samples. However the coverage of bootstrap confidence intervals can be improved by using a bias corrected or bias corrected accelerated confidence interval, explained by Efron and Tibshirani (1993), Grist et al. (2002) and Vose (2001).

2.13.2 Worst-case analysis

One approach for ecotoxicological risk assessment is worst-case analysis, which works by recognising there is uncertainty about the values of random quantities but does not model this uncertainty explicitly. The uncertainty is accounted for by selecting values in such a way that it is believed that the overall risk estimate will be conservative. The EU guidance for birds and mammals (European Commission, 2002b) contains an example where worst-case analysis is used for part of the model. The approach has been criticised by Frey (1993) because the compounding effect of using several conservative estimates is often not understood. Ferson (2002) asserts that another problem is that the conservatism is unquantified and inconsistent among different assessments. As the levels of conservatism for different analyses are unknown, they cannot be compared for decision making purposes. Worst-case analysis can be used as a screening assessment to see if further refinement is required. A comparison of worst-case analysis and a probabilistic assessment is given by Vermeire et al. (2001).

2.13.3 Interval analysis

This method uses intervals to describe the possible values that a random quantity can take. These intervals can then be manipulated using the rules of interval arithmetic. Ferson et al. (2007) discuss data with interval uncertainty including descriptions of the basic operations, addition, subtraction, division and multiplication. It is possible to compute bounds on all elementary mathematical operations. If a random quantity is repeated in the analysis, the uncertainty for the random quantity is added for each repetition leading to suboptimal bounds, where the optimal bounds are the tightest possible bounds given the inputs. When there are no repeated random quantities in the model, interval analysis is guaranteed to yield the optimal bounds given the inputs (Moore, 1966). Therefore if possible, it is better to manipulate the model so random quantities only occur once.

The advantage of interval analysis is that it can deal with any kind of uncertainty and provide bounds given the data. If the input random quantities lie within their

intervals and we combine the intervals in the correct way it can be guaranteed that the true result will lie in the output interval. Unfortunately the intervals become more conservative as more mathematical operations are performed and as they become wider they give less information on the result. So this method suffers from hyperconservatism. There is also no indication of which values are more or less likely in the interval so if the decision is based on a threshold value, interval analysis would only indicate which decision to make if the threshold value does not lie in the interval. Interval analysis for risk assessments can be performed in RiskCalc software[4]. Details of methodology with examples of applications are given by Ferson et al. (2007). Applications of interval analysis in engineering are given by Moller and Beer (2008).

2.13.4 Fuzzy arithmetic

Fuzzy numbers are a generalisation of interval analysis where we have an interval and we have a membership function which describes our beliefs about the interval in which the value of the random quantity falls. Arithmetic operations can be performed on fuzzy numbers by using interval arithmetic for each possibility level between 0 and 1. Details of a comparison between a frequentist 2D MCS and fuzzy 2D MCS are given by Kentel and Aral (2005). In the 2D fuzzy Monte Carlo, they assign membership functions for the mean and standard deviation. The membership functions must be chosen by an analyst or expert and the dependencies between parameters are not taken into account by the fuzzy method. A posterior distribution automatically takes into account the dependence between parameters and therefore it appears that 2D MCS in a Bayesian framework is preferable to the 2D fuzzy MCS.

2.13.5 Sensitivity analysis

A sensitivity analysis is often considered the most straightforward approach to determine which random quantities in the model have the most influence on the output. It also provides an indication of the range of possible outputs. The main criticism of

[4]http://www.ramas.com/riskcalc.htm

this method is that as the number of random quantities increases the complexity of considering all possible scenarios becomes cumbersome and computationally intensive. A good overview of techniques for sensitivity analysis is presented by Saltelli et al. (2000). There are methods that vary correlation coefficients, e.g. Ma (2002), but Ferson and Hajagos (2006) show that varying correlation coefficicents is not sufficient to include all possible dependencies in the sensitivity analysis. Sensitivity analysis for p-boxes has been explored by Ferson and Tucker (2006). They show how p-boxes can be pinched to a precise distribution to see what effect this has on the output.

2.14 Conclusion

This chapter has provided an insight into some of the methods that are currently being used for risk assessment, as well as some important definitions and explanations required for Chapters 3, 4 and 5. It also provided motivation for the methods developed and implemented later in the thesis.

Chapter 3

Bayesian Probability Boxes

3.1 Introduction

In this chapter we introduce Bayesian probability boxes (p-boxes) which can be used to express variability and uncertainty in risk assessment. As explained in Subsection 2.10.2, frequentist parametric p-boxes are useful as they can include different types of uncertainty, but unfortunately the way that they are constructed ignores dependence between parameters. Bayesian methods can easily deal with dependence between parameters and therefore it is natural to look at a Bayesian way of forming a p-box. The Bayesian p-box can also easily be displayed together with the modal distribution. The modal distribution is the distribution with the mode of the posterior distribution as its parameters. For example, for the Normal distribution with non-informative priors for μ and σ, the posterior is a unimodal distribution. The mode (μ_m, σ_m) is the peak of this unimodal distribution and therefore the modal distribution is $N(\mu_m, \sigma_m^2)$. Bayesian methods also have the advantages that they can deal with censored data, be updated if more data are obtained and incorporate expert opinion or other evidence through prior distributions.

The proposed Bayesian method takes a distribution-wise approach, as opposed to the Aldenberg and Jaworska (2000) pointwise method that was explained in Subsection 2.7.7. In ecotoxicological risk assessment, when the risk manager is making decisions on questions about a population, it is generally agreed that variability and uncertainty need to be modelled separately to ensure the whole population is

considered (Subsection 2.6.3). The Bayesian posterior predictive distribution does not do this so we illustrate the Bayesian posterior predictive distribution in this chapter, together with the Bayesian p-box, to show the difference between the two methods. Bayesian methods all require distributions to be chosen and therefore it is interesting to compare the results with nonparametric p-boxes which do not require a distribution to be chosen. One such nonparametric p-box is formed using the Kolmogorov-Smirnov confidence limits (Subsection 2.10.1) and is illustrated as a comparison to the other methods which assume a particular distribution.

In Section 3.2 we introduce the Bayesian p-box method, apply it to the basic case of the Exponential distribution and consider robustness of the output to the chosen prior distribution. Section 3.3 considers the more complicated case of the Normal and Lognormal distributions while Section 3.5 looks at including robustness with respect to the prior distribution(s) and how to deal with imprecise data sets. In Section 3.6, five methods, namely the Bayesian p-box, the frequentist p-box, Kolmogorov-Smirnov confidence limits, a Bayesian pointwise method and the Bayesian posterior predictive distribution, will be illustrated and compared for two different sample sizes. In Section 3.7 we look at combining Bayesian p-boxes in a basic Exposure Model (Section 2.2) and investigate the effect of the frequently used assumption of independence between random quantities by comparing it to a case where no assumption is made about dependence. In Section 3.8 we discuss all the methods previously mentioned and their usefulness in risk assessment.

Any credibility level can be chosen and evaluated, although throughout this chapter the focus will be on the 95% credibility level. In ecotoxicological risk assessment the percentile of interest is frequently the 5th percentile, whereas in human exposure risk assessment the analysts tend to choose their own percentile (e.g. the 97.5th, 99th or 99.9th percentile). For illustrative purposes we will focus on the 5th percentile for ecotoxicological risk assessment and look at several percentiles (50th, 90th and 99th) for human exposure risk assessment in this chapter.

3.2 Bayesian p-box method

In this section the proposed Bayesian p-box will be introduced. Several of its important properties will be explained and a procedure to compute the Bayesian p-box is provided. Then we illustrate the Bayesian p-box with a basic example using the Exponential distribution. In Section 3.3 the focus will be on the practically important Normal and Lognormal distributions. The method can also be used for other distributions, both discrete and continuous. In principle the method could be implemented for multivariate random quantities, but this may be difficult if the parameter space involves multiple dimensions. Also, the output may be difficult to represent in an understandable way. Hence, we restrict attention to univariate random quantities.

3.2.1 Forming a Bayesian p-box

To form a Bayesian p-box we take X to be an observable random quantity. We then assume a parametric model $X|\theta \sim f_\theta$, where f is a distribution with parameter(s) θ ($\theta \in \Theta$, where Θ may be multi-dimensional) and take $F(X|\theta)$ to be the cdf of X. We then need to choose a prior distribution for θ and combine it with the likelihood function so by Bayes Theorem we form a posterior distribution p(θ|data). For practical risk assessments, which involve communication between statisticians and risk managers, it is often easiest to focus on the observable X. Instead of using the Bayesian posterior predictive distribution, we instead consider bounds on the distributions whose parameters fall in a particular region of interest. To achieve such bounds, we select a subset, $\Theta_s(\alpha)$, of Θ, such that $1-\alpha \leq \mathrm{P}(\theta \in \Theta_s(\alpha)|$ data), with $\Theta_s(\alpha)$ in some suitable sense 'of minimal size', and find optimal bounds for $\{F(x|\theta), \theta \in \Theta_s(\alpha)\}$. For example, we could take $\alpha = 0.05$ and choose $\Theta_s(\alpha)$ to be the highest posterior density region. This would mean that the Bayesian p-box would then contain the distributions that have parameters that lie in the 95% hpd region for θ given the data.

3.2.2 Choosing $\Theta_s(\alpha)$

For the purposes of this chapter, the highest posterior density (hpd) interval or region (Subsection 2.7.1) for the parameter(s) of the distribution is used as $\Theta_s(\alpha)$. If the parametric distribution is not symmetric and unimodal, then the hpd interval displays more important features of the posterior distribution than a credible interval (Chen et al., 2001). If the posterior density is continuous and unimodal then the hpd interval or region is a compact set as it is closed and bounded. As shown in Box and Tiao (1973), it may occur that the $100(1-\alpha)\%$ credible region is identical to the $100(1-\alpha)\%$ confidence region in frequentist statistics, although the interpretation is different. This is, for example, the case for some specific non-informative prior distributions if the same sufficient statistic is used in both classical and Bayesian approaches (Turkkan and Pham-Gia, 1997). There has been some discussion as to whether the hpd region is appropriate, as it is not invariant under reparameterisation (Bernardo and Smith, 1994). Other regions, such as Bernardo's lowest posterior loss region (Bernardo, 2005), which is invariant under reparameterisation, could be used instead. In fact any subset of the parameter space Θ that is closed and bounded and has a specific posterior probability could be used to construct Bayesian p-boxes.

3.2.3 Example: Exponential Distribution

Suppose that components of a machine are stress-tested, their lifetimes are measured in days and that these lifetimes follow an Exponential distribution with parameter λ, where λ is the distribution mean. Assume that a sample, $x_1, x_2, ..., x_n$, of $n = 30$ such lifetimes is available, with sample mean 16.72 days and standard deviation 17.21 days. Consider the case $\alpha = 0.05$ and find $\Theta_s(0.05)$, here the 95% hpd interval for λ. If $\lambda \in [c_1, c_2]$, then $\Theta_s(0.05)$ is derived by calculating values of c_1 and c_2 such that the integral of the posterior distribution between c_1 and c_2 is equal to $(1-\alpha)$ and the value of the posterior probability density function is equal at c_1 and c_2.

We define the prior probability density function to be:

$$p(\lambda|a,b) \propto \lambda^{(a-1)}\exp\left(-\lambda b\right) \tag{3.1}$$

and multiply this by the likelihood function for the Exponential distribution to find the corresponding posterior probability density function:

$$p(\lambda|x_1,...x_n,a,b) \propto \lambda^{(a+n)-1}\exp\left(-\lambda\left(b+\sum_{i=1}^{n}x_i\right)\right) \tag{3.2}$$

$\Theta_s(0.05)$ for λ ($c_1 = 0.0392$ and $c_2 = 0.0816$) is illustrated in Figure 3.0.1 where we use a non-informative Gamma prior distribution with shape parameter $a = 0.001$ and inverse scale parameter $b = 1000$. $p(\lambda|x,a,b)$ represents the posterior probability density given the shape and inverse scale parameters, a and b, and the data x. Maximising and minimising the Exponential distribution over $\Theta_s(0.05)$ is equivalent to plotting the Exponential distributions with λ equal to the endpoints of $\Theta_s(0.05)$ due to the monotonicity of the Exponential cdf with respect to λ. This leads to the Exponential Bayesian p-box shown in Figure 3.0.2.

Figure 3.1: Example for the Exponential distribution

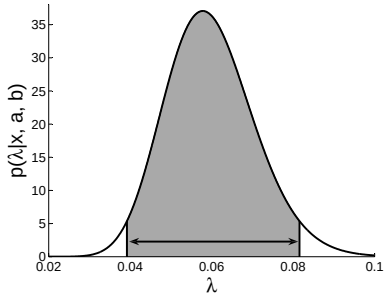

3.0.1 Posterior distribution of λ with $\Theta_s(0.05)$ (shown by the arrow)

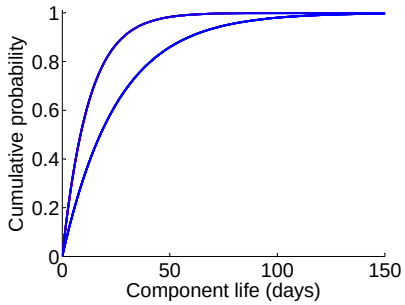

3.0.2 95% Exponential Bayesian p-box

The Exponential Bayesian p-box clearly displays uncertainty about the distribution parameter by the width of the bounds. Looking at specific percentiles shows that the 90th percentile of the random component life is between 28.2 days and 58.7 days and that the probability that the component lasts longer than 25 days, given λ is contained in $\Theta_s(0.05)$, is between 0.13 and 0.38.

3.2.4 Different credibility levels

As decision makers may not want to choose a value for α before the risk assessment is carried out, it may be attractive to produce Bayesian p-boxes for different values of α. From these they can consider the change in uncertainty at different values of α. Figure 3.1 shows the nested Exponential Bayesian p-boxes for the example above for three values of α. The 90th percentiles for each α are shown in Table 3.1.

Figure 3.1: Exponential Bayesian p-box for $\alpha = 0.5$ (black), $\alpha = 0.05$ (red) and $\alpha = 0.01$ (blue)

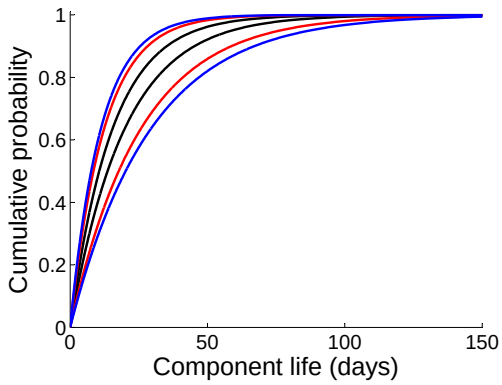

Table 3.1: Upper and lower bounds on the 90th percentile for each value of α

	90th Percentile	
α	Lower	Upper
0.5	35.219	45.282
0.05	28.227	58.725
0.01	25.538	67.055

As expected the interval for the 90th percentile widens as the credibility level in-

creases. Nested Bayesian p-boxes are useful to consider how much the uncertainty increases as the credibility level increases.

3.2.5 Robustness to the prior distribution

A common criticism of Bayesian methods is that the prior distribution may influence the posterior results of an analysis. We illustrated the use of a non-informative prior distribution in Subsection 3.2.3. One can also consider using a class of prior distributions to study robustness with respect to the prior distribution. To do this for the Exponential case, we need to choose bounds for a and b. The posterior distribution is a Gamma distribution with parameters $a+n$ and $b+\sum_{i=1}^{n} x_i$. Now suppose a priori that it is believed that the expected value of the random quantity of interest is approximately E. Then we could, for example, choose a class of prior distributions by taking s small, $a \in (1+\epsilon, s+1)$, where $\epsilon = 1e-15$ and $b \in \left(\frac{1}{2Es}, \infty\right)$. Then as λ has a Gamma distribution, $\frac{1}{\lambda}$ has an Inverse-Gamma distribution, with parameters a and $\theta = \frac{1}{b}$, and thus $\theta \in (0, 2Es)$. The expected value of $\frac{1}{\lambda}$ is $\frac{\theta}{(a-1)}$. So when $a = 1+\epsilon$, the expected value of $\frac{1}{\lambda}$ is in the interval $\left(0, \frac{2Es}{\epsilon}\right)$ and when $a = 1+s$, the expected value of $\frac{1}{\lambda}$ is in the interval $(0, 2E)$ which both seem reasonable as $\frac{1}{\lambda}$ is the mean of the Exponential distribution.

Let us consider two examples in which we use the same robustness criteria as described above $\left(a \in (1+\epsilon, s+1) \text{ and } b \in \left(\frac{1}{2Es}, \infty\right)\right)$, and the same value of s, but with two different sample sizes.

1. Choose $s = 2$, $E = 30$ and randomly generate a sample of size 10 from an Exponential distribution with $\lambda = \frac{1}{20}$. This yields $\sum_{i=1}^{n} x_i = 273.11$.

2. Choose $s = 2$, $E = 30$ and randomly generate a sample of size 100 from an Exponential distribution with $\lambda = \frac{1}{20}$. This yields $\sum_{i=1}^{n} x_i = 2034.99$.

We split a into 20 equally spaced values including the endpoints and b into 20 equally spaced values including the endpoints. Taking the envelope of the possible distributions, by using the endpoints of $\Theta_s(0.05)$, we find the 95% robust Exponential Bayesian p-boxes for these two examples. The 95% robust Exponential Bayesian

p-boxes are compared with 95% Exponential Bayesian p-boxes formed using a non-informative gamma prior distribution with $a = 0.001$ and $b = 1000$ as before, in Figures 3.2.1 and 3.2.2.

Figure 3.3: Comparison of Robust 95% Exponential Bayesian p-box (red) and 95% Exponential Bayesian p-box (blue)

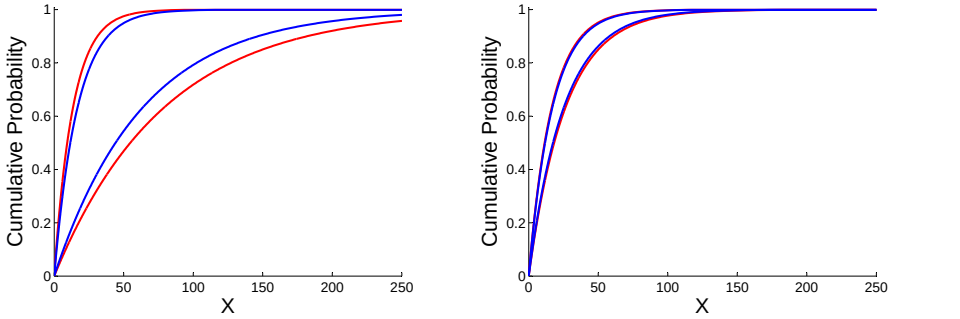

3.2.1 Small sample: $n = 10$, $\sum_{i=1}^{n} x_i = 273.11$

3.2.2 Larger sample: $n = 100$, $\sum_{i=1}^{n} x_i = 2034.99$

It is clear that the inferences from a smaller data set are more influenced by the choice of prior distribution resulting in wider bounds. Additional data lead to a more peaked likelihood function which has a stronger influence on the inferences leading to narrower bounds. The Exponential Bayesian p-box, formed using a non-informative prior distribution, is enclosed within the Exponential p-box using the class of prior distributions in both cases. The endpoints of the hpd intervals, c_1 and c_2, for the non-informative prior distribution are enclosed within the interval of $c_1 r$ and $c_2 r$, where $c_1 r$ and $c_2 r$ are the endpoints of the robust hpd interval, in both cases. As the Exponential Bayesian p-box is formed using these endpoints, the robust cases will enclose the non-informative Exponential Bayesian p-boxes for these examples. Including robustness to the prior distribution describes a little more uncertainty which is indicated by the width of the bounds. As the sample size increases, both uncertainty about λ and the influence of the prior distribution decrease. Thus, there is not a large difference between the width of the bounds using the robust class of prior distributions or the non-informative conjugate prior distribution for $n = 100$. For these data sets which were randomly generated we used 30 as an estimate of E. In practice, this value would need to be chosen by an expert or based on information

available about the random quantity prior to data collection.

In this section we have introduced the procedure to form a Bayesian p-box and illustrated it for the Exponential distribution. We have shown the possible benefit of producing Exponential p-boxes for different credibility levels and that the method can include robustness to the prior distributions. In the next section we consider how to form a Bayesian p-box for the more complicated case of the Normal distribution.

3.3 Normal and Lognormal distributions

In this section the derivation of a Bayesian p-box for the Normal and Lognormal distributions is discussed. The Lognormal distribution is frequently used in risk assessments, in particular for assessment of the magnitude of effects by estimating the proportion of species for which exposure to a chemical exceeds some threshold level (e.g. LD50 or NOEC). To describe the variation in these threshold levels between species, a species sensitivity distribution (see Section 2.5) is often used. As this is frequently assumed to be Lognormal (EFSA, 2005), the illustrative example shown in Subsection 3.3.3 is for the Lognormal distribution.

3.3.1 Bayesian P-boxes for the Normal distribution

We assume that a random quantity X has a Normal distribution with parameters μ and σ. Box and Tiao (1973) present the equation of the joint hpd region for parameters μ and σ assuming locally uniform prior distributions for μ and $\ln(\sigma)$. In this case $\Theta_s(\alpha)$ is the hpd region containing the (μ, σ) pairs with $100(1-\alpha)\%$ posterior probability. We find the hpd region by evaluating the double integral:

$$\int_R p(\mu, \sigma|\text{data}) \ \ \mathrm{d}\mu \ \mathrm{d}\sigma \tag{3.3}$$

where the region R is given by: $h(\mu,\sigma) = -(n+1)\ln(\sigma) - \frac{1}{2\sigma^2}[(n-1)s^2 + n(\mu-\overline{y})^2] \geq d$, where $\overline{y}$ is the sample mean, s is the sample standard deviation and d is a constant. To do this, we integrate numerically over R at different values of d until we find the region, $\Theta_s(\alpha)$, that contains $100(1-\alpha)\%$ probability. Then we find the (μ, σ)

pairs from $\Theta_s(\alpha)$ that optimise the Normal cdf, and use these to find bounds on the distribution of the random quantity X. So we need to calculate the (μ, σ) pairs that optimise the function $g = \Phi\left(\frac{x-\mu}{\sigma}\right)$, where $\Phi(\cdot)$ is the standard Normal cdf. It is clear that the Normal cdf is maximised (minimised) by maximising (minimising) $\left(\frac{x-\mu}{\sigma}\right)$, with fixed $x \in \mathbb{R}$, $\mu \in \mathbb{R}$ and $\sigma > 0$.

If $X \sim N(\mu, \sigma^2)$, then $\Theta_s(\alpha)$ is a strictly convex set defined by $g(\mu, \sigma) \geq d$, where d is a fixed constant, and it is closed and bounded. Therefore the gradient of the boundary of the set, that we call the contour, is continuous and constantly changing everywhere. The (μ, σ) pairs found by tracing the contour, where $\Theta_s(\alpha) = d$, maximise and minimise the cdf of X for all x, justification is given in Subsection 3.3.2. We can then form the Bayesian p-box by plotting the value of the cdf at each x given the values of each optimal (μ, σ) pair from the contour.

The parameters μ and σ are location and scale parameters respectively and this result generalises to other location-scale distributions, such as the Student t-distribution and the Cauchy distribution, as long as the derived region, $\Theta_s(\alpha)$, is closed and bounded. This result allows the use of an efficient algorithm for the computations involved in the derivation of such Bayesian p-boxes. Suppose that (μ_1, σ_1) maximises the cdf (over $\Theta_s(\alpha)$, and hence this point is on its boundary) at a particular value of x, say x_1. To find the maximum of the cdf at a point close to x_1, we only need to search the values of (μ, σ) on the boundary of $\Theta_s(\alpha)$ that are close to (μ_1, σ_1). Alternatively to speed up computation we can split the contour into several (μ, σ) pairs to give an approximate Bayesian p-box.

3.3.2 Justification

We first show that the values of μ and σ that maximise (minimise) $f = \frac{x-\mu}{\sigma}$ are on the contour. To maximise f, one needs to minimise σ. The smallest values of σ possible in $\Theta_s(\alpha)$ at any μ will fall on the contour. Similarly to minimise f, one needs to maximise σ and the maximum σ values possible at any μ will fall on the contour.

Consider the contour $h(\mu, \sigma) = d$. An example of a possible contour and the resulting Bayesian p-box is shown in Figures 3.3.1 and 3.3.2 to aid understanding.

The blue half of the contour corresponds to the resulting blue maximum bound for the Bayesian p-box and similarly the red half corresponds to the resulting minimum bound. This is a closed strictly convex set and therefore the gradient of the contour is different at all points, changes continuously and takes all directions.

Figure 3.3: Example of a possible contour and the resulting Bayesian p-box

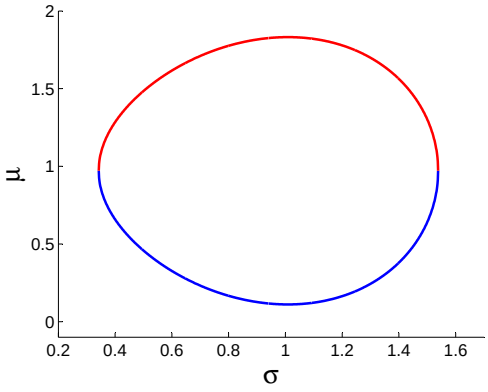

3.3.1 Possible contour

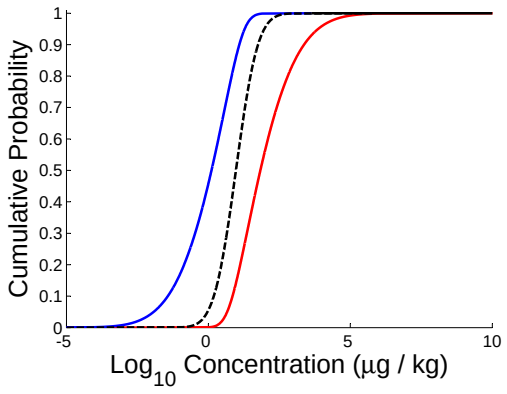

3.3.2 95% Normal Bayesian p-box with modal distribution (black)

Standard optimisation theory states that the gradient of the function f must be a negative multiple of the gradient of the contour where the contour optimises the function e.g. Boas (1983). Consider optimising the function $f = \frac{x-\mu}{\sigma}$ with respect to the contour $h(\mu, \sigma) = \mathrm{d}$. Then $\nabla(f) = -\lambda \nabla h(\mu, \sigma)$, where λ is a constant and

$$\nabla(f) = \begin{pmatrix} \frac{(\mu - x)}{\sigma^2} \\ \frac{-1}{\sigma} \end{pmatrix} \tag{3.4}$$

The first term of the vector is a continuous function of x. For $x \in \mathbb{R}$, it is clear from $\nabla h(\mu, \sigma) = \frac{\nabla(f)}{-\lambda}$ that:

$$x \to -\infty \qquad : \nabla h(\mu, \sigma) \to \begin{pmatrix} -\infty \\ \frac{1}{\lambda\sigma} \end{pmatrix} \tag{3.5}$$

$$x \to \mu \qquad : \nabla h(\mu, \sigma) \to \begin{pmatrix} 0 \\ \frac{1}{\lambda\sigma} \end{pmatrix} \tag{3.6}$$

$$x \to \infty \qquad : \nabla h(\mu, \sigma) \to \begin{pmatrix} \infty \\ \frac{1}{\lambda\sigma} \end{pmatrix} \tag{3.7}$$

so the gradient changes continuously with x. The gradient of the function h that optimises f must follow the above pattern as x increases. Therefore it is clear that the contour optimises f. To see which half of the contour is maximising f we consider the contour $h(\mu, \sigma) \leq d - \epsilon$, where ϵ is a small positive constant. This contour will be larger as it contains more probability. Again we consider the edge of the contour at $h(\mu, \sigma) = d - \epsilon$. As we move from the contour $h(\mu, \sigma) = d$ to the contour $h(\mu, \sigma) = d - \epsilon$, we find that the values of μ increase for the upper half of the contour and decrease at the lower half of the contour for given σ. This leads to an increase in $f = \frac{x-\mu}{\sigma}$ for the lower half of the contour and a decrease in f for the upper half of the contour. Therefore the upper half of the contour is minimising f and the lower half of the contour is maximising f.

3.3.3 Example: Lognormal distribution with small n

To illustrate the Bayesian p-box method, consider the No Observed Effect Concentration (NOEC) of Cadmium (μg Cd/g) of seven soil organisms data (Table 3.2) from Van Straalen and Denneman (1989), also used by Aldenberg and Jaworska (2000).

Table 3.2: NOEC for toxicity of Cadmium (μg Cd/g) of soil organisms.

Species	1	2	3	4	5	6	7
NOEC values	0.97	3.33	3.63	13.50	13.80	18.70	154.00
$\log_{10}$ (NOEC)	-0.013	0.522	0.560	1.130	1.140	1.272	2.188

Assuming that the data come from a Lognormal distribution, Log_{10}(data) follows a Normal distribution. Let us consider using the non-informative prior, $p(\mu, \sigma) = \frac{1}{\sigma}$, and take $\alpha = 0.05$. $\Theta_s(0.05)$, the 95% hpd region, is found by numerical integration, and is shown in Figure 3.4.1, where the mode of the posterior distribution is also indicated. Maximising and minimising the Normal cdf over $\Theta_s(0.05)$ leads to the 95% Normal Bayesian p-box shown in Figure 3.4.2. The uncertainty about the variability is indicated by the width of the bounds. The modal distribution, i.e. the distribution with the mode of the posterior distribution as its parameters, is also shown.

Figure 3.4: Example of $\Theta_s(0.05)$ and the Normal Bayesian p-box for the $\log_{10}$(NOEC) values given in Table 3.2

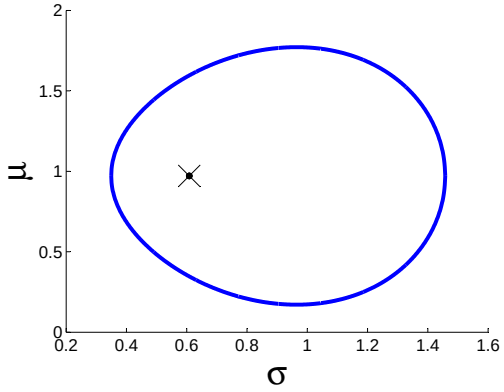

3.4.1 Mode (X) and $\Theta_s(0.05)$

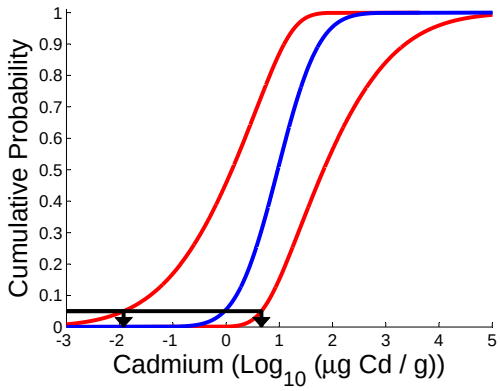

3.4.2 95% Normal Bayesian p-box (red) with modal distribution (blue) and arrows indicating the 5th percentile (black)

In effects assessments, it is assumed that if at least 95% of the species are not affected, an ecosystem is protected. Therefore, the 5th percentile of an SSD is of interest as it is the concentration of a chemical that will affect 5% of the species. Here the 95% bounds on the 5th percentile on the $\log_{10}$ scale are (-1.924, 0.663) μg Cd/g, shown in black in Figure 3.4.2. Transformed back from the $\log_{10}$ scale the 95% bounds on the 5th percentile of the Bayesian p-box are (0.012, 4.602) μg Cd/g. Therefore the concentration that will affect 5% of the species, given the (μ, σ) pairs contained in $\Theta_s(0.05)$ and thus constrained by 95% probability, can be considered to be between these bounds.

3.4 Validating Bayesian p-boxes

As (Log)Normal distributions are important in risk assessment we test the Bayesian p-box for a Normal distribution with various means and standard deviations. We begin with $\mu = 30$ and $\sigma = 3$ and take samples of different sizes ($n = 2, 10, 50$ and 100). We then form the Bayesian 95% hpd region for this Normal distribution and check if the (μ, σ) pair (30,3) fall in the hpd region. We repeat this process 100 times for each sample size and count how many times (30,3) falls in the Bayesian hpd region. To see if there is any dependence on the μ and σ used we vary them one at a time and repeat the process with new μ or σ values. For simplicity we test how

often the true μ and σ values fall in the hpd region, as then the true distribution will fall in the 95% Bayesian p-box. The results from 100 simulations for various μ and σ values are shown in Table 3.3.

Table 3.3: Results for 100 simulations

μ	σ	n	Success out of 100
30	3	2	98
		10	98
		50	97
		100	98
	5	2	96
		10	99
		50	99
		100	99
	7	2	96
		10	98
		50	98
		100	99
	9	2	95
		10	98
		50	99
		100	98
20	3	2	95
		10	97
		50	98
		100	98
40	3	2	95
		10	99
		50	99
		100	99
50	3	2	98
		10	97
		50	98
		100	100

It is clear that there is some sampling variation so some samples lead to hpd regions where the parameters of the true distribution are not included. However generally the Bayesian p-box includes the true distribution in most of the simulations, even for n as small as 2 and therefore seems a reasonably robust method to use. The method is not affected by the change of μ and σ as we would expect because the method takes the sample mean and standard deviation into account. For small samples the size of the hpd region increases, resulting in a wide Bayesian p-box, which leads to the $n = 2$ case producing good results.

3.5 Generalisations

Two topics which are of practical interest are robustness with respect to the prior distribution and imprecision in the data. In effects assessments, sample sizes may be as small as 2, so any prior distribution can have a large influence on the posterior distribution. Therefore it is useful to consider robustness with respect to the influence of the prior distribution. Robustness for the Normal distribution with respect to the prior distribution(s) for μ and σ is considered in Subsections 3.5.1 and 3.5.3. For a detailed introduction to robust Bayesian analysis we refer to Berger (1990). In practice, data sets may be given as interval data, for example when an indication of measurement uncertainty is given. A straightforward method for including such imprecision in data in the analysis is presented in Subsection 3.5.5.

3.5.1 Robustness to the prior distribution for μ

To investigate robustness with respect to the prior distribution for μ, we consider a class of Normal prior distributions for μ given values of σ. We will call this the interval class of prior distributions. The resulting Bayesian p-box will be called the 'robust Normal Bayesian p-box'. Keeping the non-informative prior distribution for σ, $p(\sigma) = \frac{1}{\sigma}$, a Normal class of prior distributions for $\mu|\sigma$ is chosen:

$$\left\{ p(\mu, \sigma) : p(\mu, \sigma) \sim N\left(a, \frac{\sigma^2}{n}\right); a \in [c, v] \right\} \tag{3.8}$$

and the prior interval for the mean, a, is chosen to be between constants c and v. Calculating the posterior distribution, and repeating the previous steps, as in Box and Tiao (1973) and Subsection 2.7.2, leads to the equation of a density contour:

$$-(n+2)\ln(\sigma) - \frac{1}{2\sigma^2}\left((n-1)s^2 + \frac{n}{2}(\overline{x}-a)^2 + 2n\left(\mu - \left(\frac{a+\overline{x}}{2}\right)\right)^2\right) = d \quad (3.9)$$

To find $\Theta_s(0.05)$, integrate the posterior distribution over different regions to find the region enclosing 95% probability. To perform the integration, values for c and v must be chosen. Here c and v are the prior limits on the mean of μ that should be chosen by an expert or based on available evidence.

3.5.2 Example: A robust Normal Bayesian p-box

We have a small data set ($n = 3$) sampled from a Normal distribution with mean 100 and standard deviation 15. The sample statistics are $\overline{x} = 96.83$ and $s = 8.58$ and we take the interval $a \in [66, 116]$. We split this interval by taking 20 equally spaced values, $a_i, i = 1, ..., 20$, including the endpoints for illustrative purposes and this produces the regions $\Theta_{s_{(a_i)}}(0.05)$. Figure 3.5.1 shows these regions and the variation in their shape as the range of σ changes at different values of a. As the interval for a is longer below $\overline{x}$ there will be larger contours at lower μ values than there will be at higher μ values. This can clearly be seen in Figure 3.5.1. This is because, as the prior value that we specify for the mean moves further away from the sample mean, the values for μ in the posterior will be lower. Therefore σ has to increase for the sample to be able to come from a distribution with such a low value for μ. The larger σ values will contribute mostly to the lower tail of the maximum (left) bound, but also slightly to the upper tail of the minimum (right) bound of the robust Normal Bayesian p-box. If the interval had been longer above $\overline{x}$, then the larger contours that we see at lower μ values would have instead been at higher μ values. These larger σ values would mostly contribute to the upper tail of the minimum (right) bound but also slightly to the lower tail of the maximum (left) bound of the robust Normal Bayesian p-box.

We also look at a larger sample ($n = 50$) from a Normal distribution with mean 100 and standard deviation 15. The sample statistics are $\overline{x} = 96.48$ and $s = 13.54$ and we take the interval $a \in [66, 116]$. Figure 3.5.2 shows the regions $\Theta_{s_{(a_i)}}(0.05)$ for this data set where the interval a is again split by taking 20 equally spaced values including the endpoints.

Figure 3.5: Examples of $\Theta_{s_{(a_i)}}(0.05)$ for both data sets

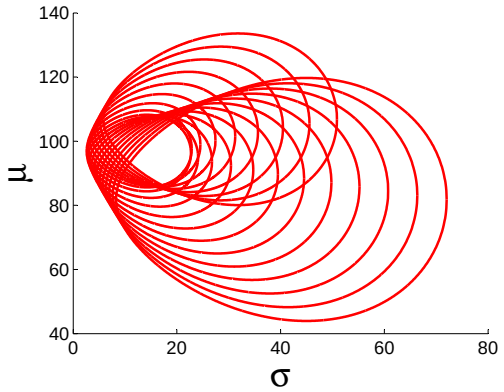

3.5.1 Example of $\Theta_{s_{(a_i)}}(0.05)$ for $n = 3$, $\overline{x} = 96.83$ and $s = 8.58$

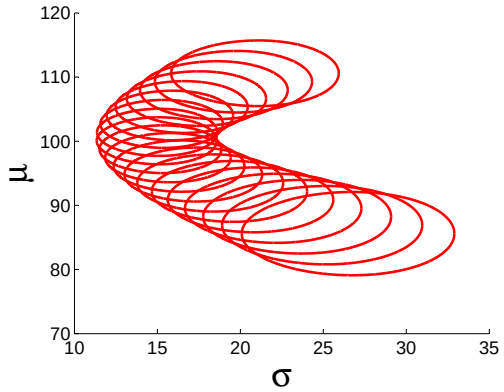

3.5.2 Example of $\Theta_{s_{(a_i)}}(0.05)$ for $n = 50$, $\overline{x} = 96.48$ and $s = 13.54$

To approximate the robust Normal Bayesian p-box for both data sets, we can take many values of a (20 equally spaced values including the endpoints in this example), maximise and minimise over the $100(1 - \alpha)\%$ contours by taking 100 (μ, σ) pairs from the boundary of each contour, and plot the envelope of all these distributions. Figure 3.6.1 shows the 95% robust Normal Bayesian p-box and the 95% Normal Bayesian p-box, using a non-informative prior, $p(\mu, \sigma) = \frac{1}{\sigma}$, for the $n = 3$ example. Figure 3.6.2 shows the 95% robust Normal Bayesian p-box and the 95% Normal Bayesian p-box for the $n = 50$ example.

Figure 3.6: Robust Normal Bayesian p-boxes

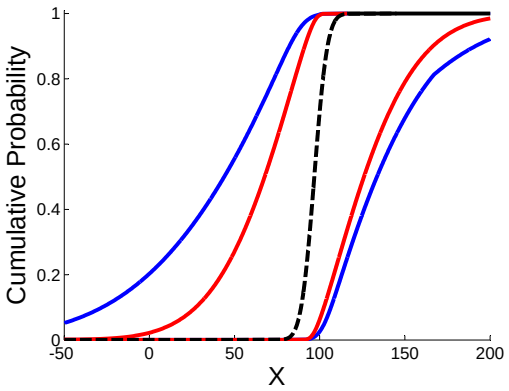

3.6.1 Robust 95% Normal Bayesian p-box for $n = 3$, $\overline{x} = 96.83$ and $s = 8.58$ (blue) with 95% Normal Bayesian p-box (red) and modal distribution (dashed)

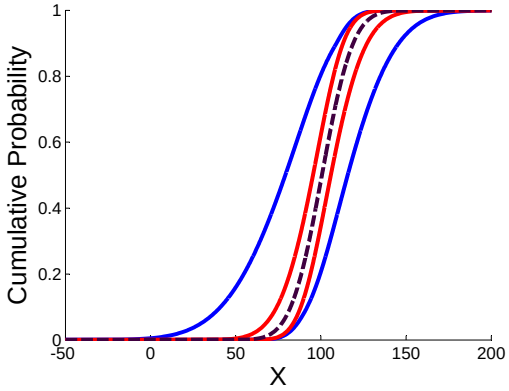

3.6.2 Robust 95% Normal Bayesian p-box for $n = 50$, $\overline{x} = 96.48$ and $s = 13.54$ (blue) with 95% Normal Bayesian p-box (red) and modal distribution (dashed)

We can see here that the larger data set leads to more certainty about the parameters and therefore a narrower p-box. It is helpful that the graphical display of any type of p-box allows an intuitive assessment of the uncertainty based on the width of the bounds. In Figures 3.7.1 and 3.7.2, we show the contour for each data set using the same non-informative prior as we used previously, $p(\mu, \sigma) = \frac{1}{\sigma}$, alongside the contours for the robust 95% Normal Bayesian p-boxes.

Figure 3.7: $\Theta_{s_{(a_i)}}(0.05)$ for the robust cases and using a non-informative prior

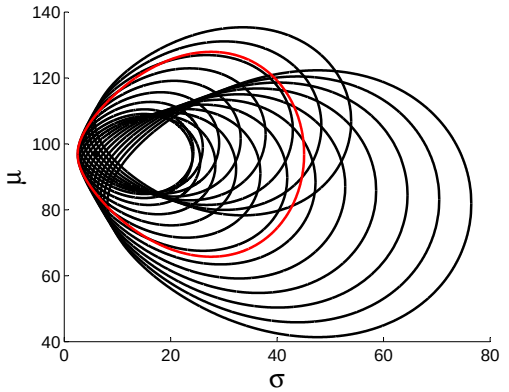

3.7.1 For $n = 3$, $\overline{x} = 96.83$ and $s = 8.58$, robust case (black) and non-informative case (red)

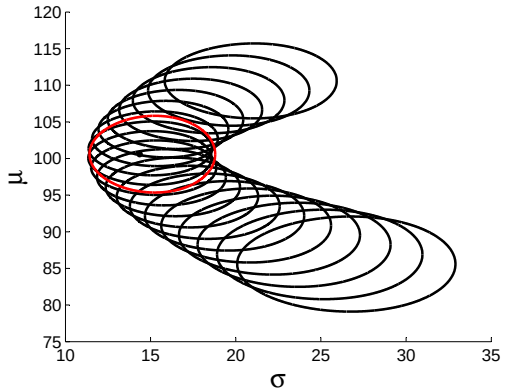

3.7.2 For $n = 50$, $\overline{x} = 96.48$ and $s = 13.54$, robust case (black) and non-informative case (red)

These regions show that the 95% Bayesian p-box should be contained within both robust 95% Normal Bayesian p-boxes. We can see this is true in Figures 3.6.1 and 3.6.2. Also, Figure 3.6.1 shows that for the $n = 3$ case, the larger contours at lower μ values lead to the extra width at the bottom of the maximum (left) bound and the top of the minimum (right) bound of the robust 95% Normal Bayesian p-box. The narrower range of σ values for larger n leads to the narrower limits on the robust 95% Normal Bayesian p-box in Figure 3.6.2.

3.5.3 Robustness to the prior distribution for μ and σ

To study robustness with respect to the prior distribution for μ and σ together, we choose a set of prior distributions for both parameters. We will call the result the 'robust (μ, σ) Normal Bayesian p-box'. Consider an interval on σ and a class of Normal prior distributions on μ given values of σ. So the joint prior distribution is as follows:

$$\left\{ p(\mu, \sigma) \sim N\left(a, \frac{\sigma_x^2}{n}\right) : \ a \in \{\mu_l, \mu_u\}, \sigma_x \in \{\sigma_l, \sigma_u\} \right\} \tag{3.10}$$

where μ_l, μ_u, σ_l and σ_u are the chosen prior limits for μ and σ respectively. Calculating the posterior distribution, and repeating the steps as in Box and Tiao (1973) and Subsection 2.7.2 for this new posterior distribution, leads to density contour:

$$-\ln(\sigma_x) - n\ln(\sigma) - \frac{n}{2\sigma_x^2}(\mu - a)^2 - \frac{1}{2\sigma^2}\left((n-1)s^2 + n\left(\overline{x} - \mu\right)^2\right) = d$$

To find $\Theta_s(\alpha)$, integrate over the posterior distribution to find the region enclosing $100(1-\alpha)\%$ probability. Values for μ_l, μ_u, σ_l and σ_u must be chosen by an expert based on available evidence.

For the numerical integration it is necessary to calculate the normalising constant k. Unfortunately this can only be derived numerically so the following results are again approximations. The lack of an exact normalising constant causes problems with numerical integration so the standard Matlab function, *contour*, is used to obtain numerical approximations to the contours. *Contour* allows the user to specify a grid of values for two random quantities (here μ and σ) and plot corresponding

contours at different heights (here at different heights of the posterior distribution).

3.5.4 Example: A robust (μ, σ) Normal Bayesian p-box

We consider a data set of size 10 ($n = 10$), randomly sampled from a Normal distribution with mean 100 and standard deviation 15. The sample statistics are $\overline{x} = 98.40$ and $s = 9.51$. Now consider the intervals from $\mu_l = 94$ to $\mu_u = 102$, and from $\sigma_l = 8$ to $\sigma_u = 11$. We need to find all the contours for each prior combination of μ and σ.

An example is shown in Figure 3.8.1, where the prior interval σ_x is split into four equal parts and the prior interval a is split into three equal parts, both including the endpoints, so the contours can be seen more clearly. We denote the different combinations of σ_x and a by r_i, $i = 1, ..., 12$, as there are 12 combinations of a and σ_x. Figure 3.8.2 shows the resulting $\Theta_{s_{(r_i)}}(0.05)$ where the prior interval for σ is split into five equal parts and the prior interval for μ is split into ten equal parts (For this case, $i = 1, ..., 50$).

Figure 3.8: Examples of $\Theta_{s_{(r_i)}}(0.05)$ for n=10, $\overline{x} = 98.40$ and $s = 9.51$

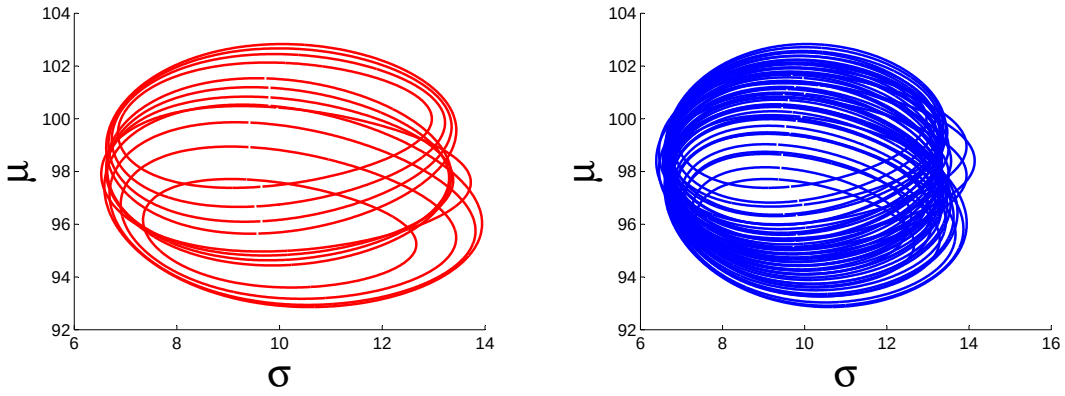

3.8.1 $\mu_l = 94$, $\mu_u = 102$, $\sigma_l = 8$, $\sigma_u = 11$

3.8.2 $\mu_l = 94$, $\mu_u = 102$, $\sigma_l = 8$, $\sigma_u = 11$

We see that the range for σ is wider for the contours where a is close to the mean of the data than for the contours where a moves away from the mean. For larger values of a the range for σ will increase again. To see this, consider the 95% highest posterior regions for $\sigma_x = 8$, with $a = 98.5, 99.5, 100.5, 101.5$ and 104, shown in Figure 3.9.

Figure 3.9: 95% hpd regions for $\sigma_x = 8$ and $a = 98.5$ (blue), 99.5 (green), 100.5 (red), 101.5 (yellow) and 104 (black)

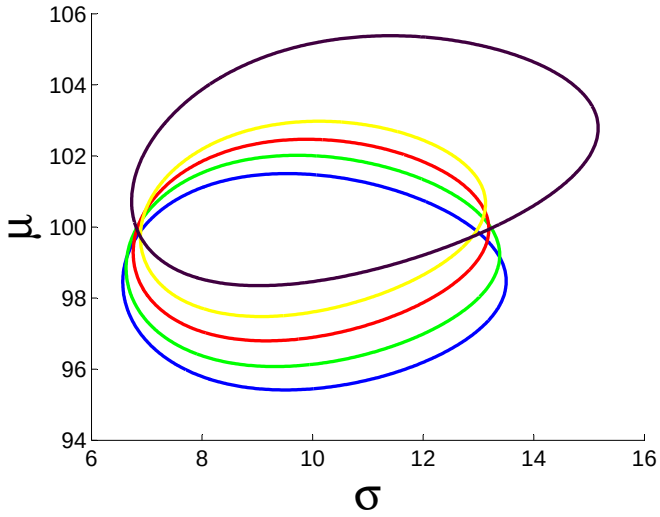

Figure 3.9 shows that the lowest contour (where $a = 98.5$) has the second largest range of σ values. This is because there is agreement between the prior value for μ (i.e. a) and the data mean ($\overline{x}$) which leads to the posterior values for μ being close to the mean value of the data. Therefore there is low probability at higher and lower values of μ as both the likelihood function and the prior distribution suggest that μ should be around the mean. For the other contours the value of a leads to a conflict between the prior value of μ and the mean of the data. The conflict leads to more μ values having higher posterior probabilities and therefore being included in the hpd region. This leads to a posterior distribution that is not symmetrical about the mean. As a increases, the hpd region becomes less and less symmetrical about the mean, leading to narrower ranges of σ. However, eventually the range of σ starts to increase again. Figure 3.9 shows the highest contour (where $a = 104$) has the largest range of σ values. This is because the mean of the data and the prior value a assigned for μ are far apart and therefore the posterior distribution

is a flatter distribution with a large variance to compensate for this difference. For example, with the prior value of $a = 104$ for μ, the data could only have come from the distribution with $\mu = a$ if σ is large.

Figure 3.10 shows the robust 95% (μ, σ) Normal Bayesian p-box resulting from the regions shown in Figure 3.8.2.

Figure 3.10: Robust 95% (μ, σ) Normal Bayesian p-box for $n = 10$, $\overline{x} = 98.40$ and $s = 9.51$ (blue), 95% Normal Bayesian p-box (red) and the modal distribution for the non robust case (grey dashed)

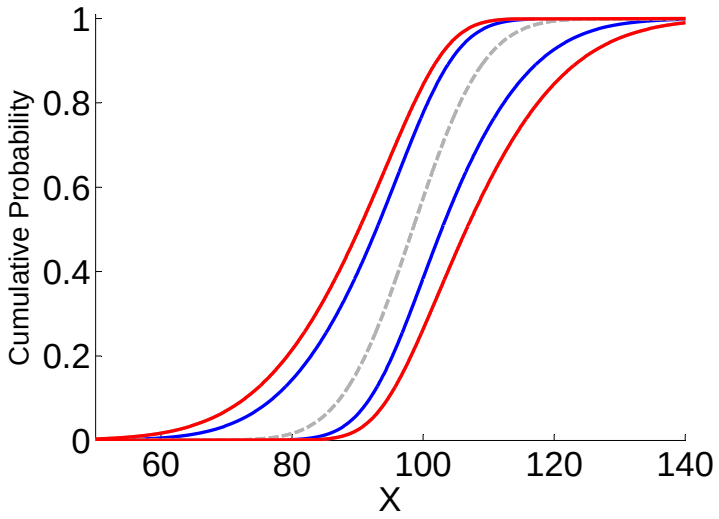

The robust (μ, σ) Normal Bayesian p-box is contained within the Normal Bayesian p-box produced with a non-informative prior distribution, $(p(\mu, \sigma) = \frac{1}{\sigma})$. The non-informative prior distribution allows a large range of different μ and σ values, whereas the set of prior distributions used for robustness leads to the exclusion of some values and thus the range of μ and σ values in $\Theta_s(0.05)$ is narrower. Therefore the distributions that are included in the robust Normal Bayesian p-box have a narrower range than those found using a non-informative prior distribution. This robust Normal Bayesian p-box is approximated because the integration constant must be evaluated numerically.

3.5.5 Imprecise data

There are many practical situations where interval data may arise, some examples are given by Ferson et al. (2007). These include cases where engineers and

other scientists report the uncertainty associated with calibration of their measuring equipment with an interval, gross ignorance where we have no data about a random quantity so we assign theoretical limits, and when numbers are rounded to significant digits. Here we consider the case where data have been provided with an indication of the measurement uncertainty surrounding the values.

Suppose that a data set, $x_1, x_2, ..., x_n$, has a particular measurement uncertainty stated, $\{-\epsilon, +\delta\}$, for $\epsilon, \delta > 0$. This means that the actual value corresponding to a reported measurement x_i is only known to be in the interval $[x_i - \epsilon, x_i + \delta]$ and all values have the same measurement error. To find the 'lowest' Normal distribution (i.e. shifted furthest to the left) that could describe the data, we can take all the values $x_i - \epsilon$, and to find the highest Normal distribution that could describe the data we would take all the values $x_i + \delta$. This follows Manski (2003), where it is stated that if y is observed to lie in $[y_-, y_+]$, then the distribution $P(y_+)$ is a feasible value of $P(y)$ and stochastically dominates all other feasible values of $P(y)$. This means that the cdf of $P(y_+)$ is less than or equal to the cdf of $P(y)$ at any value y. This is the case as $P(y_+)$ has the same shape as $P(y)$ but it is moved further to the right. Similarly the distribution $P(y_-)$ is stochastically dominated by all other feasible values of $P(y)$, as the cdf of $P(y)$ is less than or equal to the cdf of $P(y_-)$ because the cdf of $P(y_-)$ is the cdf of $P(y)$ shifted to the left.

3.5.6 Example: Normal Bayesian p-boxes for imprecise data

A random sample of size $n = 40$ is taken from a Normal distribution with mean 100 and standard deviation 15. The sample statistics are $\overline{x} = 102.31$ and $s = 13.90$. Consider very substantial data imprecision specified by $\delta = \epsilon = 10$. The procedure presented in Subsection 3.3.1 can be used to form a contour using numerical integration for each extreme case of values (i.e. taking all values $x_i - \epsilon$ or $x_i + \delta$) and the original data set. These are presented in Figure 3.11.1. We adjust the values by either adding δ to all the values or subtracting ϵ from all the values so that the sample standard deviation, s, remains the same. Therefore the contours are all the same shape and only the location of the data set is adjusted by ϵ or δ. So it is only necessary to calculate the contour for the original data set and maximise

and minimise over this contour to find lower and upper bounds. Then translate the lower bound by $-\epsilon$ and the upper bound by δ along the x-axis to form the Normal Bayesian p-box including known measurement uncertainty. The resulting Normal Bayesian p-box is shown in Figure 3.11.2 alongside the Normal Bayesian p-box that would have been obtained if data imprecision was ignored.

Figure 3.11: Examples for imprecise data

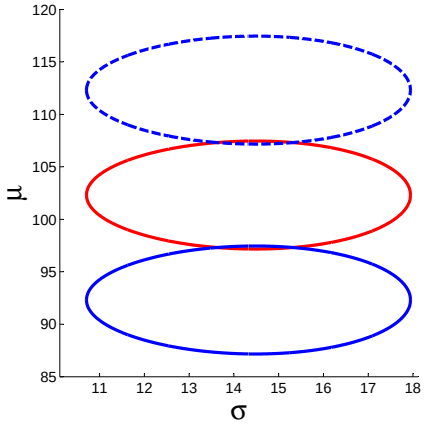

3.11.1 $\Theta_s(0.05)$ regions for $\delta = 10$ (dashed blue), $\epsilon = 10$ (blue) and $\delta = \epsilon = 0$ (red)

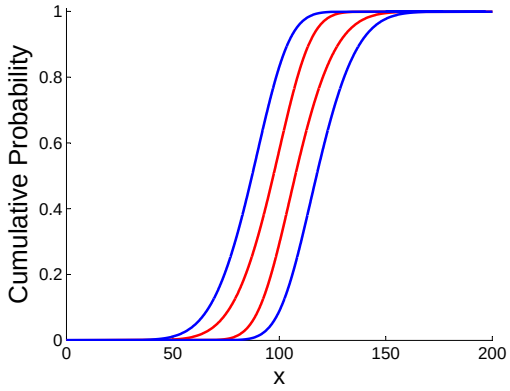

3.11.2 95% Normal Bayesian p-box including measurement uncertainty (blue) with 95% Normal Bayesian p-box without measurement uncertainty (red)

The interval uncertainty may be caused by, for example, known measurement (in)accuracy or rounding of data. If this information is available or can be assessed, then it is easy to incorporate in the analysis. For more complicated cases of data imprecision, for example where the measurement uncertainty is not known exactly, a different approach may be required.

The methods in Subsections 3.5.1 or 3.5.3 could be combined in an analysis with the methods in this section to include both robustness and measurement uncertainty.

3.6 Comparison of different methods

This section compares a parametric Normal frequentist p-box, KS confidence limits, the pointwise Bayesian approach, the Bayesian posterior predictive distribution (all explained in Chapter 2), and the Normal Bayesian p-box approach. Here we construct the frequentist parametric p-box for the Normal distribution using 95%

frequentist confidence intervals for μ and σ (Aughenbaugh and Paredis, 2006).

3.6.1 Example: Comparing methods for small n

For small n, consider a typical data set for avian risk assessment for pesticides. In the European Council Directive 91/414/EEC, it is stated that the acute oral toxicity of an active substance must be determined for either a quail species or the mallard duck. There are typically two species available and the same two are generally used. Suppose that for a certain pesticide, toxicity tests were conducted on these species resulting in median lethal doses (LD50 in mg/kg bw) of 400 (quail) and 2000 (mallard). It is assumed that these two data points come from a Lognormal distribution. The bounds from each method at the 5th percentile are shown in Table 3.4. Figures 3.12.1 and 3.12.2 present the results of the different methods with 95% confidence or credibility levels. In Figure 3.12.2, the modal distribution is omitted so that the median can be clearly seen. The Bayesian posterior predictive distribution gives a 5th percentile of 1.971 mg/kg bw on the $\log_{10}$ scale. In the current legislation for birds, European Commission (2002b), the toxicity-exposure ratio (TER) is found by taking the lowest data point and dividing by an exposure value. This is then compared with a threshold level of 10. So when the TER > 10, the chemical is considered safe. Rearranging the equation shows us that the chemical is considered to be safe if exposure is less than 40 mg/kg bw. On the $\log_{10}$ scale this equates to 1.6 mg/kg bw. This suggests that the current approach is not conservative when compared to the results for the probabilistic methods shown in Table 3.4, because it is not below their lower limits. However it is more conservative than the posterior predictive distribution on the $\log_{10}$ scale (1.971 mg/kg bw). However the approaches shown in Table 3.4 all envelope the current method which indicates that a safe level could be much lower than implied by the current approach.

Table 3.4: Comparison of bounds on 5th percentile in $\log_{10}$ (mg/kg bw)

	Lower	Upper
95% parametric Normal frequentist p-box	-27.43	7.03
95% Normal Bayesian p-box approach	-14.99	3.95
95% KS confidence limits	- ∞	3.3010
95% pointwise Bayesian approach	-23.03	2.82

Figure 3.12: Examples for a small sample size

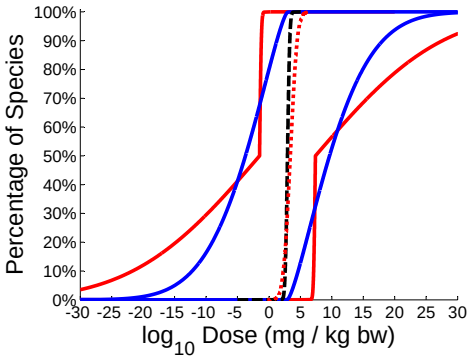

3.12.1 95% parametric Normal frequentist p-box (red), 95% Normal Bayesian p-box (blue), modal disribution (black dashed), Bayesian posterior predictive distribution (red dotted)

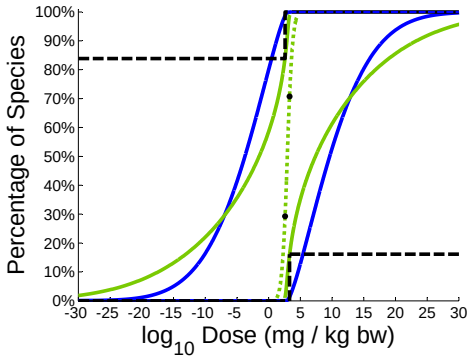

3.12.2 95% Normal Bayesian p-box (blue), 95% KS confidence limits (black dashed), 95% pointwise Bayesian method (green), median distribution (green dotted) and data (black dots)

The values in Table 3.4 appear to be similar because they are given on a $\log_{10}$ scale, but there are actually large differences between the methods. The Normal frequentist p-box method gives wider bounds than the other methods at high and low percentiles. This may be due to the fact that the subspace of Θ in the Normal frequentist p-box method is a rectangle between the smallest and largest μ and σ pairs, whereas in the Normal Bayesian p-box method it is a strictly convex set, here oval-shaped, where the dependence of μ and σ is taken into account. This indicates that ignoring the dependence between parameters leads to wider bounds at the higher and lower percentiles than when dependence is taken into account. If narrower confidence intervals for μ and σ had been chosen, so the rectangular subspace of Θ was enclosed in the Bayesian oval, the Normal frequentist p-box would fall within the Normal Bayesian p-box. At the 50th percentile, it is clear that the Normal frequentist p-box is narrower than the other methods because of the way it is constructed, ignoring dependence between μ and σ. If the frequentist Normal

p-box was constructed using, for example, a joint confidence region for μ and σ, as described in Burmaster and Thompson (1998), it may provide bounds closer to the Bayesian p-box bounds as the joint confidence region is designed to take dependencies between μ and σ into account. However both confidence regions described in Burmaster and Thompson (1998) use approximations. One uses a χ^2 approximation which may not be appropriate for small n, the other uses a Taylor series approximation and it is not clear what effect these approximations will have on the output. The KS confidence limits are based on no assumptions about distribution shape and are very wide to include the large sampling uncertainty due to the small sample size. The lower limit is $-\infty$, although there may be practical reasons to bound this at a particular value.

The lower and upper bounds according to the Bayesian pointwise method are lower, at the 5th percentile, than those based on the Normal Bayesian p-box. This is because in the former method the uncertainty is estimated about the percentile, irrespective of the rest of the distribution, and a scaled non-central t-distribution is used to calculate the bounds. The Normal Bayesian p-box takes the whole distribution into account when finding the bounds as it takes the (μ, σ) pairs from the $100(1-\alpha)\%$ hpd region, whereas the pointwise method finds the $\frac{\alpha}{2}$ and $\frac{(1-\alpha)}{2}$-percentiles of the scaled non-central t-distribution at each percentile.

The 5th percentile of the Bayesian posterior predictive distribution is a prediction for a random individual and produces a single line rather than upper and lower bounds. The Bayesian posterior predictive distribution would be appropriate when a random species is of interest, or it can be used for checking the underlying assumptions of the model (Lee, 2004). This can be done by simulating samples from the Bayesian posterior predictive distribution and comparing these samples with the observed data set. If there are large differences between them this may indicate that the chosen model is not appropriate (Gelman et al., 1995).

Clearly which method should be used depends on whether the specific percentile or the whole distribution is of interest. In practice, it will often be useful to present methods together to get a better picture of the uncertainty and variability involved.

However, the results and the differences between the methods would need to be clearly communicated to risk managers to avoid confusion.

3.6.2 Example: Comparing methods for larger n

We consider a larger data set ($n = 50$) sampled from a Normal distribution with mean 200 and standard deviation 20. The sample statistics are $\overline{x} = 194.71$ and $s = 18.75$. For this n, an approximate Normal Bayesian p-box may be formed by finding $\Theta_s(\alpha)$ using a χ^2 approximation, and maximising and minimising over this. The results from all the methods (assuming $\alpha = 0.05$) are shown in Figures 3.13.1 and 3.13.2.

Figure 3.13: Examples for $n = 50$

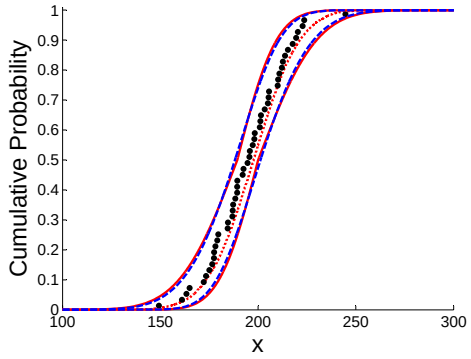

3.13.1 95% Normal frequentist p-box (red), 95% approximate (χ^2) Normal Bayesian p-box (blue dashed), Bayesian posterior predictive distribution (dotted red) and data (black dots)

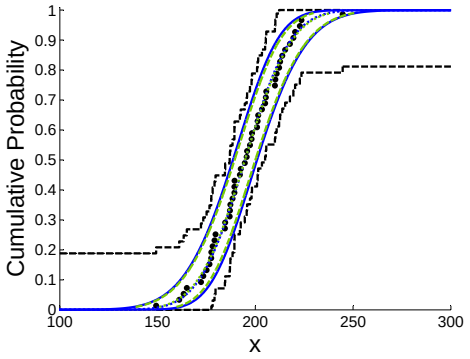

3.13.2 95% Normal Bayesian p-box (blue), 95% KS confidence limits (black dashed), 95% Bayesian pointwise method (green dashed), median distribution (green dotted) and data (black dots)

The Normal frequentist p-box is slightly wider than the Bayesian methods at lower and higher percentiles and narrower at the median, although there is not a large difference. The χ^2 approximation results are close to the Normal Bayesian p-box. As n increases to infinity the bounds will converge to the true distribution (assuming the true distribution was Normal). The Bayesian pointwise method bounds are now enclosed within the Normal Bayesian p-box. These narrower pointwise bounds are due to the shape of the scaled non-central t-distribution with $n - 1$ degrees of freedom. This becomes more peaked and less skewed as n increases and so the percentiles enclosing 95% become narrower. KS confidence limits are particularly

useful when there is no reason to assume any specific distribution, as they provide limits on the empirical distribution function. The Bayesian posterior predictive distribution indicates a prediction for a random individual and is contained within all the other p-boxes shown here. To illustrate the uncertainties involved it is again useful to represent the results from several methods. If a decision is to be made about a population, then methods that form bounds on variability should be used. If a decision is about a random individual from a population then predictive methods should be implemented.

The computation of frequentist parametric p-boxes is not affected by large n, as it only requires intervals for the input parameters. A large n does not cause problems with computation of KS confidence limits because it is a simple calculation based on n and α. The Bayesian posterior predictive distribution is not affected by large n as it uses the sufficient sample statistics. The Bayesian pointwise method becomes slower as n increases and as the number of percentiles evaluated increases. However, even for $n = 1000$, finding the bounds on 1000 percentiles using the pointwise Bayesian method only takes around 45 seconds on a computer with a 1.6Ghz Intel Pentium processor with 1 Gb of RAM. For large samples (say $n > 300$) the time taken to calculate the Normal Bayesian p-box using numerical integration can become prohibitive and the normalising constant becomes large, which complicates the calculations. In such cases, $\Theta_s(\alpha)$ can be easily formed using a χ^2 approximation, as shown by Box and Tiao (1973), and this can then be used to form an approximate Normal Bayesian p-box.

3.7 Dependence

The use of Bayesian p-boxes for more complex models with multiple random quantities is not straightforward. In principle the Bayesian p-box could be used for any random quantity or model, but practically it may be difficult to implement. To calculate Bayesian p-boxes for a more complex model, for example the simple Exposure Model (Section 2.2), requires the calculation of a multi-dimensional posterior distribution and derivation of the corresponding $\Theta_s(\alpha)$. If the posterior distribution has

more than three dimensions, we would need to find a mode and integrate outwards equally in all directions to find the $100(1-\alpha)\%$ hpd space.

A useful tool in probability bounds analysis is the possible combination of different p-boxes using Fréchet bounds, which are computed using a method by Williamson and Downs (1990). This method enables the analyst to combine bounds, such as the pointwise bounds, Bayesian p-boxes, frequentist parametric p-boxes and KS confidence limits when nothing is assumed about dependence between the random quantities. As sometimes little is known about the dependence between random quantities, it is useful to visualise these bounds and compare them to the bounds produced under the assumption of independence, which is often used by default. In many risk assessments the assumption of independence is used, for example by Fan et al. (2005), Chow et al. (2005) and Havelaar et al. (2000), because of a lack of methods that can deal with unknown dependence. In the following example we illustrate the Williamson and Downs method by combining Bayesian p-boxes without making any assumption about dependence. This method may be a way forward for applying Bayesian p-boxes in more complicated models. However, this will provide no information on the modal distribution and only provides a range of values for the probability contained within the final Bayesian p-box, as explained and illustrated in the example below.

3.7.1 Example: Combining random quantities

This example compares the Bayesian p-box formed for the Exposure Model assuming independence between the random quantities, with the Bayesian p-box formed using the Williamson and Downs method (1990). We consider the exposure of young children between 1.5 and 4 years old to benzene in soft drinks with simulated data sets. We take a sample of size 100 from a Normal distribution with mean 20 kg and standard deviation 2 kg for their bodyweight and with mean 1 kg/day and standard deviation 0.2 kg/day for their intake. A sample of size 100 is taken from a Lognormal distribution with mean 4.48 μg/kg and standard deviation 5.87 μg/kg for concentration. The sufficient sample statistics for bodyweight are: $\overline{x} = 20.16$ kg, $s = 2.01$ kg; intake: $\overline{x} = 0.49$ kg/day, $s = 0.10$ kg/day; and Log_{10}(concentration):

$\overline{x} = 0.42$ μg/kg, $s = 0.40$ μg/kg.

The methods described previously are used to calculate the Normal Bayesian p-boxes for each random quantity. Here we calculate 98.3% Normal Bayesian p-boxes so that when we assume independence the final probability within the Bayesian p-box will be $0.983^3 \approx 0.95$. Then these Bayesian p-boxes are combined both by assuming independence (which we call the B_I p-box) and by using Fréchet bounds in the method by Williamson and Downs (which we call the B_F p-box). The results are shown in Figures 3.14.1 and 3.14.2. Figure 3.14.2 is on a $\log_{10}$ scale to show the differences between the methods more clearly.

Figure 3.14: 95% B_I p-box (red) and between 94.91 and 98.3% B_F p-box (blue)

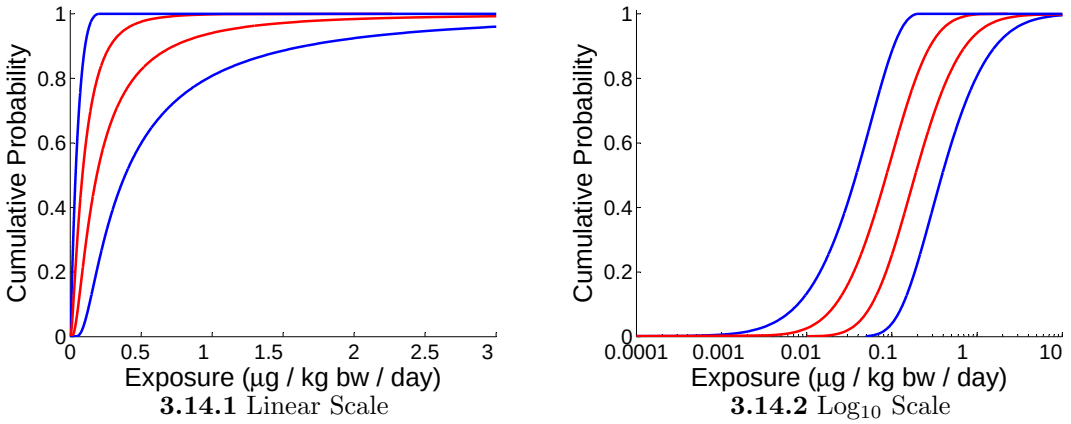

3.14.1 Linear Scale **3.14.2** Log_{10} Scale

The probability within the B_F p-box is between 94.91% and 98.3%. These values are calculated using Fréchet bounds on the probability. The lower and upper bounds for $P(A_1 \,\&\, A_2 \,\&\, A_3)$ (where & indicates the conjunction of events) are $[\max(0,\ a1\ +\ a2 +\ a3 - 2),\ \min(a1, a2, a3)]$ for three events as explained in Subsection 2.11.2, where $a1,\ a2,\ a3$ are the probabilities for the events. In this example the probabilities are the credible levels of the random quantities (e.g. 0.95 for 95%). The 10th, 50th and 90th upper and lower percentiles for both Bayesian p-boxes are given in Table 3.5.

Table 3.5: Upper and lower percentiles for both Bayesian p-boxes (on the linear scale)

Output	50th Percentile		90th Percentile		99th Percentile	
	Lower	Upper	Lower	Upper	Lower	Upper
95% B_I p-box	0.0861	0.1874	0.2812	0.7282	0.6623	2.5334
94.91% - 98.3% B_F p-box	0.0380	0.3872	0.1050	1.6470	0.1651	6.4228

It is clear that assuming independence makes a large difference to the results, although part of the difference is due to the B_F p-box potentially enclosing more probability. The bounds for the B_F p-box will always be at least as wide as those for the B_I p-box, because independence is one of the dependencies that is included in the B_F p-box. Decision makers and risk managers may find it useful to consider both these Bayesian p-boxes so they can see the effect of assuming independence on the inferences. Unfortunately, a modal distribution cannot be found easily when the Bayesian p-boxes have been combined using the Williamson and Downs method. To find the modal distribution, the multi-dimensional posterior probability density function would have to be calculated. The parameter values which combine to provide the highest posterior probability density value would be the mode and the modal distribution would then be the distribution formed with these parameter values.

3.8 Conclusion

There is no best method for the kind of risk assessment discussed in this chapter, it clearly depends on the specific problem considered by the analyst. If a risk manager is interested in the population as a whole, and thus in the entire distribution, it is useful to consider the Bayesian p-box as introduced in this chapter. Nested Bayesian p-boxes can give an analyst or risk manager a clear indication of the changes at different credibility levels. However, if the interest is only in a single percentile, e.g. the 90th percentile exposure, then the pointwise Bayesian method is more appropriate than the Bayesian p-box. This is because the Bayesian pointwise method finds bounds on the uncertainty about percentiles themselves, whereas the

Bayesian p-box takes the parameter values from the $100(1-\alpha)\%$ hpd region and then produces bounds based on the distributions with these parameters.

There are many uncertainties that need to be accounted for in risk analyses including choice of distribution, parameter uncertainty and assumptions on dependence between random quantities. Bayesian p-boxes can deal with the uncertainty of distribution shape by forming separate p-boxes for each possible input distribution. The envelope of all the Bayesian p-boxes can then be taken. The Normal Bayesian p-box includes parameter dependence and parameter uncertainty in the bounds. Robustness can, in principle, be included, but computations may be cumbersome for many distributions. Also the modal distribution can be displayed, as illustrated in examples in this chapter. To account for uncertainty about the dependence between random quantities, the Williamson and Downs method, as mentioned in Section 3.7, can be used on any type of p-box to compare the effect of dependence assumptions. The Bayesian p-box method is versatile in that it can use any strictly convex bounded region of the posterior parameter space to form a Bayesian p-box, using the procedures described in this chapter. A disadvantage of Bayesian methods is that a distributional assumption has to be made.

The KS confidence limits bound the empirical distribution function and make no assumption about distribution shape. Using these limits or other nonparametric p-boxes (Subsection 2.10.1) would be useful in situations where an analyst prefers not to assume a particular distribution. However for small sample sizes these usually lead to wide bounds. The Normal frequentist p-box neglects parameter dependence, and therefore it does not seem reasonable to use these bounds except when alternatives cannot be used because no data are available. A disadvantage of both the Normal frequentist p-box and the KS confidence limits is that they give no indication of how likely any of the distributions within the bounds are.

The Bayesian p-boxes introduced in this chapter provide a means of characterising variability and uncertainty in risk assessment, while avoiding simplistic and often invalid assumptions of independence between parameters. Bayesian p-boxes can contribute to addressing the need for information about the degree of variability and uncertainty in risk estimates (Codex, 2007; Madelin, 2004). This allows risk

managers to take account of the range of possible outcomes in decision-making. In particular, this is useful for support of risk managers in judging when the degree of uncertainty is sufficient to justify precautionary action (European Commission, 2000).

Chapter 4

Nonparametric predictive assessment of exposure risk

4.1 Introduction

Nonparametric Predictive Inference (NPI) is a method that provides lower and upper probabilities for the predicted value(s) of one or more future observation(s) of random quantities. NPI is introduced with references to applications of NPI in Section 2.9. In this chapter we present NPI lower and upper cdfs for the simple Exposure Model that was introduced in Section 2.2. This is the first use of NPI for this type of risk assessment. Currently many of the methods used in exposure risk assessment use parametric probability distributions. Here we consider the application of NPI to assess the exposure of a random individual to a chemical without making any distributional assumptions.

In Section 4.2 we explain how to calculate NPI lower and upper cdfs for random quantities and briefly consider NPI for censored data sets. We explore calculating exposure values for a random individual using the simple Exposure Model for a case study in Section 4.3. Section 4.4 explores how strongly and weakly correlated data affect the NPI lower and upper cdfs by using simulations. We discuss difficulties in computation in Section 4.5 and the effect of different sample sizes in Section 4.6.

We show how to include known measurement uncertainty in an analysis in Section 4.7. Section 4.8 compares NPI with the Bayesian posterior predictive distribution and in Section 4.9 we propose an ad hoc method for robust NPI.

4.2 Nonparametric Predictive Inference

As discussed in Section 2.9, NPI is based on the assumption, $A_{(n)}$, proposed by Hill (1968) for making predictions when there is very vague a priori knowledge about the form of the underlying distribution of a random quantity. The NPI framework is particularly useful because it provides a probability that the predicted value of the next observation of a random quantity will fall in various intervals. NPI also has the advantage that it does not require any further assumptions to be added. NPI includes uncertainty by using interval probability and does not use any information other than that provided by the data. Therefore it gives the best possible bounds without making any assumptions other than $A_{(n)}$ for each random quantity.

In risk assessments for food safety, risk managers could be interested in the distribution for a random individual's exposure to a chemical or the exposure distribution of a population to a chemical. As introduced in Section 2.2, a simple way to calculate exposure is by the Exposure Model:

$$\text{Exposure} = \frac{\text{Intake} \times \text{Concentration}}{\text{Bodyweight}}$$

NPI provides predictive probabilities for an individual. Although we do not consider it further in this thesis, NPI could be used if individuals would like to predict their own exposure. This can be done by taking their own intakes of a food type, their own bodyweight and a data set of concentrations for a particular chemical in the food type. The NPI lower and upper probabilities based on their own data can then be formed following the procedure presented in Subsection 4.2.2. The probability in the intervals between the calculated exposure values for one person will then be $[(n_c+1)(n_i+1)(n_{bw}+1)]^{-1}$, where n_c is the size of the concentration data set, n_i is the size of the intake data set and n_{bw} is the size of the bodyweight data set (which is 1), assuming there are no ties in any of the data sets and no ties in the

exposure values that are calculated. Combining these lower and upper probabilities leads to NPI lower and upper cdfs for the individual's exposure. This could easily be extended to take concentrations of a chemical in multiple food types into account. Next we look at an example of calculating NPI for one random quantity and then an example for calculating NPI lower and upper cdfs for Exposure.

4.2.1 Example: NPI for a single random quantity

To calculate the tightest lower and upper bounds on the cumulative distribution function (cdf) of a random quantity corresponding to the assumption $A_{(n)}$, we form lower and upper cdfs ($\underline{F}$ and $\overline{F}$ respectively) for the probability that the next value will fall in the intervals formed by the observed values. As a brief example, suppose we have an ordered data set $\{2, 2, 4, 5, 6\}$ for positive random quantities $X_i, i = 1, ..5$. Following $A_{(5)}$, the lower and upper cdfs can be calculated as explained in Subsection 2.9.2 where the set B is $(-\infty, x]$. where $x \in (0, \infty)$. The M function for X_6 is:

$$\begin{array}{lcllcl} M_{X_6}(0,\ 2) & = & 1/6 & M_{X_6}(4,\ 5) & = & 1/6 \\ M_{X_6}\ (2) & = & 1/6 & M_{X_6}(5,\ 6) & = & 1/6 \\ M_{X_6}(2,\ 4) & = & 1/6 & M_{X_6}(6, \infty) & = & 1/6 \end{array}$$

The lower and upper cdfs for X_6 can be plotted as shown in Figure 4.1. The final value of the lower cdf for X_6, $\underline{F}_{X_6}(x)$, is $\frac{5}{6}$, for $x > x_5$.

Figure 4.1: NPI lower and upper cdfs

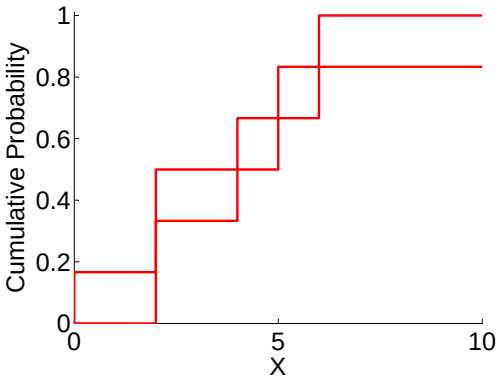

As n tends to ∞, the NPI lower and upper cdfs converge to the empirical distribution function of the data. The cdf of the empirical distribution function, F_e, will always lie in $[\underline{F}_{X_{n+1}}(x), \overline{F}_{X_{n+1}}(x)]$ for all x, where n is the number of observations.

4.2.2 Example: NPI for the Exposure Model

Now we look at calculating NPI lower and upper cdfs for the Exposure Model that was described in Section 2.2. Assume we have ordered observations x_1, x_2, for the random quantities X_1 and X_2 respectively. Then $n_x = 2$ is the total number of observations and we have intervals $(0, x_1)$, (x_1, x_2), (x_2, ∞). Assuming $A_{(2)}$, the probability that the next observation falls in any of these intervals is $\frac{1}{n_x+1} = \frac{1}{3}$. Assume we also have ordered observations y_1, y_2, y_3 for random quantities Y_1, Y_2, and Y_3 respectively and $n_y = 3$ is the total number of observations. This leads to intervals $(0, y_1), (y_1, y_2), (y_2, y_3), (y_3, \infty)$ and assuming $A_{(3)}$, the probability that the next observation falls in any of these intervals is $\frac{1}{n_y+1} = \frac{1}{4}$. Taking the product of the intervals for the random quantities X_3 and Y_4, leads to 12 intervals each with probability $\frac{1}{12}$, assuming there are no ties, for the random quantity that we call XY_{new}. We combine the intervals by multiplying the minimum values of each interval for X_3 with the minimum values of each interval for Y_4 and the maximum values of each interval for X_3 with the maximum values of each interval for Y_4. For example to multiply (x_1, x_2) with (y_1, y_2), we multiply x_1 with y_1 and x_2 with y_2 to form the interval (x_1y_1, x_2y_2). Notice that this is the widest the interval can be, as combining the other endpoints, e.g. y_2 with x_1 will always produce values that fall in this interval due to their ordering. Now assume we have ordered observations z_1, z_2 for random quantities Z_1 and Z_2 respectively. Assuming $A_{(2)}$, the probability that the next observation falls in any of the intervals $(0, z_1)$, (z_1, z_2), (z_2, ∞) is $\frac{1}{3}$. Combining the random quantities X_3, Y_4 and Z_3 in the Exposure Model leads to 36 intervals each with probability $\frac{1}{36}$ assuming there are no ties. The M function for the predicted value of the next observation, $\frac{XY}{Z}_{new}$, is shown below, where $\exp_j$ represents the jth ordered value that forms the intervals for $\frac{XY}{Z}_{new}$, and $j = 1, ..., 34$.

$$\begin{aligned} M_{\frac{XY}{Z}_{new}}(0,\ \exp_1) &= 1/36 \\ M_{\frac{XY}{Z}_{new}}(\exp_j, \exp_{j+1}) &= 1/36 \\ M_{\frac{XY}{Z}_{new}}(\exp_{35},\ \infty) &= 1/36 \end{aligned}$$

The NPI lower and upper cdfs are formed as explained in Subsection 2.9.2.

4.2.3 NPI for left-censored data

The distribution of probability mass for a data set with left-censored values (explained in Section 2.4) can also be represented using M functions. It is often the case with concentration data that there is a limit of detection (LOD) below which concentration of chemicals cannot be measured. This leads to left-censored data where some values are reported as $<$ LOD. The censoring will be between 0 and the LOD because concentration cannot be negative.

Example: NPI lower and upper cdfs for left-censored data

Assume that the LOD is 1 and we have an ordered data set $\{x_1, x_2, x_3, x_4\}$ for concentration and x_1 is a censored value that is between 0 and 1. The uncertainty about the value of x_1 can be represented by overlapping intervals in the M function, which takes into account that the censored value may be 0, or any value between 0 and 1. So the partial description of probability mass for a new observation X_5, based on $A_{(4)}$, can be represented as below:

$$\begin{aligned} M_{X_5}(0\ ,\ \ 1) &= 1/5 \quad M_{X_5}(x_3,\ x_4) = 1/5 \\ M_{X_5}(0,\ \ x_2) &= 1/5 \quad M_{X_5}(x_4,\ \infty) = 1/5 \\ M_{X_5}(x_2,\ x_3) &= 1/5 \end{aligned}$$

The NPI lower and upper cdfs calculated from this M function will describe the tightest possible bounds given the information we have available and $A_{(4)}$. Figure 4.2 shows the NPI lower and upper cdfs for this example.

Figure 4.2: NPI lower and upper cdfs for X_5

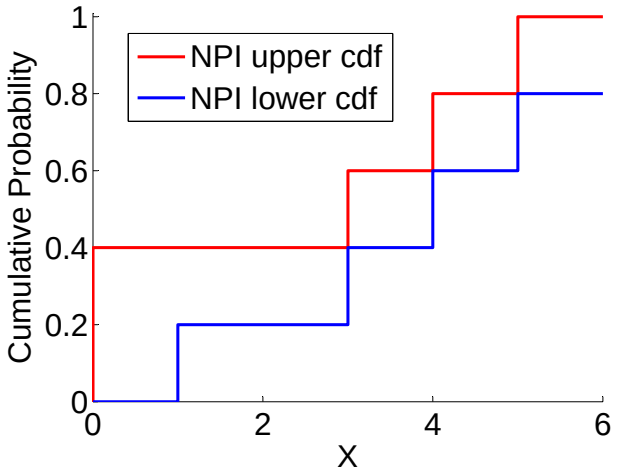

There is a problem that if, for example, the censored value happened to be 0.2, then the intervals $(0, 0.2)$ and $(0.2, x_2)$ should each have probability mass $\frac{1}{5}$ rather than the probability masses assigned to the intervals in the previous M function. However, without knowing anything more than the censored value is less than 1, the tightest bounds given $A_{(4)}$ and the censoring are represented by the M function given previously. The bounds will enclose the possible lower and upper cdfs that would correspond to all possible values of x_1.

We are interested in the exposure of individuals to a particular chemical. Although it is informative to see how much uncertainty in the exposure is caused by the censored concentration values, often the risk associated with exposure is based on upper tail exposures. This is because higher exposures to chemicals are generally more harmful than low exposures. Since the left-censored concentration values only contribute to the lower tail of the exposure distribution, they are generally considered to be less important in risk assessments. However if the LOD is large, or the safe exposure level is very low, the censoring may contribute substantially making it useful to be able to form such lower and upper cdfs for a random individual.

4.3 Case Study: Benzene Exposure

In this section we show how to calculate NPI lower and upper cdfs for the Exposure Model where we have data for the exposure of young children to benzene in soft drinks. We have data for each of the three non-negative random quantities, concentration, intake and bodyweight. A description of the data sets that we will use for the analysis is given in Subsection 4.3.1. We calculate the NPI lower and upper cdfs for exposure for a random individual, for two different cases and then we compare them. First we consider the case where we calculate NPI lower and upper cdfs for exposure for a random individual, for the three random quantities separately. Then, for the second case, we combine each individual's bodyweight with their average intake and treat this as one random quantity which we call IR. We then calculate the NPI lower and upper cdfs for exposure for a random individual, using the two random quantities, concentration and IR.

4.3.1 The data

Concentration data for benzene in soft drinks were obtained from the Food Standards Agency Survey from March 2006[1]. Out of 150 samples, 109 were below the Limit Of Detection (LOD) of 1 μg/kg. Assuming $A_{(150)}$, the probability of the next observation of benzene concentration falling in the interval $(0, 1)$ is $\frac{122}{151}$. Usually the probability of X_{151} falling in the interval $(0, 1)$ would be $\frac{109}{151}$ but here the lowest measured datum that is not censored is equal to the LOD. Therefore there is a probability of $\frac{110}{151}$ that X_{151} falls in the interval $(0, 1)$. The concentration data is given in Table 4.1.

[1] http://www.food.gov.uk/science/surveillance/fsisbranch2006/fsis0606

Table 4.1: Concentration data

Data value	Frequency	Data value	Frequency
< 1	109	7	4
1	13	8	1
2	13	9	1
3	3	10	1
4	3	23	1
5	1		

Intake and bodyweight data were obtained from the UK Data Archive Study No. 3481. National Diet, Nutrition and Dental Survey of Children Aged 1.5 - 4.5 years (1992 - 1993)[2]. It is a 4 day survey of 1717 children giving information about their weight, food and drink intake and other covariates such as age, height, region and social class. Only individuals with no missing values (i.e. individuals with intake values for every day of the survey and a recorded bodyweight) were used in the analysis. We excluded 23 individuals, whose bodyweights were not recorded, leaving us with data for 1694 individuals. Omitting these individuals from the analysis may lead to bias, particularly if they all had large or small bodyweights. Also, if they were heavy consumers of soft drinks then their exposure may be higher than the exposure of the general population. However their average intakes of drink were between 0.025 kg/day and 0.418 kg/day compared with the minimum of 0 kg/day and maximum of 1.239 kg/day for all the other individuals, so it is unlikely that they would lead to higher exposures than individuals that are included unless they have very small bodyweights.

As an illustration of the use of NPI in risk assessment we include non-consumers in the analysis and consider the average intake over the 4 days of the survey. We can only make inferences about the random quantities that we have data for. Therefore the conclusions reached can only be predictions for the average exposure for a random individual on the particular four days of the survey. They cannot provide any information about the exposure of an individual for the rest of the year.

As we have bodyweight and average intake values for each individual it is possible to treat bodyweight and average intake as separate random quantities and generate

[2]http://www.esds.ac.uk/findingdata/snDescription.asp?sn=3481&key=coding

NPI lower and upper cdfs based on this assumption. This is presented in the next section. However, it is generally believed that bodyweight and average intake are dependent on each other. Therefore we also consider using IR as a random quantity. This loses some information as we no longer separate the random quantities, average intake and bodyweight, but it does naturally include dependencies between these random quantities. The differences caused by using IR are discussed in Subsection 4.3.2. We use the average intake over the 4 days of the survey throughout this chapter so for ease of presentation we will henceforth refer to this as 'intake'.

4.3.2 NPI lower and upper cdfs

In this example we derive NPI lower and upper cdfs for exposure for a random individual using the data sets that were described in the previous section. We compare the results of treating all three random quantities separately, which we will call the 'independent case', and using the IR, which we will call the 'dependent case'. It is interesting to look at both cases, although using IR has the advantage that it takes dependencies between intake and bodyweight into account. For the situation where all the random quantities are assumed to be independent, we first calculate the NPI lower and upper cdfs for the exposure as described in Subsection 4.2.2. In the second situation we calculate the IR and then calculate the NPI lower and upper cdfs on the product of concentration and IR.

To calculate the NPI lower and upper cdfs for exposure for a random individual, we first add a minimum and a maximum to each data set. For concentration and intake, zero and ∞ are appropriate. However for bodyweight we use 1e-15 and ∞ as we cannot divide by zero.

For the independent case, we have ties at 135 bodyweight values and 1194 intake values, both from an original sample size of 1694. The tied values from the original data set and their frequency of occurrence are stored and the correct probability is assigned to the tied values themselves or to the intervals if the value is not tied. Working with the tied values speeds up computation and avoids problems with computer memory (computational issues are discussed in Section 4.5). First we look at a scatterplot of bodyweight and intake to see if there appears to be any

correlation between them. The scatterplot is shown in Figure 4.3.

Figure 4.3: Scatterplot of Intake versus Bodyweight

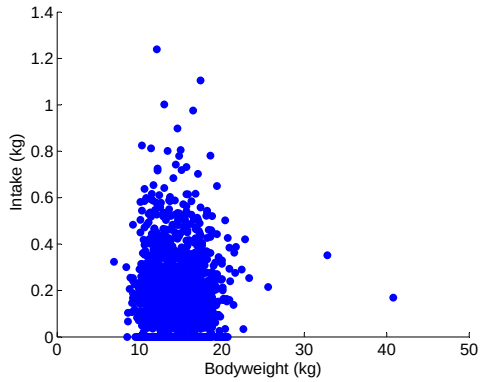

The scatterplot does not show any obvious correlation between bodyweight and intake. To check the strength of correlation we consider Spearman's rank correlation coefficient which ranges between -1 and 1, where -1 indicates a very strong negative correlation and 1 indicates a very strong positive correlation. Around zero indicates very weak correlation. Spearman's rank correlation coefficient is -0.0071, indicating a weak negative correlation between bodyweight and intake. The weak correlation suggests that there is no strong dependence between the random quantities.

Figure 4.4.1 shows the NPI lower and upper cdfs for exposure for a random individual for both cases. Part of the upper tail is displayed in more detail in Figure 4.4.2 to show the differences between the two cases. It is clear that the dependent case resembles a step function more closely than the independent case. This is due to the smaller number of exposure values generated in the dependent case which leads to fewer steps with larger jumps at many values. The independent case has many more exposure values so it appears to be much smoother, but it is still a step function, with small jumps at several values.

Figure 4.4: NPI lower and upper cdfs for a random individual

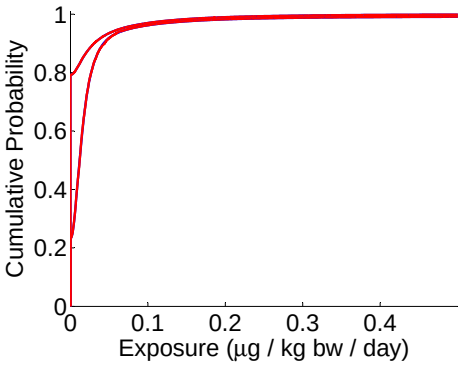

4.4.1 NPI lower and upper cdfs for the independent case (blue line) and the dependent case (red line) on a linear scale

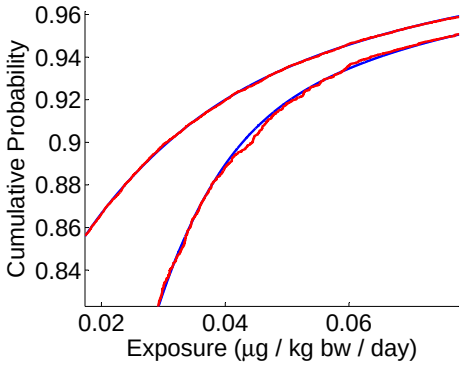

4.4.2 A close up of part of the NPI lower and upper cdfs for the independent case (blue line) and the dependent case (red line)

There is not much difference between the results from the independent and dependent cases. There are small differences at some exposure values and neither set of NPI lower and upper cdfs is enclosed within the other. One observable difference is that the final value of the lower cdf for independence (0.9922) is lower than the final value of the lower cdf for the dependent case (0.9928). The difference in the final value of the lower cdfs might be informative for an individual and may be useful for risk managers to see how much dependence is influencing the results. The difference is due to the larger number of data values combined in the independent case where bodyweight and intake are combined separately. In the dependent case intake is divided by bodyweight and then the resulting values combined with concentration values leading to fewer exposure values. Therefore in the M function for exposure for a random individual, M_{exp}, there is a larger probability mass in $M^{(3)}_{\text{exp}}(\text{exp}_N, \infty)$ (where $M^{(i)}_{\text{exp}}(\text{exp}_N, \infty)$ represents the M function value for the interval between the highest exposure value and ∞ for exposure for a random individual, calculated using i random quantities) than in $M^{(2)}_{\text{exp}}(\text{exp}_N, \infty)$.

For the case where we use IR the final value of the lower cdf is given by

$$1 - \frac{(n_c + 1 + n_{IR})}{(n_c + 1)(n_{IR} + 1)} = 0.9928 \tag{4.1}$$

as $M^{(2)}_{\text{exp}}(\text{exp}_N, \infty) = \frac{(n_c+1+n_{IR})}{(n_c+1)(n_{IR}+1)}$, where n_c is the concentration sample size (here 150) and n_{IR} is the IR sample size (here 1694). Similarly in the independent case $M^{(3)}_{\text{exp}}(\text{exp}_N, \infty) = \frac{((n_c+1+n_{int})n_{bw}+(n_c+1)(n_{int}+1))}{(n_c+1)(n_{int}+1)(n_{bw}+1)}$ so the final value of the lower cdf in this case is

$$\left(1 - \frac{((n_c + 1 + n_{int})n_{bw} + (n_c + 1)(n_{int} + 1))}{(n_c + 1)(n_{int} + 1)(n_{bw} + 1)}\right) = 0.9922 \tag{4.2}$$

where n_{bw} is the bodyweight sample size (here 1694) and n_{int} is the intake sample size (here 1694) and as before n_c is the concentration sample size (here 150).

4.4 Exploring dependence for NPI by simulation

We keep X (in μg / kg) as a fixed sample from a Lognormal distribution with mean, $\mu_x = 1.5$ and standard deviation, $\sigma_x = 2.8$. We consider the effect of varying the correlation between Y (in kg /day), which we assume to have a Lognormal distribution with mean, $\mu_y = 1.27$ and standard deviation, $\sigma_y = 1.03$ and Z (in kg), which we assume to have a Normal distribution with mean, $\mu_z = 30$, and standard deviation, $\sigma_z = 3$. We consider 1000 simulations for two values of n (50 and 100) and we vary ρ between -1 and 1. The exposure percentiles are estimated by taking very large samples (1,000,000) from the relevant distributions and combining them as in the simple Exposure Model. Then we take the 10th, 50th and 90th percentiles for comparison purposes and call them the true exposure percentiles. We compare the 10th, 50th and 90th percentiles from the independent and dependent NPI methods with the true exposure percentiles. We count how many times the true exposure percentiles fall in the intervals generated by the dependent and independent NPI.

We also consider whether the NPI methods over- or underestimate the true exposure percentile.

4.4.1 Varying n

In this section we consider two different values of n and then compare how well NPI predicts for 1000 samples for each of these n. The results for $n = 50$ are shown in Table 4.2. The results for $n = 100$ are shown in Table 4.3.

Table 4.2: Results from 1000 simulations when $n = 50$

ρ	Method		Percentile		
			10th	50th	90th
1	Dependent	Success	719	351	350
		Underestimates	233	256	1
		Overestimates	48	393	649
0.5	Dependent	Success	651	348	360
		Underestimates	273	246	9
		Overestimates	76	406	631
0	Dependent	Success	654	365	380
		Underestimates	278	218	8
		Overestimates	68	417	612
-0.5	Dependent	Success	655	375	404
		Underestimates	287	220	8
		Overestimates	58	405	588
-1	Dependent	Success	582	308	396
		Underestimates	336	258	26
		Overestimates	82	434	578
1	Independent	Success	478	571	172
		Underestimates	522	138	0
		Overestimates	0	291	828
0.5	Independent	Success	617	560	278
		Underestimates	383	151	0
		Overestimates	0	289	722
0	Independent	Success	759	549	422
		Underestimates	240	144	0
		Overestimates	1	307	578
-0.5	Independent	Success	871	567	592
		Underestimates	126	144	0
		Overestimates	3	289	408
-1	Independent	Success	857	461	679
		Underestimates	130	195	6
		Overestimates	13	344	315

Table 4.3: Results from 1000 simulations when $n = 100$

ρ	Method		Percentile		
			10th	50th	90th
1	Dependent	Success	687	351	269
		Underestimates	206	221	4
		Overestimates	107	428	727
0.5	Dependent	Success	673	337	280
		Underestimates	225	217	6
		Overestimates	102	446	714
0	Dependent	Success	653	352	284
		Underestimates	244	189	4
		Overestimates	103	459	712
-0.5	Dependent	Success	629	340	283
		Underestimates	271	208	6
		Overestimates	100	452	711
-1	Dependent	Success	546	273	329
		Underestimates	339	241	28
		Overestimates	115	486	643
1	Independent	Success	348	498	49
		Underestimates	652	126	0
		Overestimates	0	376	951
0.5	Independent	Success	626	489	156
		Underestimates	372	129	0
		Overestimates	2	382	844
0	Independent	Success	777	488	310
		Underestimates	212	120	1
		Overestimates	11	392	689
-0.5	Independent	Success	865	487	541
		Underestimates	97	146	3
		Overestimates	38	367	456
-1	Independent	Success	784	394	653
		Underestimates	98	187	30
		Overestimates	118	419	317

Generally the 10th percentile is captured best by both methods regardless of n. The general trend for the dependent case is that as ρ decreases from 1 to -1, the dependent method captures the 10th percentile less often. The trend is less clear in the independent case as the 10th percentile is captured more often as ρ decreases from 1 to 0 but increases for $\rho = -0.5$ and decreases again for $\rho = -1$. As n increases the percentage of times that the 10th percentile is captured, by both methods, decreases slightly. This is probably due to the narrowing of the intervals

in the NPI lower and upper cdfs because of the larger data samples used. Both methods appear to underestimate the 10th percentile more than they overestimate it, for both n, except for the independent case where $\rho = -1$ and $n = 100$. Here the overestimates are slightly higher than the underestimates. This is probably due to the gradient of the exposure distribution when ρ is negative as discussed later.

The 50th percentile is captured between 27.3 and 37.5% of the time for the dependent method and between 39.4 and 57.1% of the time for the independent method. There is the same general trend as with the 10th percentile, that as n increases the percentage of times that the 50th percentile is captured decreases slightly. There is a general trend in the independent case that as ρ decreases from 1 to -1, the 50th percentile is captured fewer times, although again $\rho = -0.5$ performs better than $\rho = -1$. For the dependent case the results are similar for different values of ρ although $\rho = -1$ leads to the lowest percentage of times that the 50th percentile is captured. Again this is probably due to the gradient of the exposure distribution at different values of ρ. Generally the 50th percentile is overestimated more than it is underestimated.

The 90th percentile is captured between 26.9 and 40.4% of the time for the dependent case whereas it is captured between 4.9 and 67.9% of the time by the independent case. For the dependent case there is a general trend that the 90th percentile is captured more often as ρ decreases from 1 to -1, regardless of n. However for $n = 50$ there is a decrease from 40.4% for $\rho = -0.5$ to 39.6% for $\rho = -1$. This decrease does not occur when $n = 100$ so it is probably due to sampling variation. Both the dependent and independent methods generally overestimate the 90th percentile, particularly the independent case which does not underestimate the 90th percentile for most of the results in this example. The cases where the independent method does underestimate the 90th percentile are generally at negative rank correlations. This is explained by the gradient of the exposure distribution for negative values of ρ as discussed below.

When $\rho = 1$, the gradient of the exposure distribution at low percentiles is lower than the gradient of the exposure distribution when $\rho = -1$. At higher percentiles this is reversed and the gradient of the exposure distribution when $\rho = 1$ is higher

than the gradient when $\rho = -1$. This means that the exposure distribution when $\rho = -1$ is much flatter and spread out than the exposure distribution for $\rho = 1$. The exposure distributions for each value of ρ are shown in Figure 4.5.1 on a log scale. Figure 4.5.2 shows a close up of the lower half of the distributions. The independent NPI tends to underestimate the 10th percentile and overestimate the 90th percentile. This is because it allows every combination of values for X, Y and Z ignoring any dependency between them. Therefore the smallest values are divided by the largest values and the largest values are divided by the smallest values regardless of the specified rank correlation. This leads to a flat distribution where the values are spread out.

In the dependent case this does not happen because, for example, if $\rho = 1$, then the smallest value of Y will be divided by the smallest value of Z and the largest value of Y will be divided by the largest value of Z. Similarly for $\rho = -1$, the smallest value of Y will be divided by the largest value of Z etc. Therefore there are fewer values in the dependent case and there are less extreme values compared to the independent case. The independent case appears to perform better on the negative correlation than the positive correlation. This is probably because the lower predictions for the 10th percentile and higher predictions for the 90th percentile mean the NPI upper and lower cdfs do not increase steeply. Therefore the cdf more closely resembles that of the cdf when $\rho = -1$ than the cdf when $\rho = 1$.

The dependent case appears to be an improvement on the independent case for positive correlations, but not for the zero rank correlation. As the dependent case is taking the rank correlation into account, we would expect the dependent case to be better than the independent case for correlated data but not for uncorrelated data (i.e. when $\rho = 0$). However we would also expect the dependent case to perform better for the negative correlations which it does not appear to do. The dependent case considers fewer values as it only uses the data for X and $\frac{Y}{Z}$, whereas the independent case uses all the data for X, Y and Z separately. Therefore the dependent case not performing as well as the independent case may be due to the independent case having cdfs that more closely resemble the cdf of the case with negative correlation. The dependent case has less values with higher probability and

grows more steeply, which is closer to the positive correlation case.

Figure 4.5: Exposure distributions with various values for ρ

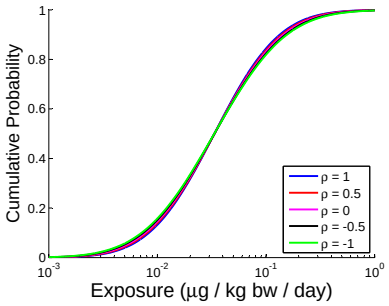

4.5.1 Exposure distribution with varying ρ

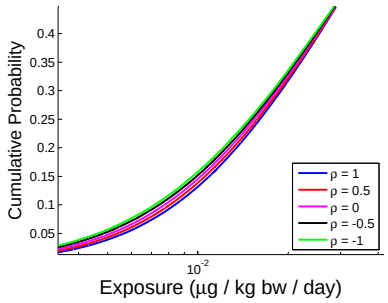

4.5.2 Close-up of exposure distribution with varying ρ

4.4.2 Varying μ_z and σ_z

In this section we only consider samples of size 50 and we take $\rho = 1$ and $\rho = -1$. We vary σ_z first while keeping μ_z fixed and then we consider the case where we fix σ_z and vary μ_z.

Varying σ_z

We begin by keeping μ_z fixed at 30, while taking σ_z to be 5 and 7. The results for $\rho = 1$ are shown in Table 4.4 and the results for $\rho = -1$ are shown in Table 4.5. We re-use the results from Table 4.2 above where $\sigma_z = 3$.

Table 4.4: Results from 1000 simulations with $\sigma_z = 3$, 5 and 7 and $\rho = 1$

σ_z	Method		Percentile		
			10th	50th	90th
3	Dependent	Success	719	351	350
		Underestimates	233	256	1
		Overestimates	48	393	649
5	Dependent	Success	787	389	342
		Underestimates	180	237	0
		Overestimates	33	374	658
7	Dependent	Success	546	397	228
		Underestimates	450	280	1
		Overestimates	4	323	771
3	Independent	Success	478	571	172
		Underestimates	522	138	0
		Overestimates	0	291	828
5	Independent	Success	232	630	41
		Underestimates	768	83	0
		Overestimates	0	287	959
7	Independent	Success	95	618	20
		Underestimates	905	128	0
		Overestimates	0	254	980

For $\rho = 1$ we can see that increasing σ_z from 5 to 7 leads to lower success rates for the 10th and 90th percentiles for the dependent case. The 50th percentile for both cases was fairly consistent because the 50th percentile does not depend on σ_z as much as the tails of the distribution do. The independent case shows a very clear decrease in success rates for the 10th and 90th percentiles as σ_z varies from 3 to 7. Also the 10th percentile is always underestimated and the 90th percentile is always overestimated (in this example). This is expected because as we saw earlier the NPI independent case combines every possible combination of all the data values. As σ_z increases, the spread of exposure values increases leading to flatter NPI lower and upper cdfs. At the same time, as σ_z increases, the true exposure distribution becomes a steeper distribution. Therefore we would expect that the independent case performs better for smaller σ_z. The dependent case performs better than the independent case. This is probably because it takes the rank correlation into account so the NPI lower and upper cdfs do not become as flat as in the independent case.

Table 4.5: Results from 1000 simulations with σ_z = 3,5 and 7 and $\rho = -1$

σ_z	Method		Percentile		
			10th	50th	90th
3	Dependent	Success	582	308	396
		Underestimates	336	258	26
		Overestimates	82	434	578
5	Dependent	Success	566	276	367
		Underestimates	319	252	47
		Overestimates	115	472	586
7	Dependent	Success	600	303	550
		Underestimates	241	297	143
		Overestimates	159	400	307
3	Independent	Success	857	461	679
		Underestimates	130	195	6
		Overestimates	13	344	315
5	Independent	Success	879	419	747
		Underestimates	75	191	20
		Overestimates	46	390	233
7	Independent	Success	886	445	827
		Underestimates	40	226	101
		Overestimates	74	329	72

For $\rho = -1$, we see the reverse situation from $\rho = 1$, where the success rates for the 10th and 90th percentiles improve as σ_z increases, although the difference is not as large as it was for the independent case for $\rho = 1$. The independent case improves slightly as σ_z increases. This is again because the independent case produces a flatter distribution due to the larger spread of exposure values for increased σ_z. As σ_z increases, the true exposure distribution becomes flatter. Therefore we would expect that the independent case performs better for larger σ_z.

Varying μ_z

Here we keep $n = 50$, $\rho = 1$ and $\rho = -1$, we fix σ_z to be 3 and take μ_z to be 20 and 40. The results are shown in Table 4.6 for $\rho = 1$ and in Table 4.7 for $\rho = -1$. We re-use the results from Table 4.2 where $\mu_z = 30$ and $\sigma_z = 3$.

Table 4.6: Results from 1000 simulations with $\mu_z = 20$, 30 and 40 and $\rho = 1$

μ_z	Method		Percentile		
			10th	50th	90th
20	Dependent	Success	745	367	338
		Underestimates	228	248	4
		Overestimates	27	385	658
30	Dependent	Success	719	351	350
		Underestimates	233	256	1
		Overestimates	48	393	649
40	Dependent	Success	666	341	360
		Underestimates	295	231	6
		Overestimates	39	428	634
20	Independent	Success	255	608	75
		Underestimates	745	102	0
		Overestimates	0	290	925
30	Independent	Success	478	571	172
		Underestimates	522	138	0
		Overestimates	0	291	828
40	Independent	Success	529	545	246
		Underestimates	471	143	0
		Overestimates	0	312	754

Table 4.7: Results from 1000 simulations with $\mu_z = 20$, 30 and 40 and $\rho = -1$

μ_z	Method		Percentile		
			10th	50th	90th
20	Dependent	Success	559	298	396
		Underestimates	341	276	39
		Overestimates	100	426	565
30	Dependent	Success	582	308	396
		Underestimates	336	258	26
		Overestimates	82	434	578
40	Dependent	Success	581	293	375
		Underestimates	328	263	23
		Overestimates	91	444	602
20	Independent	Success	891	434	753
		Underestimates	80	212	19
		Overestimates	29	354	228
30	Independent	Success	857	461	679
		Underestimates	130	195	6
		Overestimates	13	344	315
40	Independent	Success	838	468	615
		Underestimates	156	180	2
		Overestimates	6	352	383

We would not expect that increasing μ_z would have a large influence on the results because increasing μ_z only affects the location of the exposure distribution. This is particularly true for the dependent case because there is little variance in the results as μ increases for both values of ρ. It is also the case for the independent case when $\rho = -1$, where there are only small differences in the number of successes for each percentile at different values of μ_z. The results for the independent case are better for $\rho = -1$ than for $\rho = 1$, whereas for the dependent case the results are better for $\rho = 1$. This was expected given the results discussed previously. For $\rho = 1$, the success rate of the 10th and 90th percentiles for the independent case improves as μ_z increases. This is probably due to the NPI lower and upper cdfs becoming steeper and therefore closer to the true exposure distribution as μ_z increases.

4.4.3 Discussion

In this example, i.e. for a division, we have seen that the dependent case appears to perform better for positive rank correlations, whereas the independent case appears to perform better for negative correlations and correlations equal to zero. Varying σ_z and varying μ_z also affected the results in the ways described above. We have counted how many intervals overestimated or underestimated the true percentiles but not given an indication of how much they over- or underestimate by. Generally, the independent case underestimated the 10th percentile, or overestimated the 90th percentile by more than the dependent case. This is because the independent case does not account for the specified correlation so it produces flatter distributions.

We would not expect predictive methods to produce exact predictions based on samples such as those used in these examples. If we used different predictive methods, e.g. the Bayesian posterior predictive distribution, the results would be dependent on distributional assumptions and how well the sample represents the distribution that it has been sampled from. As seen in Chapter 5, both NPI and the Bayesian posterior predictive distribution can produce good predictions and poor predictions depending on the samples and the distributions that are sampled from.

Here we used 1,000 simulations to try and allow for sampling variation. Sampling variation will strongly affect the NPI results for small samples because it only uses the samples and an assumption of $A_{(n)}$ for the analysis. For larger samples there will be less effect from sampling variation (as illustrated in Chapter 5), but the NPI intervals become narrower. Therefore the NPI lower and upper cdfs for smaller samples may perform better (as we saw in our example) because the intervals are wider and include more uncertainty about the exposure percentiles so it is more likely that they will enclose the true percentiles.

4.5 Computational issues

In this section we briefly discuss some computational problems that arise when modelling NPI with large data sets. The large number of values in the intake and bodyweight data sets described in Subsection 4.3.1 led to problems with computer memory as we needed to store all the possible combinations of all the values of all three data sets. As the data sets were $n_c = 150$, $n_{int} = 1694$ and $n_{bw} = 1694$ in length (and adding a minimum or maximum depending on which cdf we consider) this leads to $(n_c + 1)(n_{int} + 1)(n_{bw} + 1) = 433,826,775$ values for each cdf. These need to be stored along with the cumulative probabilities for each interval so that we can plot the NPI lower and upper cdfs. One way in which we solved this problem was by looking for repeated values in the data sets. Fortunately there were only 135 tied bodyweight values which made it possible to calculate NPI lower and upper cdfs for exposure for a random individual in the way explained below.

When there are repeated values in the data sets we can speed up the calculation by counting the number of tied values and then only using one in the calculation. This means that instead of having $(n_c + 1)(n_{int} + 1)(n_{bw} + 1)$ values to consider for each cdf we only have to calculate $(T_c + 1)(T_{int} + 1)(T_{bw} + 1)$ where T_c, T_{int} and T_{bw} are the number of tied values in the data sets for concentration, intake and bodyweight respectively. Eliminating repeated values can be done at each stage so the calculation is only done with the minimum possible number of values.

The probabilities for each interval are calculated based on the number of repeated values that occur in the data sets.

If it is the case that even after checking for repeated values, the data sets are still too large, it is still possible to calculate NPI lower and upper cdfs. It can be done by calculating all the values and counting how many are less than various threshold values. This eliminates problems with storing many values but it only becomes accurate by using a large number of threshold values. Several threshold values are needed because the smaller the interval between the threshold values, the closer to the actual lower and upper cdfs the results will be. However, as we would only use this method when there are very large data sets, it gives a good approximation for lower numbers of threshold values. Using many threshold values makes the method slow, but when the data sets are so large that there is no other method available, it gives a useful approximation. A relatively quick approximation can be made using the *histc* function in Matlab, which counts the number of values in each interval between threshold values. However it is only fast for smaller numbers of threshold values (e.g. for 1000 threshold values for the data sets in the case study (Section 4.3), it took approximately 3.5 minutes on a computer with a 1.6Ghz Intel Pentium processor with 1 Gb of RAM).

4.6 The effect of different sample sizes

In this section we look at how taking different sample sizes affects the NPI lower and upper cdfs. For simplicity we consider a case without censoring in the concentration data set and look at the effect of sample size on the NPI lower and upper cdfs for exposure for a random individual, again using the Exposure Model. For comparison we keep the size of the concentration data set at $n_c = 100$ and sample different size data sets for intake and bodyweight. The concentration data set is sampled from a Lognormal distribution with mean 9.02 μg/kg and standard deviation 66.07 μg/kg. We sample intake from a Lognormal distribution with mean 1.13 kg/day and standard deviation 0.60 kg/day and sample bodyweight from a Normal distribution with mean 30 kg and standard deviation 3 kg. Again these distributions are chosen

so the samples resemble the data sets that we have for young children. We consider samples of size $10, 30, 50$ and 100. The results are shown on the linear scale in Figure 4.6.1 and on the log scale in Figure 4.6.2.

Figure 4.6: NPI lower and upper cdfs using different sample sizes

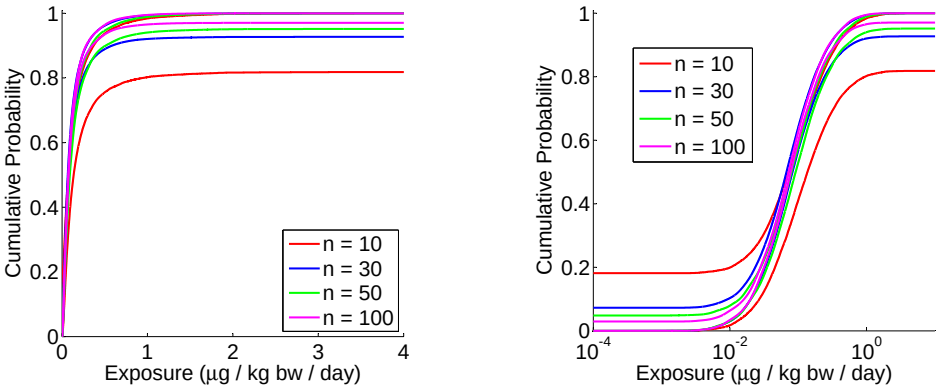

4.6.1 Linear scale

4.6.2 Log_{10} scale

Figures 4.6.1 and 4.6.2 show that, as the sample size increases, the uncertainty reduces so the NPI lower and upper cdfs get narrower. This is to be expected because including more observations in NPI leads to less uncertainty about variability and therefore narrower bounds. The general shape remains the same for the values of n shown here. The NPI lower and upper cdfs for the smaller values of n do not entirely enclose the NPI lower and upper cdfs for other sample sizes. This is due to variation between samples. We briefly investigate the effect of sampling variation for a sample of size 10 and a sample of size 100 below. For each sample size we take 5 different samples and plot the NPI lower and upper cdfs on a $\log_{10}$ scale in Figures 4.7.1 and 4.7.2 respectively.

Figure 4.7: NPI lower and upper cdfs for 5 different samples from each sample size

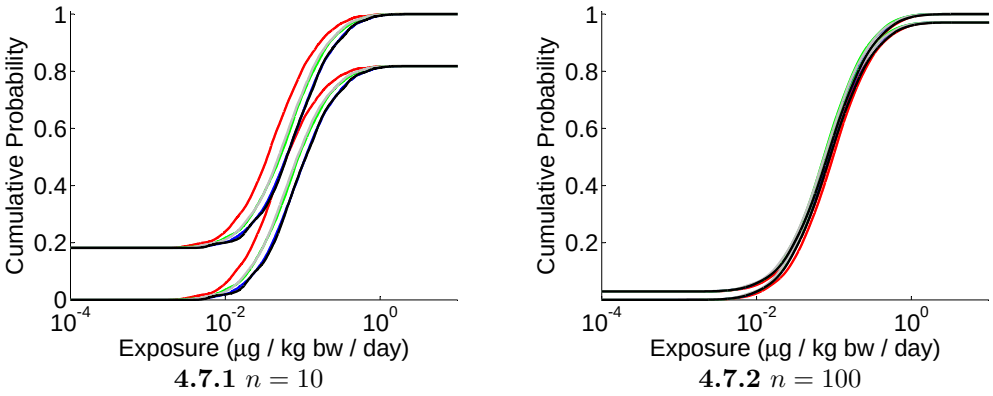

4.7.1 $n = 10$ **4.7.2** $n = 100$

As we expected Figures 4.7.1 and 4.7.2 show that there is more sampling variation when we consider a sample of size 10 than there is for a sample of size 100. This can be seen as the distance between the NPI lower and upper cdfs for the sample size of 10 is larger than the distance between the NPI lower and upper cdfs for the sample size of 100.

4.7 Imprecise data

In practice, data sets may be given as interval data, such as when an indication of measurement uncertainty is given as discussed in Subsection 3.5.5. An example of how to calculate NPI lower and upper cdfs with measurement uncertainty is presented here.

Suppose that the maximum measurement error of some apparatus used to measure the concentration of benzene in soft drinks is known. There may of course also be human error but we ignore that here. Assume that the maximum measurement error is $\delta = 0.3$. Then we can form NPI lower and upper cdfs on the concentration data (the benzene data used in Subsection 4.3.1) by considering the values $y_i = x_i + \delta$ and $z_i = x_i - \delta$. Let $x_{(1)}, x_{(2)}, ..., x_{(n)}$ be the order statistics of data $x_1, x_2, ..., x_n$ and let X_i be the corresponding pre-data random quantities so the data consist of the realized values $X_i = x_i, i = 1, ..., n$. Let Y_i and Z_i be observable random quantities with observations y_i and z_i respectively. The cdf for the next random quantity Y_{n+1}, is the NPI lower cdf because we find the NPI lower cdf by taking the envelope

of the M functions for X_{n+1}, Y_{n+1} and Z_{n+1}. The M function for Y_{n+1} describes probability mass at higher concentration values than either of the M functions for X_{n+1} and Z_{n+1}. Therefore the NPI lower cdf for Y_{n+1} becomes the NPI lower cdf for X_{n+1} including measurement uncertainty. Similarly the upper cdf for Z_{n+1} forms the NPI upper cdf as the M function for Z_{n+1} describes probability mass at lower concentrations than the M functions for X_{n+1} and Y_{n+1}.

The maximum value that the censored values can take is 1, so we take the censored point including measurement uncertainty to be $1 + \delta$. One could argue that we should take the limit to be 1, as if it is above 1 then we assume that the concentration is high enough to be detected. However if the apparatus can measure inaccurately up to $\pm\delta$, then it is possible that some values recorded as 1 are actually lower than the limit of detection, and some values recorded as < 1 are actually higher than 1 so we take $1 + \delta$ to be the maximum value that censored values can take. The NPI lower and upper cdfs including fixed measurement uncertainty ($\delta = 0.3$) for the concentration data (see Subsection 4.3.1) are shown with the NPI lower and upper cdfs for the original concentration data set in Figure 4.8.

Figure 4.8: NPI lower and upper cdfs with fixed measurement uncertainty (red) and for the original data set (blue)

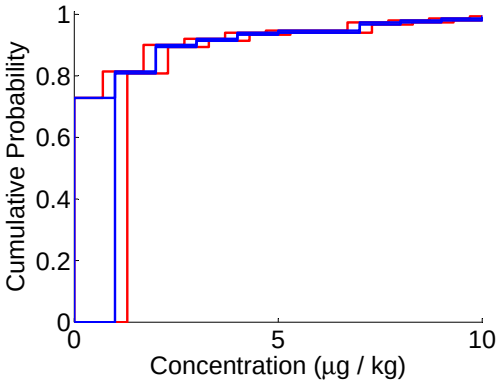

Including the measurement uncertainty leads to NPI lower and upper cdfs that increase at different values of concentration. We can see from Figure 4.8 that the measurement uncertainty leads to more uncertainty around the original data values,

but for the values that are not within $\pm\delta$ of an observed data value the lower and upper probabilities remain the same.

If information on measurement uncertainty is provided with data as a constant, it is easy to incorporate into the NPI lower and upper cdfs as shown here. We can combine such NPI lower and upper cdfs that incorporate measurement uncertainty with other NPI lower and upper cdfs for other random quantities. This is illustrated next with the original data sets (see Subsection 4.3.1) for bodyweight, intake and concentration. We form two sets of NPI lower and upper cdfs for exposure for a random individual, one set with no measurement uncertainty and one set with fixed measurement uncertainty ($\delta = 0.3$) for the concentration data set. These NPI lower and upper cdfs are shown in Figure 4.9.

Figure 4.9: NPI lower and upper cdfs with fixed measurement uncertainty (red) and no measurement uncertainty (blue)

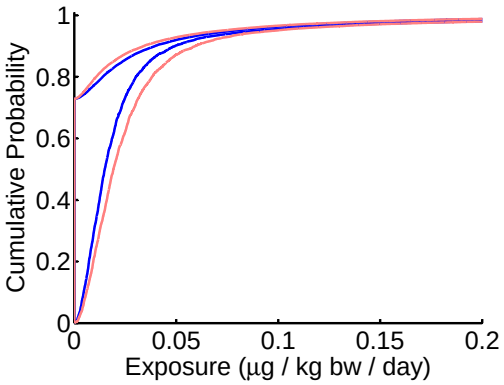

As shown in Figure 4.9, the NPI lower and upper cdfs including measurement uncertainty enclose the NPI lower and upper cdfs for the original data set. The difference in the width of NPI lower and upper cdfs is simply due to the size of δ.

4.8 Comparison to Bayesian methods

NPI focuses on predicting a future observation for a random quantitiy or a combination of random quantities. We therefore begin by comparing it to a Bayesian

posterior predictive distribution, where a prediction is obtained for a random individual. To calculate the Bayesian posterior predictive distribution, it is necessary to choose a prior distribution and a likelihood function. Independence is assumed between random quantities in many analyses because it is difficult to choose a joint distribution that describes the (unknown) dependence accurately. We calculate the Bayesian posterior predictive distributions for the random quantities concentration and *IR*, where we assume that both random quantities have a Lognormal distribution. Then we take 10,000 random samples from their Bayesian posterior predictive distributions and calculate the product. We calculate the NPI lower and upper cdfs on the product of concentration and *IR*. The results from both methods are shown in Figures 4.10.1 and 4.10.2.

Figure 4.10: Comparison of the Bayesian posterior predictive distribution (black dots) and NPI lower and upper cdfs (red lines)

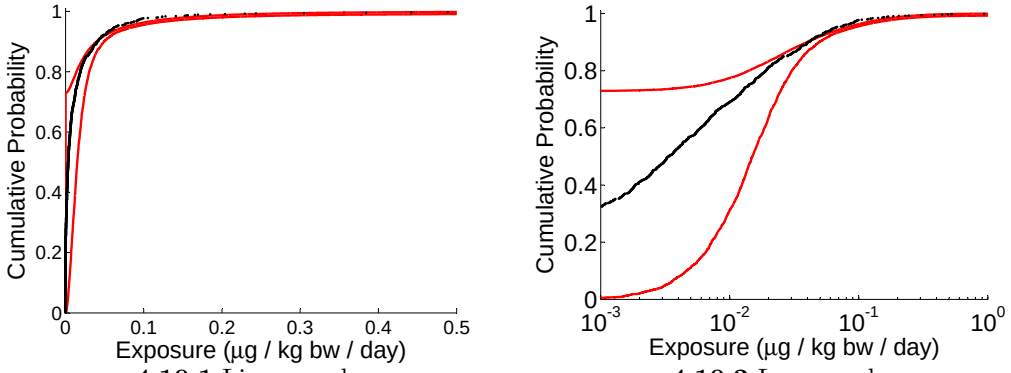

4.10.1 Linear scale **4.10.2** Log_{10} scale

The results of the Bayesian posterior predictive distributions are above the NPI lower and upper cdfs at around 0.1 μg/kg bw/day, leading to a less conservative indication of exposure than the NPI cdfs. It is less conservative in the sense that the Bayesian bounds indicate that, for example, the 99th percentile exposure is lower than indicated by NPI. The differences between the NPI and Bayesian results are due to the distributional assumptions made for the Bayesian posterior predictive distribution. The Bayesian method makes the assumptions that the *IR* and the concentration data are Lognormally distributed. The censored values in the concentration data set were dealt with using data augmentation (see Section 2.7.6) for the Bayesian posterior predictive distribution.

Figures 4.10.1 and 4.10.2 show that distributional assumptions have an effect on the final exposure distribution, and may lead to overestimates or underestimates of exposure for different percentiles, depending on the distributional assumption used. NPI is nonparametric and therefore does not share this problem of the influence of a distributional assumption. This is useful, particularly as there are many problems with fitting distributions to data sets, e.g. if the data set is small almost any distribution will fit, and if the data set is large, often no standard distributions such as Normal or Lognormal distributions will fit. NPI performs best on medium to large data sets. For small data sets there is often little information available which leads to large uncertainty, as indicated by the width between the lower and upper cdfs. The NPI lower and upper cdfs are very far apart at zero and low exposure values, due to the censoring included in the concentration and the presence of non-consumers who have an intake of zero. At larger exposure values the bounds get closer together again as the censored values only contribute to the lower tail. It is not surprising that the NPI lower and upper cdfs and the Bayesian posterior predictive methods differ as they are quite extreme cases; one assumes a specific, fully specified distribution and the other only assumes $A_{(n)}$.

We briefly consider the situation where we assume independence between all three random quantities. For the Bayesian method we assume Lognormal distributions for bodyweight, intake and concentration and combine them by randomly sampling 10,000 values for each random quantity from their Bayesian posterior predictive distribution. We then combine the values as in the Exposure Model to produce predictions for exposure. We find NPI lower and upper cdfs as previously described. The results for these methods are shown in Figures 4.11.1 and 4.11.2.

Figure 4.11: Comparison of the Bayesian posterior predictive distribution (black dots) and NPI lower and upper cdfs (blue lines)

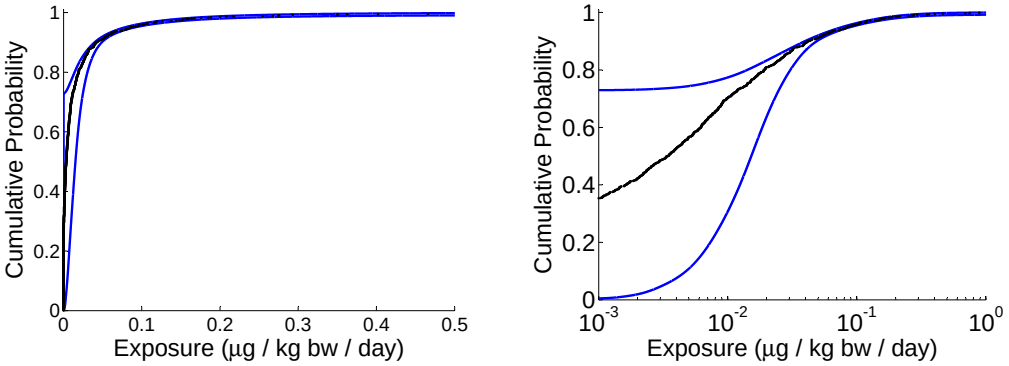

4.11.1 Linear scale

4.11.2 Log_{10} scale

The NPI lower and upper cdfs for the three separate random quantities are smoother than the NPI lower and upper cdfs for the product of concentration and IR because of the larger number of exposure values calculated. The small changes in the Bayesian predictions are due to the new assumptions about the distributions of the input random quantities which lead to the Bayesian predictions now lying between the NPI lower and upper cdfs. There is still the large difference that we saw before in the NPI lower and upper cdfs near zero due to the censored values and non-consumers in the analysis.

4.9 Robust NPI

In this section we consider an ad hoc method for which the theoretical foundation requires further investigation. We call this method robust NPI and illustrate an example here. We will explore the use of the method as part of a robust model in Chapter 5.

4.9.1 Example: Robust NPI lower and upper cdfs

In a Bayesian analysis we include robustness by considering different parameter values for distributions. As we have no parameters for NPI, one option we have is to assign the probability $\frac{1}{n+1}$ to the intervals as before, but spread the $\frac{1}{n+1}$ probability over the intervals on either side of every interval. This is an ad hoc method which

seems attractive to make NPI more robust to problems such as sampling variation.

We illustrate robust NPI with an example for random quantity X_{n+1} where we have observations $x_i = 1, 2, 3, 4, 5$. The M function for X_6 with robustness is:

$$\begin{aligned} M_{X_6}(0,\ x_2) &= \tfrac{1}{6} \\ M_{X_6}(0,\ x_3) &= \tfrac{1}{6} \\ M_{X_6}(x_1,\ x_4) &= \tfrac{1}{6} \\ M_{X_6}(x_2,\ x_5) &= \tfrac{1}{6} \\ M_{X_6}(x_3,\ \infty) &= \tfrac{1}{6} \\ M_{X_6}(x_4,\ \infty) &= \tfrac{1}{6} \end{aligned}$$

The NPI lower and upper cdfs for X_6 with robustness are shown in Figure 4.12 with the NPI lower and upper cdfs for X_6 without robustness for comparison.

Figure 4.12: NPI lower and upper cdfs for X_6 with robustness (red) and without robustness (blue)

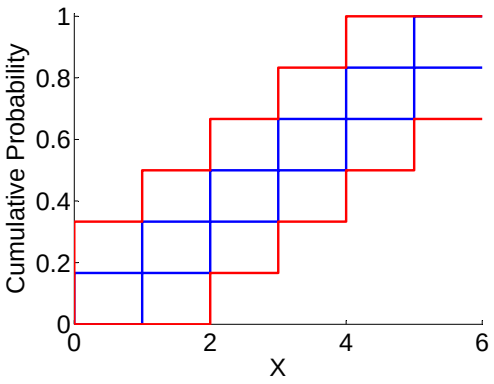

Notice that the upper cdf including robustness is the same upper cdf as without robustness but the probability that was at x_j is now at x_{j-1}. Similarly the lower cdf including robustness is the same lower cdf as without robustness but the probability that was at x_j is now at x_{j+1}.

If we use the robust NPI approach for two positive random quantities X_{n_x+1} and Y_{n_y+1}, the intervals in the M function for $XY_{(n_x+1)(n_y+1)}$ will be similar to the

M function for a standard NPI analysis except the intervals will be wider. For example, the interval that would be (xy_1, xy_2) in standard NPI will now be $(0, xy_3)$ and the interval that was (xy_2, xy_3) will now be (xy_1, xy_4) etc, where xy_k is the kth ordered value for XY. Similarly for three random quantities, as we have in the Exposure Model, the intervals will be wider when using robust NPI than when we use standard NPI. To incorporate more robustness for any of the random quantities we could assign $\frac{1}{n+1}$ probability over two intervals either side of every interval etc. This may be appropriate for small sample sizes.

Any theoretical properties for the robust method used for NPI need investigation but it seems a sensible approach to indicate the uncertainty about the predicted value of the next observation. As n increases, these robust NPI lower and upper cdfs will converge to the empirical distribution, as the NPI lower and upper cdfs do. However the convergence will be slower. Also we can see that robust NPI makes sense when we have one observation as it produces the output that the next observation has a probability between 0 and 1 of falling in the interval $(-\infty, \infty)$. This statement is true given our current state of information and is more cautious about predictions than the NPI method.

4.10 Conclusion

In this chapter we have shown how NPI can be implemented for an exposure risk assessment including censored data. An example with real data sets has been presented and we have explored the effect of correlations on the NPI bounds. We briefly discussed how to solve the computational challenges with implementing NPI either by only using one of each tied value in the sample or by using a threshold approach. We looked at the effect of different sample sizes and saw that larger sample sizes lead to less uncertainty about the next observation and therefore the NPI lower and upper cdfs are closer together. Fixed measurement uncertainty can be included in the NPI lower and upper cdfs.

We compared the results from an NPI analysis with the Bayesian posterior predictive distribution, where it compares favourably due to the fact that no assumption

is needed about the distribution and that NPI includes interval uncertainty due to the assumption $A_{(n)}$. We saw that the assumptions necessary in the Bayesian framework led to differing results, whereas the NPI results were similar for both two and three random quantities in the exposure model. The main difference was the final probability of the NPI lower cdf due to the sample sizes, as discussed in Subsection 4.3.2. We introduced an ad hoc method where we included robustness for NPI. This helps to make NPI more robust to sampling variation and may be useful for small sample sizes because it introduces more uncertainty about the predicted value of the next observation. So in this chapter we have shown that NPI can be applied in the field of exposure risk assessment even when there is censored data. It is also useful when we want to avoid making distributional assumptions and has the potential to be made robust for smaller sample sizes.

Chapter 5

Combining NPI and Bayesian methods

5.1 Introduction

In this chapter we present a hybrid method that can be used to combine nonparametric predictive inference (NPI) with Bayesian methods. This hybrid method, which we will call the NPI-Bayes hybrid method, will be useful in practice when we want to combine random quantities for which we make different assumptions based on the level of information available. If we do not have enough information to justify the assumption of a particular distribution, we can implement NPI for that random quantity and combine it with other random quantities for which we have enough evidence available to make distributional assumptions. As the majority of methods used in probabilistic risk assessments require distributional assumptions, it is interesting to compare nonparametric methods such as NPI with distributional methods, such as the Bayesian posterior predictive distribution. The NPI-Bayes hybrid method allows us to combine and compare these methods.

In Section 5.2 we explain how the NPI-Bayes hybrid method works and illustrate it with an example. We implement the NPI-Bayes hybrid method for the simple Exposure Model (Section 2.2) with different assumptions made about each random quantity in the model in Section 5.3. We consider the case where all the random quantities are modelled by NPI and another case where all the random quantities

are modelled by Bayesian posterior predictive distributions. We also consider all the other possible combinations (e.g. one random quantity represented by NPI and two by Bayesian posterior predictive distributions, etc.) using the NPI-Bayes hybrid method. For the simple Exposure Model we use simulated data sets to describe the exposure of young children to benzene from soft drinks. We then compare the results for all the different combinations of NPI and the Bayesian posterior predictive distribution for the random quantities using the NPI-Bayes hybrid method. Throughout this chapter we assume (Log)Normality for the random quantities that are described using the Bayesian posterior predictive distribution. However it would be possible to implement the NPI-Bayes hybrid method when assuming other distributions by sampling from the corresponding posterior predictive distributions. We also consider how sampling variation and sample size affect the results by simulating multiple samples, of two different sizes, for each random quantity in the Exposure Model and comparing the results.

In Section 5.4 we show how the NPI-Bayes hybrid method can be adapted to include robustness to the prior distribution for the random quantities for which we use a Bayesian posterior predictive distribution. For these random quantities, robustness to the prior distribution is implemented for two different classes of prior distributions and compared with the Bayesian method when we use a non-infomative prior distribution. Next we provide an algorithm for incorporating robustness in the NPI-Bayes hybrid method. In Section 5.5 we present two examples including robustness for the Exposure Model, one where robust Bayesian methods are used for all the random quantities and one where robust NPI is used for all the random quantities. Then all the different possible combinations are compared by looking at their 10th, 50th and 90th percentiles. In Section 5.6 we show that NPI can be combined with two-dimensional Monte Carlo simulation (2D MCS) using an example with the Exposure Model.

5.2 The NPI-Bayes hybrid method

In this section we explain the NPI-Bayes hybrid method for combining NPI and a Bayesian posterior predictive distribution. Assume that we have n_x observations x_i, where $i = 1, ..., n_x$, for random quantities X_i and that these observations come from a Normal distribution. We also have n_y observations y_j, $j = 1, ..., n_y$, for positive random quantities, Y_j. As we have no further information about the Y_j we choose to use NPI for Y_{n_y+1}. To apply the NPI-Bayes hybrid method we assume independence between the X_i and Y_j.

The Bayesian posterior predictive distribution for the X_i with a non-informative prior, $p(\mu, \sigma^2) = \frac{1}{\sigma^2}$, is a scaled Student t-distribution with $(n_x - 1)$ degrees of freedom, location parameter $\overline{x}$ and scale parameter $\sqrt{\left(1 + (\frac{1}{n_x})s_x\right)}$, where $\overline{x}$ is the sample mean, s_x is the sample standard deviation and n_x is the number of observations of X (Gelman et al., 1995). We invert the cdf at n_p percentiles of the Student t-distribution between 0 and 1 and assign each value probability $p_i = \frac{1}{n_p}$. By inverting the cdf we capture the range of values for the X_i.

We want to find bounds on the prediction for the next observation, XY_{new}. To do this we use the following algorithm.

1. Take n_p values, which we denote v_i, $i = 1, ..., n_p$, by inverting the Student t-distribution with $n_x - 1$ degrees of freedom, location parameter $\overline{x}$ and scale parameter $\sqrt{\left(1 + (\frac{1}{n_x})s_x\right)}$ at n_p percentiles.

2. Take the set of ordered observed values for Y_j, $j = 1, ..., n_y$, and add ∞ so we have $n_y + 1$ values, call this set L (this leads to the values that form the intervals for the lower cdf for xy_{new}).

3. Take the set of ordered observed values for Y_j and add 0 so we have $n_y + 1$ values, call this set U (this will lead to the values that form the intervals for the upper cdf for xy_{new}).

4. Find all the intervals between the ordered values $(v_i y_j)_k$ for $\underline{F}_{XY_{new}}(xy)$ by multiplying the values v_i from the Student t-distribution, with the set L, where $k = 1, ..., n_p(n_y + 1)$, $i = 1, ..., n_p$ and $j = 1, ..., n_y$.

5. Similarly find all the intervals between the ordered values $(v_i y_j)_k$ for $\overline{F}_{XY_{new}}(xy)$ by multiplying the values v_i with the set U, with i, j and k as before.

6. The probability on the intervals between each $v_i y_j$ value is $\frac{1}{n_p(n_y+1)}$

7. Plot $\underline{F}_{XY_{new}}(xy)$ and $\overline{F}_{XY_{new}}(xy)$

The combinations of $(v_i y_j)$ for the lower and upper cdfs will be the same, apart from the infinities generated for the lower cdf and the zeroes generated for the upper cdf. Therefore it is only necessary to combine the values from the scaled Student t-distribution with the observed values for Y_j once. We can describe the resulting probabilities using an M function. We order all the values $v_i y_j$ and call them b and use the index r to denote their place in the ordering.

$$\begin{aligned} M_{XY_{new}}(0, b_1) &= 1/n_p(n_y+1) \\ M_{XY_{new}}(b_r, b_{r+1}) &= 1/n_p(n_y+1) \\ M_{XY_{new}}(b_{(n_p(n_y+1)-1)},\ \infty) &= 1/n_p(n_y+1) \end{aligned}$$

for $r = 1, ..., (n_p(n_y+1) - 2)$.

We now illustrate the NPI-Bayes hybrid method using an example where we use the NPI approach for one random quantity and use the Bayesian posterior predictive distribution for the other random quantity.

Take $Y > 0$ and assume that we have observations [1,2,3] for the Y_j, $j = 1, ..., 3$. We assume $A_{(3)}$ for Y_4 and therefore the M function is as follows:

$$\begin{aligned} M_{Y_4}(0,\ 1) &= 1/4 \\ M_{Y_4}(1,\ 2) &= 1/4 \\ M_{Y_4}(2,\ 3) &= 1/4 \\ M_{Y_4}(3,\ \infty) &= 1/4 \end{aligned}$$

Generally we would only recommend using NPI for medium to large samples, but for illustrative purposes we use it for small n here. We take a sample of 20 values, $x_i, i = 1, ..., 20$ for the X_i from a Normal distribution with mean 5 and standard

deviation 0.2. The sample mean, $\overline{x} = 5.00$ and the sample standard deviation, $s_x = 0.17$. Then we invert the cdf of the Student t-distribution at 5000 percentiles. We can see that the probability for each interval will be $\frac{1}{4(5000)}$ as each of the 5000 v_i values for the X_i have probability $\frac{1}{n_p}$ which is $\frac{1}{5000}$ and each Y_4 value has probability $\frac{1}{4}$ of falling in each of the intervals shown in the M function. We then proceed as with a NPI analysis to find the lower and upper cdfs. An example is shown in Figure 5.1.

Figure 5.1: Example of NPI-Bayes hybrid method

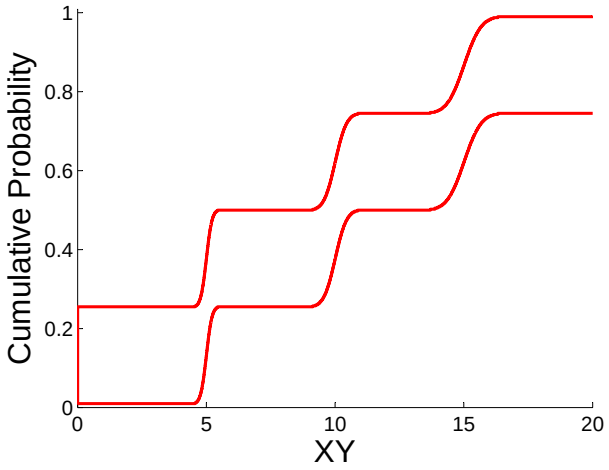

The influence of the Y_j is very clear in the four different parts of the lower and upper cdfs obtained. This is because of the small sample size that was used in this example. The final value of the lower cdf will be $\frac{3}{4}$ because the probability that the random quantity falls in an interval between the largest finite value for XY_{new} and ∞ will be $\frac{1}{n_y+1}$. If we instead had 50 observations, and thus $Y_j, j = 1, ..., 50$, (sampled from a Normal distribution with mean 2 and standard deviation 0.2) and we again use NPI for the Y_j and model the X_i as before, we would get results as shown in Figure 5.2. The final value of the lower cdf will now be $\frac{50}{51}$.

Figure 5.2: Combining NPI and Bayesian posterior predictive distribution for a larger sample size for Y

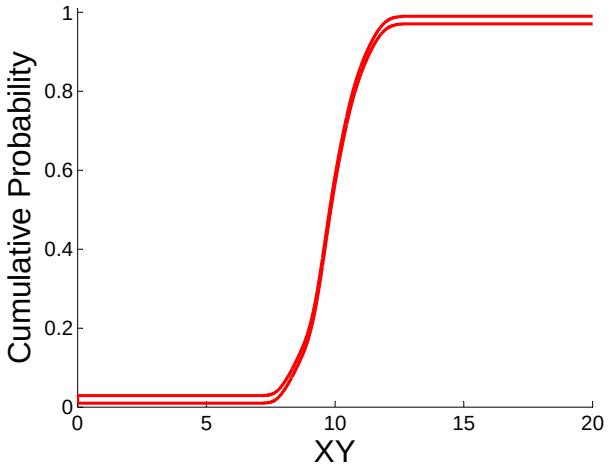

So we have shown that the NPI-Bayes hybrid method allows us to combine NPI and the Bayesian posterior predictive distribution for different random quantities. Our example is for the Normal distribution and can be used when an analyst assumes a Normal or Lognormal distribution. However the Bayesian posterior predictive distribution for any distribution could be combined with NPI in a similar way if it is possible to sample from the Bayesian posterior predictive distribution. In the next section we show how we can apply the NPI-Bayes hybrid method to the Exposure Model.

5.3 Predicting exposure using the NPI-Bayes hybrid method

We consider the simple Exposure Model described in Section 2.2:

$$\text{Exposure} = \frac{X \times Y}{Z} \tag{5.1}$$

where X is concentration, Y is intake and Z is bodyweight. We begin by simulating

a sample from a (Log)Normal distribution for each random quantity. We look at how well NPI and the Bayesian posterior predictive distribution describe the (Log)Normal distributions that we have taken the samples from. Then we calculate exposure by combining NPI for some random quantities and the Bayesian posterior predictive distribution for other random quantities. We compare the results for each of these combinations. We will use the following notation for the different possible combinations: NX indicates that the NPI approach was used for the random quantities X_i and BX that the Bayesian posterior predictive distribution was used for the random quantities X_i. Similarly we use NY, BY, NZ and BZ.

5.3.1 Data sets

To illustrate the NPI-Bayes hybrid method for calculating exposure, we need to have a sample for each random quantity in the model. In this example we choose distributions for each random quantity so that the data sets resemble those from Section 4.3 which described young children's exposure to benzene in soft drinks. We simulate 20 concentration (x) values from a Lognormal distribution with mean 1.4993 μg/kg and standard deviation 1.6749 μg/kg, 20 intake (y) values from a Lognormal distribution with mean 1.2776 kg/day and standard deviation 1.0159 kg/day and 20 bodyweight (z) values from a Normal distribution with mean 30 kg and standard deviation 3 kg. The ordered samples are:

X	0.1703	0.1828	0.3059	0.4278	0.4439	0.4994	0.5459	0.6037,
	0.6118	0.8656	0.8700	0.9074	1.175	1.471	1.472	1.569,
	2.346	2.663	4.036	12.12				
Y	0.2758	0.3199	0.4195	0.4397	0.4815	0.5377	0.6922	0.6997,
	0.7477	0.7675	0.8732	0.9954	1.130	1.174	1.348	1.403,
	1.629	1.632	1.653	2.769				
Z	25.86	25.93	26.58	26.65	26.93	28.61	28.83	28.98,
	29.37	30.95	31.11	31.51	32.12	32.18	33.11	33.57,
	34.66	35.59	35.87	36.34				

Figures 5.3.1, 5.3.2 and 5.3.3 show the NPI lower and upper cdfs, the cdf of the

Bayesian posterior predictive distribution given the assumption of (Log)Normality, the cdf of the distribution that each data set was sampled from and the empirical cdf for each random quantity. We display the distributions from which the data were sampled so we can see how closely the results from the different methods resemble these distributions. However, in a real-life risk assessment it is unlikely that we would know which distributions the data were sampled from and the data probably would not have come from a random sampling process.

Figure 5.3: NPI lower and upper cdfs (blue lines), Bayesian posterior predictive distribution (red line), empirical cdf of the data (green) and distribution that the data were sampled from (black line) for each random quantity

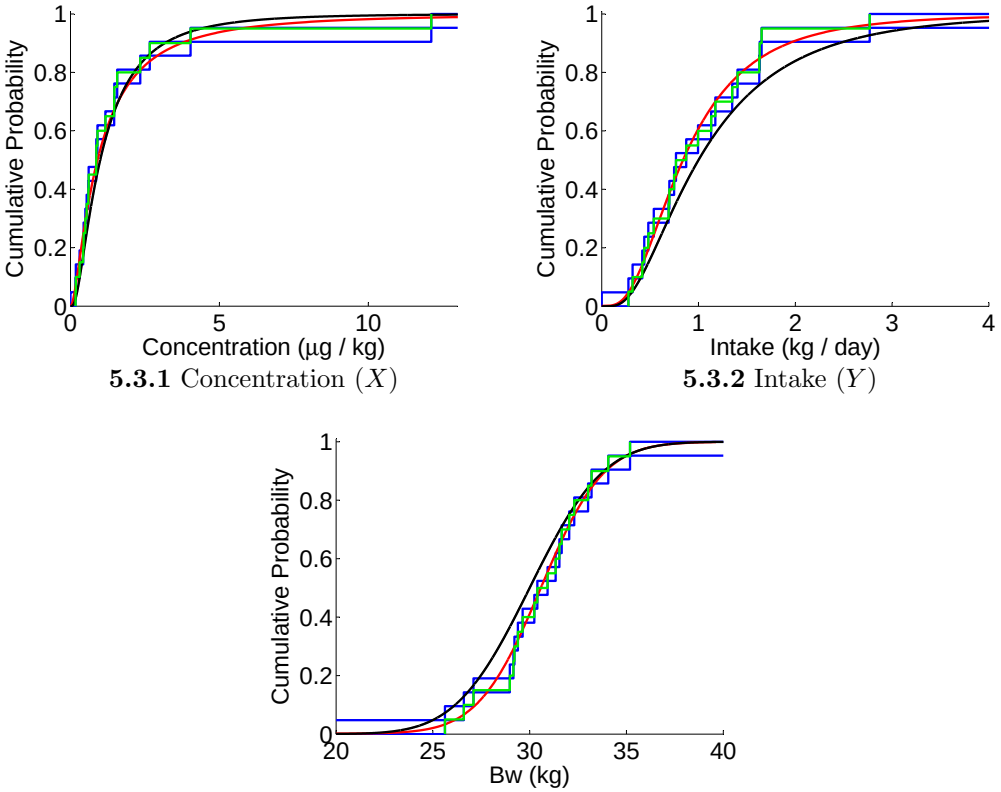

5.3.1 Concentration (X)

5.3.2 Intake (Y)

5.3.3 Bodyweight (Z)

Figure 5.3.1 shows that for this sample of concentration values, the Bayesian posterior predictive cdf overestimates the concentration at high percentiles (above about the 80th percentile) but it is very close to the cdf of the distribution that the data were sampled from at lower percentiles. The NPI lower and upper cdfs are generally close to the cdf of the distribution that the data were sampled from except at very high percentiles. Figure 5.3.2 shows that the Bayesian posterior predictive

cdf underestimates intake for most percentiles of the cdf of the distribution that the data were sampled from. The NPI lower and upper cdfs are close to or enclose the cdf of the distribution from which the data were sampled for most percentiles. The large intervals in the upper tail of the NPI lower and upper cdfs for concentration and intake, are due to fewer data points being sampled from the tails than from the middle of the distributions that the data were sampled from. Figure 5.3.3 shows that the Bayesian posterior predictive cdf overestimates the bodyweight for low percentiles and is close to the upper tail of the cdf of the distribution from which the data were sampled. The NPI lower and upper cdfs enclose the cdf of the distribution from which the data were sampled in the lower and upper tails and predicts values that are higher for the middle percentiles. Generally we tend to be more interested in the lower tail because people with smaller bodyweights are potentially more at risk from exposure to a chemical.

The Bayesian posterior predictive distribution is determined by the mean and standard deviation of the sample and by the shape of the Student t-distribution imposed on it because of the Normality assumption. NPI also depends on the values in the sample but does not make distributional assumptions and the NPI lower and upper cdfs will always enclose the empirical cdf of the data. Therefore different samples lead to different results so we explore the effect of sampling variation in Subsection 5.3.3.

5.3.2 Calculating exposure

We consider all different combinations of random quantities, using the NPI approach for some random quantities and the Bayesian posterior predictive distribution for the other random quantities, in the Exposure Model. For ease of presentation, we display the results of each combination by the 10th, 50th, and 90th percentiles. These percentiles are either intervals, if they use the NPI approach for some random quantities, or point values if they only use the Bayesian posterior predictive distribution for all the random quantities. We represent these by plotting the intervals for each percentile in Figure 5.4 as horizontal lines. We combine the distributions that the data were sampled from assuming independence between the random quantities

and call this the approximate exposure distribution. We show the percentiles of the approximate exposure distribution as vertical grey lines, so it is clear which intervals include the percentiles of the approximate exposure distribution. Although it cannot be seen in Figure 5.4, the lower bound for the 10th percentile for the case (NX, NY, NZ) extends down to 0, and the upper bound for the 90th percentile for (NX,NY,NZ) extends to ∞.

Figure 5.4: Percentiles for Exposure for combinations of Bayes and NPI

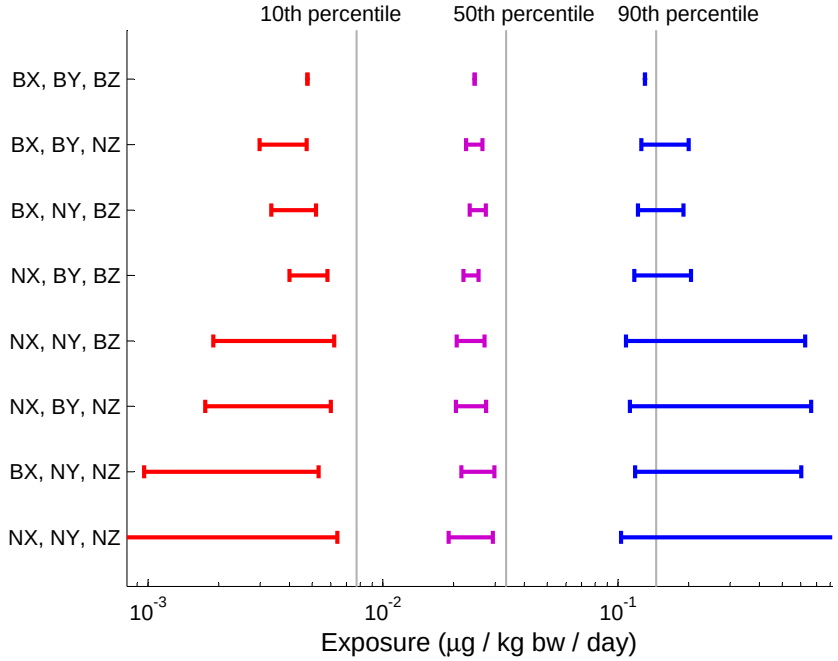

As can be seen from Figure 5.4, the 10th and 50th percentiles of the approximate exposure distribution do not lie within the corresponding lower and upper cdfs of any of the cases. However the 90th percentile of the approximate exposure distribution lies within the lower and upper cdfs of all the cases except (BX, BY, BZ). The lower and upper cdfs on the 10th and 50th percentiles are all lower than the percentiles of the approximate exposure distribution. This is due to the combination of the higher and lower predictions for each random quantity (See Figures 5.3.1, 5.3.2 and 5.3.3). The higher predictions for bodyweight for middle and low percentiles and the lower predictions for intake would lead to lower exposure values in general. However when combined with the higher predictions for upper percentiles for concentration, the values for the upper percentiles of exposure are larger. This explains why the 90th percentile of the approximate exposure distribution lies within the lower and upper

cdfs of all the cases except (BX, BY, BZ).

The combinations where the NPI approach is used for more random quantities lead to the widest intervals. Therefore if we were uncertain about the distribution that the data were sampled from, we would recommend combining all the random quantities using NPI because we are more likely to capture the percentiles of the approximate exposure distribution.

5.3.3 Sampling variation

In this section we explore sampling variation by comparing the differences in results for each of the eight cases, (NX, NY, NZ), (NX, NY, BZ), etc., when we use different samples for each random quantity in the model.

We simulate 10 samples of size 20 from the Lognormal distributions that we assigned for concentration and intake and 10 samples of size 20 from the Normal distribution that we assumed for bodyweight (see Subsection 5.3.1). We combine these samples to produce 10 different lower and upper cdfs for the 10th, 50th and 90th percentiles of exposure for each of the eight different combinations of random quantities (NX, NY, NZ), etc. We then compare how the 10th, 50th and 90th percentiles differ for each case and compare the results between cases. We plot the results with the percentiles of the approximate exposure distribution (vertical grey lines) for comparison. The 10th, 50th and 90th percentiles obtained by using the NPI-Bayes hybrid method for each of the 10 different sets of samples are shown in Figures 5.5.1 - 5.5.6 and Figures 5.6.1 - 5.6.2. We denote each set of three samples by Sample 1 to 10 for simplicity in the Figures.

Figure 5.5: Percentiles for different samples for each combination

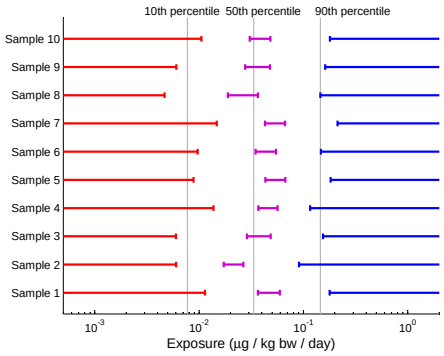

5.5.1 (NX, NY, NZ)

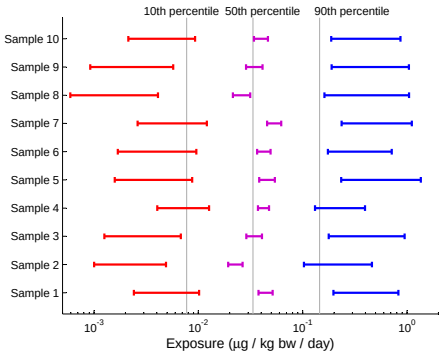

5.5.2 (BX, NY, NZ)

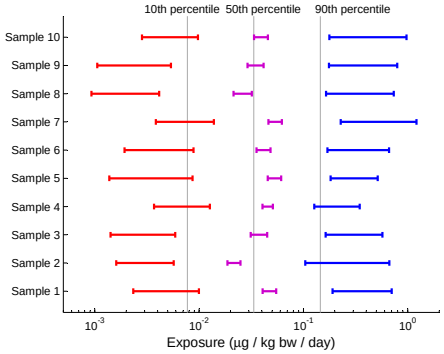

5.5.3 (NX, BY, NZ)

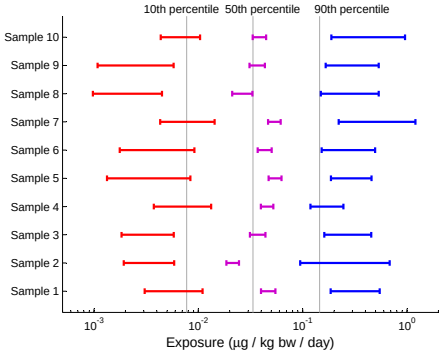

5.5.4 (NX, NY, BZ)

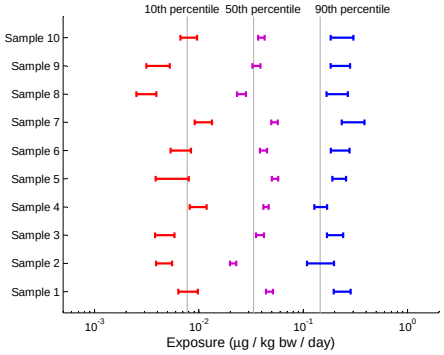

5.5.5 (NX, BY, BZ)

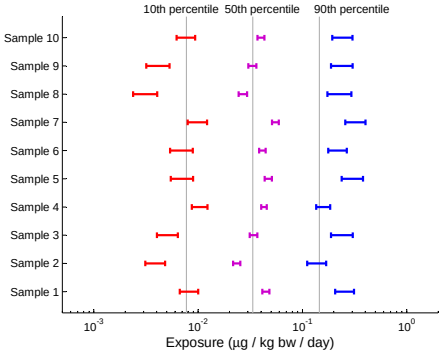

5.5.6 (BX, NY, BZ)

Figure 5.6: Percentiles for different samples for each combination

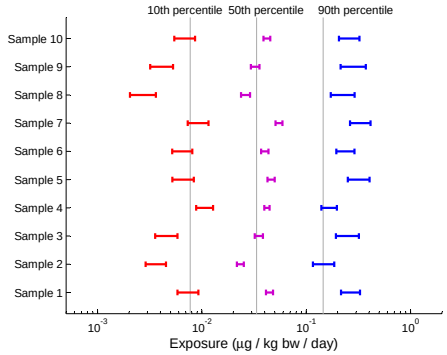

5.6.1 (BX, BY, NZ)

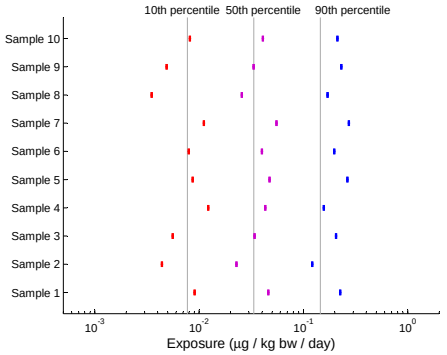

5.6.2 (BX, BY, BZ)

We can see from Figures 5.5.1 - 5.5.6 and Figures 5.6.1 - 5.6.2 that the intervals for all the percentiles become narrower as we use the NPI approach for fewer random quantities. The intervals for the 50th percentile tend to be narrower than the intervals for the 10th and 90th percentiles. This is due to the lack of data describing the tails of the distribution, so there is more uncertainty about the higher and lower percentiles than about the 50th percentile. For the (NX, NY, NZ) case the lower limit of the 10th percentile for all the samples is 0, and the upper limit for the 90th percentile for all the samples is ∞. The intervals for this case overlap for different samples. Therefore using the NPI approach for random quantities is more robust to sampling variation than the Bayesian method which only produces point estimates which underestimate or overestimate the percentiles. However, even using the NPI approach for all the random quantities in the Exposure Model does not lead to the percentiles of the approximate exposure distribution lying within the lower and upper cdfs. This may be due to the small sample size that we used. In the next section we look at the difference when we use a larger sample size.

5.3.4 Larger sample sizes

In this section we explore the effect of sample size on the percentiles for exposure and again compare the difference in results for each of the eight cases (NX, NY, NZ), etc. As before we simulate 10 samples from the Lognormal distributions that we assigned for concentration and intake and 10 samples from the Normal distribution that we

assumed for bodyweight. However, here we take samples of size 100. We combine these samples for each of the eight different combinations of random quantities to produce 10 different lower and upper cdfs for the 10th, 50th and 90th percentiles of exposure. We plot the results with the percentiles of the approximate exposure distribution (vertical grey lines) for comparison. The 10th, 50th and 90th percentiles obtained by using the NPI-Bayes hybrid method for each of the 10 different sets of samples are shown in Figures 5.7.1 - 5.7.4 and Figures 5.8.1 - 5.8.4. We compare these results with those given in Figures 5.5.1 - 5.5.6 and Figures 5.6.1 - 5.6.2 for samples of size 20.

Figure 5.7: Percentiles for different samples of size 100

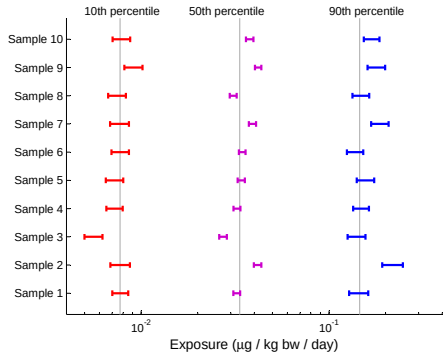

5.7.1 (NX, NY, NZ)

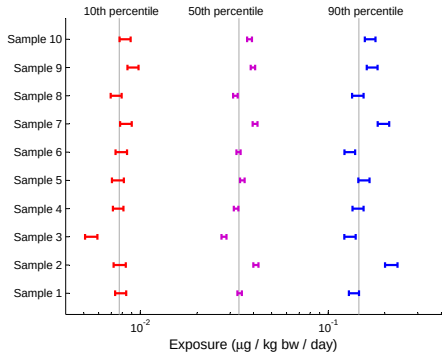

5.7.2 (BX, NY, NZ)

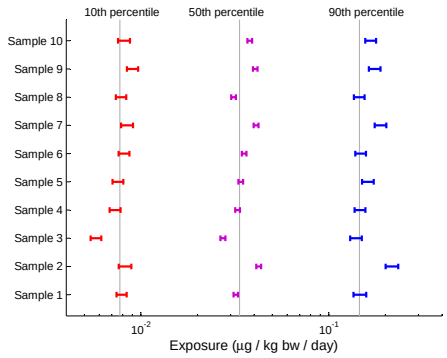

5.7.3 (NX, BY, NZ)

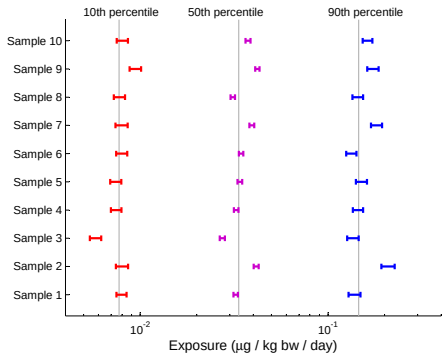

5.7.4 (NX, NY, BZ)

Figure 5.8: Percentiles for different samples of size 100

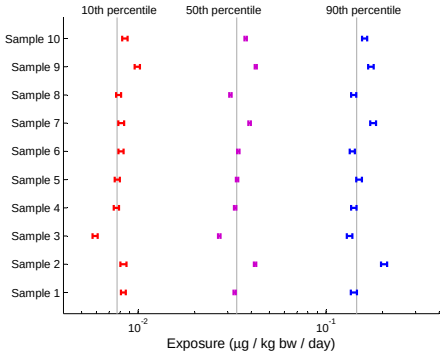

5.8.1 (NX, BY, BZ)

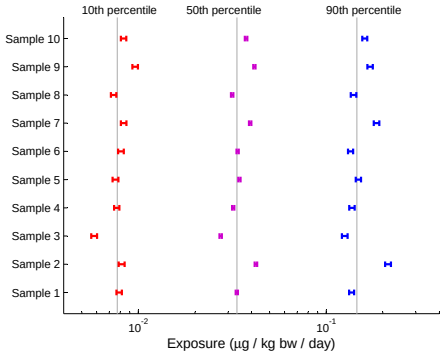

5.8.2 (BX, NY, BZ)

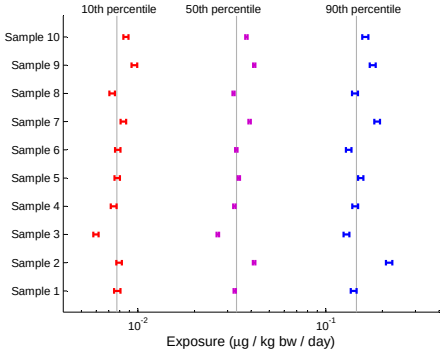

5.8.3 (BX, BY, NZ)

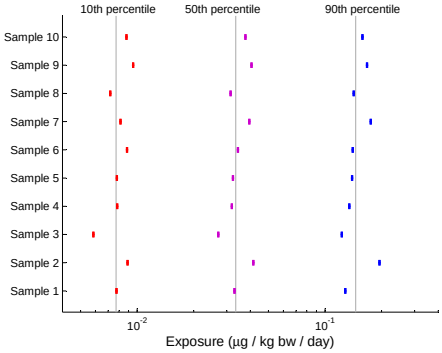

5.8.4 (BX, BY, BZ)

The main difference in results between the application with a small sample size and with a larger sample size is that the intervals for the percentiles are much narrower. These narrower intervals for NPI are due to the larger sample size which provides more information about the distribution. Generally the percentiles of the approximate exposure distribution lie in more intervals, particularly for the (NX, NY, NZ) case and the cases where the NPI approach is used for two of the random quantities. The intervals for the 50th percentile still tend to be narrower than those at the 10th and 90th percentile, although the difference in width is smaller than it was for the small sample size. The Bayesian posterior predictive distribution does not capture uncertainty about the estimates for the percentiles and thus can lead to incorrect results. NPI captures more uncertainty than the Bayesian method due to NPI's inclusion of interval uncertainty.

As the sample size increases, the performance of NPI will improve because it only uses information from the data and distributional assumptions for the data are not needed. This makes NPI particularly useful if the distribution is unknown or the data do not follow a standard parametric distribution (e.g. Normal, Lognormal, etc.). The estimates given by the Bayesian posterior predictive distribution may not improve as n increases if an incorrect distributional assumption is made. However if the assumed distribution is the correct distribution, then as $n \to \infty$, the Bayesian estimates will be closer to the distribution that the data were sampled from. As we have seen, even with a sample size of 100 there is variation in the results and the percentiles for the approximate exposure distribution do not always lie within the lower and upper bounds. Therefore if we are interested in the tails and the uncertainty about the tails, predictive methods may not be the most appropriate choice. One solution to include more uncertainty about the tails in the analysis is to include robustness. In the next section we discuss how to include robustness to the prior distribution when we use a Bayesian approach for a random quantity and how to include robustness in the NPI-Bayes hybrid method for the Exposure Model.

5.4 Robustness

5.4.1 Robustness for the Normal distribution

In this section we explain how our proposed hybrid method can be combined with robustness when we use the Bayesian approach for random quantities. We begin by explaining two different classes of prior distributions, a class of interval prior distributions for μ that we used in Subsection 3.5.1 and a class of Normal-Gamma prior distributions. We then explain the algorithm used to include robustness in the NPI-Bayes hybrid method for the Exposure Model.

Robustness to the prior for μ

To include robustness to the prior for μ, we consider the class of Normal prior distributions on $\mu|\sigma$ used in Subsection 3.5.1. The corresponding Bayesian posterior predictive distribution is a Student t-distribution with $n-1$ degrees of freedom, location parameter $\left(\frac{a+\overline{x}}{2}\right)$ and scale parameter $\sqrt{\frac{(2n+1)\left((n-1)s^2+\frac{n(\overline{x}-a)^2}{2}\right)}{2n(n-1)}}$, where $\overline{x}$ is the sample mean, n is the sample size and s is the sample standard deviation. When we use this class of prior distributions, we will call the resulting bounds the 'robust interval posterior predictive box'.

Robustness to prior distribution for (μ, σ)

Another possible class of prior distributions can be obtained by using a conjugate Normal-Gamma prior. If we assume this prior distribution

$$p(\mu,\sigma) \propto \frac{1}{\sigma^2}^{a} \exp\left[-\frac{c}{2\sigma^2}(\mu-m)^2 - \frac{b}{\sigma^2}\right],\ -\infty<\mu<\infty,\ \sigma^2>0$$

the Bayesian posterior predictive distribution for the X_i given this conjugate prior distribution can be shown by basic exercise to be a Student t-distribution with $2a^*-3$ degrees of freedom, location parameter m^* and scale parameter $\sqrt{\frac{2b^*(1+c^*)}{(c^*(2a^*-3))}}$, where $a^* = a+\frac{n}{2}$, $b^* = b+\frac{s^2(n-1)}{2}+\frac{(nd)}{2(n+c)}(\overline{x}-m)^2$, $c^* = c+n$, $m^* = \frac{cm+n\overline{x}}{c+n}$. When we use this class of Normal-Gamma prior distributions, we will call the resulting bounds the 'robust Normal-Gamma posterior predictive box'.

We now illustrate the algorithm for including robustness in the NPI-Bayes hybrid method. It is most easily represented with a diagram. In this algorithm we assume that we want to include robustness for every random quantity. If this is not the case, an approach combining this algorithm and the algorithm for the original NPI-Bayes hybrid method can be used instead.

5.4.2 Diagram showing how to include robustness for the Exposure Model

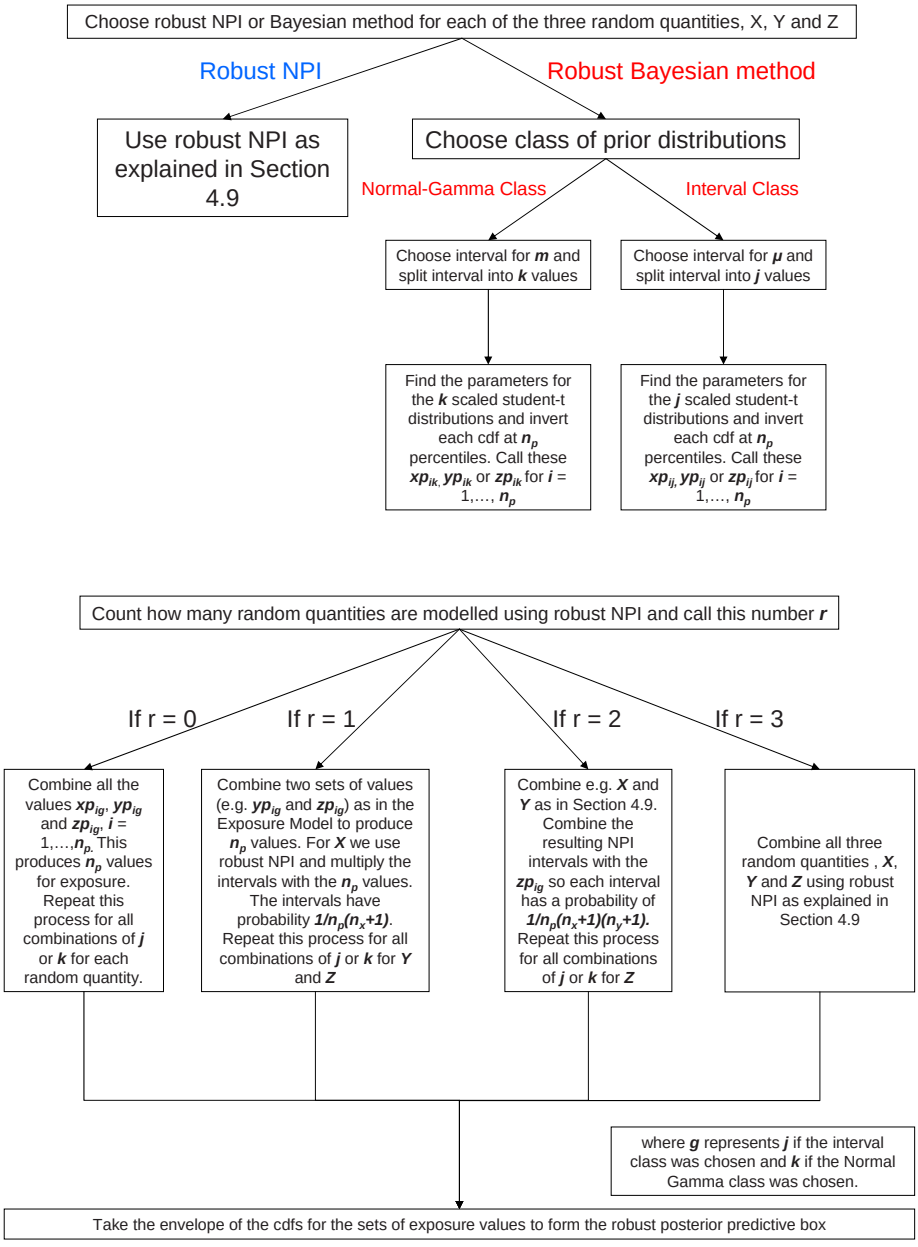

5.5 Examples: NPI-Bayes robust hybrid method

In this section we look at the results of incorporating robustness into the hybrid method for the Exposure Model. We compare the results for assuming each of the previously described classes of prior distributions for the case (BX, BY, BZ) with each other and with the results when we assume a non-robust, non-informative prior, $p(\mu, \sigma) = \frac{1}{\sigma}$ for all three random quantities. We then show the results for the (NX, NY, NZ) case where we use robust NPI for all the random quantities. We compare this with the case where we use NPI without robustness for all three random quantities. These examples allow us to illustrate the proposed NPI-Bayes robust hybrid method for the two most extreme cases. We illustrate the approximate exposure distribution to show how close the combinations are to the percentiles of the approximate exposure distribution. In the model, we can combine robust and non-robust random quantities, but for illustration of the method here we concentrate on the case where we include robustness for all the random quantities. We show the percentiles for all the other possible combinations of random quantities including robustness for each random quantity. We use r to denote that we are including robustness, e.g. BX_r indicates that we are using robust Bayesian methods for random quantity X.

5.5.1 Case (BX_r, BY_r, BZ_r)

We consider the case where bodyweight, the log of concentration and the log of intake are modelled by the robust Bayesian posterior predictive distribution with the assumption of Normality. We again use the data sets introduced in Subsection 5.3.1. We compare the results from assuming a non-informative prior for all three random quantities, assuming an interval class of prior distributions for all three random quantities and assuming a class of Normal-Gamma prior distributions for all three random quantities. Combinations of different classes of prior distributions could be considered if desired.

Let μ_{bw}, μ_{int} and μ_{conc} be the intervals for the mean of the prior distribution for bodyweight, intake and concentration respectively for the interval class of prior

distributions. Also, let m_{bw}, m_{int} and m_{conc} be the intervals for the mean of the prior distribution for bodyweight, intake and concentration respectively for the Normal-Gamma class of prior distributions. Take μ_{bw} and m_{bw} to be 10 equally spaced values between 25 kg and 35 kg, μ_{int} and m_{int} to be 10 equally spaced values between 0.5 kg/day and 1.2 kg/day and μ_{conc} and m_{conc} to be 10 equally spaced values between 0.3 μg/kg and 3 μg/kg. For the Normal-Gamma prior we use parameters $a = c = 10, b = 0.01$ for all the random quantities. Figure 5.9 shows the results for the non-informative prior, the two different classes of prior distribution and the approximate exposure distribution for comparison.

Figure 5.9: Non-informative posterior predictive distribution (black line), robust interval posterior predictive box (red line), robust Normal-Gamma posterior predictive box (blue line) and approximate exposure distribution (green line)

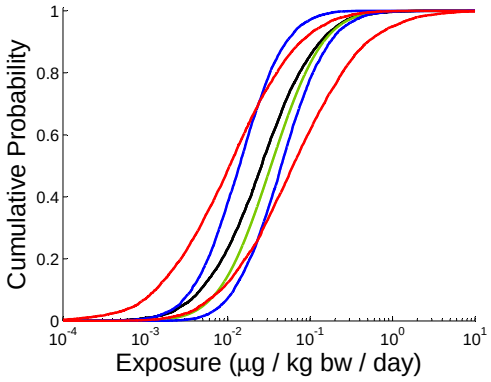

In Figure 5.9 we see that the robust Normal-Gamma posterior predictive box follows the shape of the approximate exposure distribution for lower percentiles and encloses the approximate exposure distribution. The robust interval posterior predictive box nearly encloses the approximate exposure distribution, although it slightly underestimates the lower percentiles of exposure. The non-informative posterior predictive distribution is only a single line here and underestimates the approximate exposure distribution for most percentiles until it reaches very high percentiles. This is probably due to the shape constraints of the Student t-distributions used to form the non-informative posterior predictive distribution and the lack of uncertainty included by the prior distribution.

5.5.2 Case (NX_r, NY_r, NZ_r)

In this section we use robust NPI for all three random quantities. We combine them as described in Section 4.9 to find the robust NPI lower and upper cdfs for exposure. The results are shown in Figure 5.10 with the approximate exposure distribution for comparison. An advantage of NPI is that we do not need to assume any distributions or choose any prior distributions or values for the prior distributions for the random quantities.

Figure 5.10: Robust NPI lower and upper cdfs for exposure (blue lines), NPI lower and upper cdfs without robustness (red lines) and approximate exposure distribution (green line)

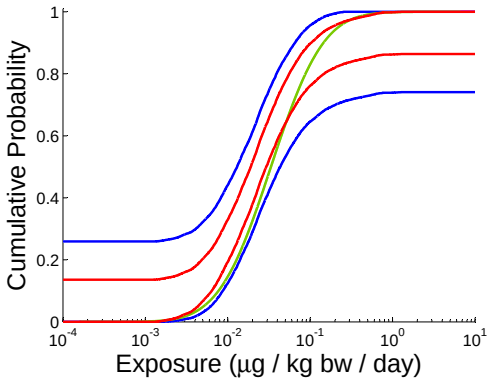

The original NPI lower and upper cdfs did not enclose the approximate exposure distribution while the robust NPI lower and upper cdfs do enclose the approximate exposure distribution. Therefore we can see that adding robustness to the analysis results in bounds containing the distribution that we are trying to predict. We compare the 10th, 50th and 90th percentiles of this case and (BX, BY, BZ) with all the other cases in the next subsection.

5.5.3 Comparing all the cases

In this section we consider all the cases (NX, NY, NZ) etc. including robustness for each random quantity. For illustration we use the Normal-Gamma class of prior distributions when we use Bayesian methods for the random quantities, as it per-

formed well in the (BX, BY, BZ) case. We take m_{bw}, m_{int} and m_{conc} as before. The 10th, 50th and 90th percentiles are shown in Table 5.1.

Table 5.1: Percentiles for all cases including robustness

Case	10th Percentile		50th Percentile		90th Percentile	
	Lower	Upper	Lower	Upper	Lower	Upper
(NX_r, NY_r, NZ_r)	0	0.0087	0.0130	0.0435	0.0655	∞
(BX_r, NY_r, NZ_r)	0	0.0112	0.0121	0.0537	0.0548	∞
(NX_r, BY_r, NZ_r)	0	0.0095	0.0137	0.0377	0.0595	∞
(NX_r, NY_r, BZ_r)	0	0.0089	0.0147	0.0384	0.0655	∞
(NX_r, BY_r, BZ_r)	0.0016	0.0095	0.0151	0.0344	0.0603	0.7663
(BX_r, NY_r, BZ_r)	0.0009	0.0115	0.0136	0.0497	0.0570	0.7610
(BX_r, BY_r, NZ_r)	0.0009	0.0118	0.0121	0.0490	0.0527	0.6789
(BX_r, BY_r, BZ_r)	0.0036	0.0118	0.0139	0.0446	0.0515	0.1760

The 10th, 50th and 90th percentiles for the approximate exposure distribution are 0.0077, 0.0335 and 0.1455 μg/kg bw/day respectively. We can see that the 10th, 50th and 90th percentiles of the approximate exposure distribution all lie in the lower and upper bounds for the 10th, 50th and 90th percentiles for all the cases. Therefore adding robustness to all the random quantities leads to results that again enclose the 10th, 50th and 90th percentiles of the approximate exposure distribution.

In this section we have seen that it is possible to include robustness when we use Bayesian methods for random quantities and when we use NPI for random quantities. We have compared the different cases of combining the random quantities with the different robust methods. Including robustness is useful as it resulted in all the cases enclosing the 10th, 50th and 90th percentiles of the approximate exposure distribution. For the Bayesian case different classes of prior distributions could be chosen to reflect prior beliefs about the random quantities. For the NPI case different levels of robustness could be incorporated. For small samples, we could perhaps assign the probability $\frac{1}{n+1}$ to two intervals on either side of every interval.

This would include more robustness to represent the increased uncertainty about the distribution that the data were sampled from for a small sample.

5.6 Combining NPI with Bayesian 2D MCS

We have illustrated combining NPI with the Bayesian posterior predictive distribution in this chapter. However it may be the case that we want to combine a predictive method with a Bayesian 2D method (one that separates variability and uncertainty). We illustrate a NPI-2D Bayes hybrid method with the Exposure Model. Suppose we want to calculate exposure based on predictions of the bodyweight of a young child. Usually to combine a Bayesian posterior predictive distribution with a Bayesian 2D MCS, we would sample from the Bayesian posterior predictive distribution for bodyweight in the outer loop of a 2D MCS. We would then combine the predicted value with the values calculated in the inner loop of the 2D MCS.

Here we do not want to choose a distribution for bodyweight so we predict the bodyweights using NPI. We again use the data sets provided in Subsection 5.3.1. We use a Bayesian 2D MCS for concentration and intake assuming that both random quantities are Lognormally distributed. We combine concentration and intake in a 2D MCS with 1000 inner loops and 1000 outer loops to include uncertainty about the distribution parameters. Then we find NPI lower and upper cdfs for the product of intake and concentration including parameter uncertainty by using the values that form the envelope of the 2D MCS output. These NPI lower and upper cdfs can then be combined with the NPI lower and upper cdfs for bodyweight as done previously in Section 4.3 to find bounds on exposure. The resulting lower and upper NPI cdfs are shown in Figure 5.11.

Figure 5.11: NPI lower and upper cdfs for exposure

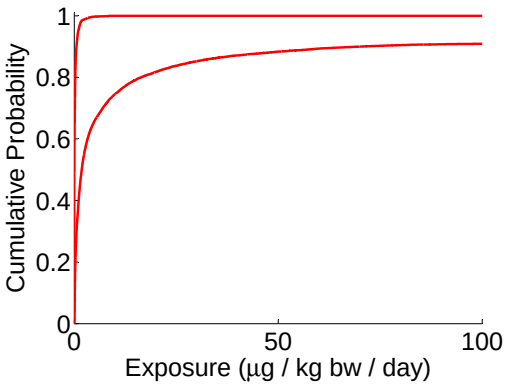

So here we have combined the NPI predictions for the next bodyweight observation with the 2D MCS results to include parameter uncertainty for concentration and intake.

5.7 Conclusions

In this chapter we have shown that we can combine NPI and the Bayesian posterior predictive distribution by using the NPI-Bayes hybrid method and the NPI-Bayes robust hybrid method. We have also shown that it is possible to combine NPI with 2D Bayesian methods such as 2D MCS. The NPI-Bayes hybrid method is useful where there are different levels of information available for random quantities. NPI can be used for random quantities for which we do not have enough information available to assume a distribution and the Bayesian posterior predictive distribution or 2D Bayesian MCS can be used for random quantities about which we have more information. It is common in practice that this situation, where we have lots of information about some random quantities and less information about other random quantities, will occur. For example, there is often little information about concentration of chemicals in different food types but lots of information available about the bodyweights of the population.

We saw in Subsection 5.3.4 that even when using samples with 100 values, the

percentiles of the approximate exposure distribution did not lie in the intervals for all the cases for all the samples. We would expect that as the sample size, n, increases, the lower and upper cdfs would converge to the approximate exposure distribution. Therefore as some of the combinations failed to fully represent the percentiles of the approximate exposure distribution for $n = 100$, we added robustness to each random quantity to improve the hybrid method.

To incorporate robustness we created a new robust hybrid method that can combine random quantities using either robust NPI or the Bayesian posterior predictive distribution with robustness. We considered two different classes of prior distributions for the Bayesian posterior predictive distribution, and our method could easily be adapted to include other possible classes of prior distributions. The Bayesian part of the NPI-Bayes robust hybrid method could be applied to any distribution (e.g. Weibull or Exponential distribution), as long as we can sample from the posterior predictive distribution. We can also represent different levels of robustness for NPI. Including robustness allows us to account for more uncertainty and led to both cases (NX_r, NY_r, NZ_r) and (BX_r, BY_r, BZ_r) enclosing the approximate exposure distribution. Also, all the cases where robustness was included for all the random quantities produced intervals containing the 10th, 50th and 90th percentiles of the approximate exposure distribution. This was not the case without robustness. This indicates that when using predictive methods on smaller samples, the NPI-Bayes robust hybrid method can represent the uncertainty about the approximate exposure distribution.

In practice, the NPI-Bayes robust hybrid method allows us to take account of the information available about random quantities such as intake whilst including robustness for random quantities such as concentration. It also allows us the option of not having to assume a distribution for all the random quantities in the model. We can use a mixture of the NPI-Bayes hybrid method and robust hybrid method to implement robustness for some random quantities and not for others. If the sample sizes are large then the hybrid method will provide results close to the approximate exposure distribution when the random quantities are combined. However if the sample sizes are small the robust hybrid method will provide better results than

the hybrid method because it is more likely to contain the approximate exposure distribution in the resulting bounds.

The results from all three of these methods require more investigation as it is not clear how the resulting bounds should be interpreted. The NPI-Bayes hybrid method, the NPI-Bayes robust hybrid method and the NPI-2D Bayes hybrid method introduced in this chapter are useful tools to combine random quantities in practice. The choice of which method to use and which combination to use will depend on many factors, such as sample size, whether there is enough information to make distributional assumptions and whether there are experts available to choose classes of prior distributions.

Chapter 6

Conclusions and Future Research

This chapter provides a short summary of the main results presented in this thesis, and discusses important challenges for future research.

6.1 Conclusions

In this thesis we have introduced new methods that add to the choice of methods available for risk assessment. The appropriate method to use will depend on factors such as whether the decision is about a population or an individual, how many data are available and if there is enough information about the random quantities for the analyst to assume a particular distribution. It also depends on whether the whole distribution or a percentile for a population is of interest. If the decision maker would like to estimate the risk based on the whole distribution, Bayesian p-boxes could be implemented. If the question is about a random individual NPI could be appropriate, as NPI only assumes $A_{(n)}$ and includes interval uncertainty. If there are some random quantities in a model about which we do not want to make a distributional assumption and others that we are prepared to assume distributions for, then the NPI-Bayes or robust NPI-Bayes hybrid method could be used.

In Chapter 3, we have seen that nested Bayesian p-boxes can give an analyst or risk manager a clear indication of the changes at different credibility levels. Bayesian p-boxes should be used instead of frequentist p-boxes when working with distributions with more than one parameter, particularly for small sample sizes. This is be-

cause the frequentist p-boxes ignore dependence between parameters and therefore do not lead to the tightest possible bounds given the information available. Bayesian p-boxes can be formed using any subset of the posterior parameter space, as long as it is closed and bounded. We have shown that the Bayesian p-box method can take fixed measurement uncertainty and robustness to the prior distribution into account. We focused on including robustness to the prior distribution for the practically important cases of the Normal and Lognormal distributions. We have explained how Bayesian p-boxes can be combined under the assumption of independence or under no assumptions about dependence using the Williamson and Downs method. It may be useful to risk managers to see both outputs so they can see how much reduction in uncertainty there is under the assumption of independence. Bayesian p-boxes can include distribution uncertainty and model uncertainty by forming Bayesian p-boxes separately for each distribution or model and then taking the envelope of the results. Displaying the results from different distributions or models may provide more insight into the risk distribution and provide a clearer picture for the risk manager. When a risk manager has to make a decision about a population, this method can be used to illustrate bounds on the distribution of the population.

In Chapter 4, we have shown that NPI provides an alternative method for predicting the exposure of a random individual to a chemical. For a medium or large data set, NPI provides a better representation of the exposure than methods such as the Bayesian posterior predictive distributions due to the inclusion of interval uncertainty and the lack of distributional assumptions. NPI can be used where we have left-censored data and known measurement uncertainty and will produce the tightest possible lower and upper cdfs given this information. We explored the effect of strong and weak correlations in an example and it seemed that neither of them strongly influenced the NPI analysis. We also suggested an ad hoc method to include more uncertainty in the NPI analysis which we called 'robust NPI'. This method seems to work well and may provide a way to use NPI for small samples but requires further investigation.

In Chapter 5, we introduced a NPI-Bayes hybrid method that allows us to combine random quantities where some random quantities are modelled with NPI and

others are modelled with Bayesian methods. We have shown that NPI can be combined with both one-dimensional methods, such as the Bayesian posterior predictive distribution and two-dimensional methods such as 2D Monte Carlo Simulation. We showed how robustness could be incorporated in the hybrid method for both NPI and the Bayesian posterior predictive distribution methods. Including robustness to the prior distribution can partially reduce the effect of distributional assumptions, as including the additional uncertainty increases the chance that the true distribution will fall within the bounds. However, robustness may also reduce the uncertainty if narrower ranges are selected for the priors. Further research is required into the interpretation of the output bounds. NPI is a frequentist method, that is also consistent with the Bayesian framework and it is unclear how to interpret the bounds when mixing a frequentist and a Bayesian method together.

All methods that we have presented and explored in this thesis help to model the uncertainties involved more transparently than they currently are in the deterministic risk assessments. We have focused on Bayesian methods because they have the advantage that parameter dependence can be incorporated and the results can be updated with future observations. NPI has been investigated due to the advantage of not having to assume a distribution and because it includes interval uncertainty. As both NPI and Bayesian methods have advantages we then combined them in a NPI-Bayes hybrid method. Further research is required into extensions of these methods. We briefly describe possible future research topics in Section 6.2.

6.2 Topics for future research

In this section we discuss possible areas of future research which build on the work presented in this thesis. All these areas would add to the expansion of quantifying uncertainty in risk assessments.

6.2.1 Uncertainty about correlations

It is possible to combine various types of bounds, e.g. Bayesian p-boxes, by using the method presented by Williamson and Downs (1990). We have also briefly introduced

copulas which are a method of combining random quantities with a fixed correlation. However when we do not know much about the dependence but we do know that the random quantities are, for example, definitely not negatively correlated, the Williamson and Downs method will not be able to exclude this particular correlation. Further research is needed into excluding known dependencies from the resulting bounds. If the result of combining two random quantities with a specific correlation falls completely within the bounds formed using the Williamson and Downs method, excluding the specific correlation may not have any effect on the outer bounds. If we knew that there was a range of possible correlations, it may be possible to combine the bounds assuming various correlations in the interval. If these behave in a linear way (i.e. the lowest correlation leads to the lowest possible bound and as the correlation increases the upper bounds increase) then it may be possible to draw a p-box around the results. Further research into eliciting and modelling dependencies between random quantities is necessary to make the risk assessments more realistic.

6.2.2 Bayesian p-boxes for other distributions

In this thesis we have presented Bayesian p-boxes for the Exponential and Normal distributions. Bayesian p-boxes could be formed for other distributions, as long as we can calculate the highest posterior density or similar region from the posterior distribution. The region needs to be closed and bounded so we can minimise and maximise the corresponding cdf over the region to form the lower and upper bounds on the random quantity. If we had a multi-modal distribution, we could have various closed and bounded regions. It would in theory be possible to minimise and maximise the cdf of the distribution over these regions separately and then form multiple p-boxes to represent the different regions. When these p-boxes are considered all together they should represent the $100(1-\alpha)\%$ probability that, for example, the distribution for a random quantity X falls in the p-boxes. However, if we can only sample from the posterior distribution, it may not be possible to calculate a highest posterior density or any other region with a certain credible level. The justification for the minimum and maximum bounds being formed by the (μ, σ) pairs on the contour applies to location-scale distributions. However if distributions have more

than two parameters, it will become more complicated to calculate regions and to present the results in a meaningful way. It would be interesting and also important for risk assessment to develop Bayesian p-boxes for other distributions.

6.2.3 More realistic models

Throughout this thesis we have used the simple Exposure Model to illustrate our methods. It would be beneficial to consider developing the methods for more complicated exposure models or for models in other fields. We have already discussed developing Bayesian p-boxes for other distributions, but there is also research needed on combining the Bayesian p-boxes for different random quantities in a model. It would be useful to research how we could find the hpd region, or a similar region, from the posterior distribution for several combined random quantities as this would then allow us to find, for example, 95% bounds on the whole model. NPI could be used for more complicated models, although more research needs to be done on how to do this in the most computationally efficient way. As models become more complicated and include more random quantities it can potentially make it difficult to store all the possible values on a computer. It would also be useful to look at combining random quantities with different dependencies which is currently not possible in the NPI framework. The NPI-Bayes hybrid methods could be used for more complicated models, although this too will be limited by the computation required for the random quantities that NPI is used for in the model.

Appendix

A Distributions used in this thesis

Normal distribution

X has a Normal distribution with mean μ and variance σ^2, denoted $X \sim N(\mu, \sigma^2)$, if it has density

$$p(X) = \frac{1}{\sigma\sqrt{2\pi}}\exp\left(\frac{-(x-\mu)^2}{2\sigma^2}\right) \qquad (-\infty < x < \infty)$$

As the distribution is symmetric and unimodal, the median and mode are both equal to the mean. If $\mu = 0$ and $\sigma = 1$, X is said to have a Standard Normal distribution. μ can be referred to as the location parameter and σ can be referred to as the scale parameter.

Lognormal distribution

X has a Lognormal distribution if it has density

$$p(X) = \frac{1}{x\sigma\sqrt{2\pi}}\exp\left(\frac{-(log(x)-\mu)^2}{2\sigma^2}\right)$$

where μ and σ are the mean and standard deviation of the Normal distribution for $\log(X)$.

Student t distribution

X has a Student t distribution on ν degrees of freedom, denoted $X \sim t_\mu$, if it has density

$$p(X) = \frac{\Gamma(\frac{\nu+1}{2})}{\sqrt{\pi\nu}\Gamma(\frac{\nu}{2})}\left(1+\frac{x^2}{\nu}\right)^{-\frac{\nu+1}{2}}$$

The non-central t distribution is a generalisation of Student's t distribution with a non-centrality parameter that measures the normalised distance between the true population mean and the population mean, μ, that we have assumed.

Gamma distribution

X has a two parameter Gamma distribution with parameters a and b, denoted $X \sim G(a, b)$, if it has density

$$p(X) = \frac{1}{b^a \Gamma(a)} x^{a-1} \exp\left(\frac{-x}{b}\right)$$

This is a conjugate prior distribution for the Exponential distribution in Bayesian statistics.

χ^2 distribution

X has a χ^2 distribution on ν degrees of freedom, denoted $X \sim \chi^2_\nu$, if it has density

$$p(X) = \frac{1}{2^{\frac{\nu}{2}} \Gamma\left(\frac{\nu}{2}\right)} x^{\frac{\nu-2}{2}} \exp\left(\frac{-x}{2}\right)$$

This is a special case of the Gamma distribution with $a = \frac{\nu}{2}$ and $b = 2$.

Exponential Distribution

X has an Exponential distibution with parameter λ if it has the density

$$p(X) = \lambda \exp\left(-\lambda x\right)$$

Bibliography

Aitio A. (2008). Research needs for environmental health risk assessment. *Journal of Toxicology and Environmental Health Part A*, **71** (18): 1254 – 1258

Aldenberg T. and Jaworska J.S. (2000). Uncertainty of the Hazardous Concentration and Fraction Affected for Normal Species Sensitivity Distributions. *Ecotoxicology and Environmental Safety*, **46** (1): 1 – 18

Aughenbaugh J.M. and Paredis C.J.J. (2006). The value of using imprecise probabilities in engineering design. *Journal of Mechanical Design*, **128** (4): 969 – 979

Augustin T. and Coolen F.P.A. (2004). Nonparametric predictive inference and interval probability. *Journal of Statistical Planning and Inference*, **124** (2): 251 – 272

Berger J.O. (1985). *Statistical Decision Theory and Bayesian Analysis*. New York: Springer-Verlag, Second Edition

Berger J.O. (1990). Robust Bayesian analysis: sensitivity to the prior. *Journal of Statistical Planning and Inference*, **25** (3): 303 – 328

Berger J.O. (2000). Bayesian analysis: A look at today and thoughts of tomorrow. *Journal of the American Statistical Association*, **95** (452): 1269 – 1276

Berger J.O. and Berliner L.M. (1986). Robust Bayes and Empirical Bayes Analysis with ϵ-contaminated priors. *The Annals of Statistics*, **14** (2): 461 – 486

Bernardo J.M. (2005). Intrinsic credible regions: An objective Bayesian approach to interval estimation. *Test*, **14** (2): 317 – 384

Bernardo J.M. and Smith A.F.M. (1994). *Bayesian Theory*. John Wiley and Sons, First Edition

Blasco A. (2005). The use of Bayesian statistics in meat quality analyses: a review. *Meat Science*, **69** (1): 115 – 122

Boas M.L. (1983). *Mathematical Methods in the Physical Sciences*. John Wiley and Sons, Second Edition

Bose S. (1994). Bayesian robustness with mixture classes of priors. *The Annals of Statistics*, **22** (2): 652 – 667

Box G.E.P. and Tiao G.C. (1973). *Bayesian Inference in Statistical Analysis*. Addison-Wesley, Reading, MA

Brand E., Otte P.F. and Lijzen J.P.A. (2007). CSOIL 2000 an exposure model for human risk assessment of soil contamination. A model description. Technical report. RIVM, Bilthoven, The Netherlands. Available at http://rivm.openrepository.com/rivm/bitstream/10029/7382/1/601501022.pdf

Bryan B., , McMahan H.B., Shafer C.M. and Schneider J. (2007). Efficiently computing minimax expected-size confidence regions. In *Proceedings of the 24th International Conference on Machine Learning, Corvallis, OR*

Burmaster D.E. and Thompson K.M. (1998). Fitting second-order parametric distributions to data using maximum likelihood estimation. *Human and Ecological Risk Assessment*, **4** (2): 319 – 339

Burmaster D.E. and Wilson A.M. (1996). An introduction to second-order random variables in human health risk assessments. *Human and Ecological Risk Assessment*, **2** (4): 892 – 919

Chaturvedi A. (1996). Robust Bayesian analysis of the linear regression model. *Journal of Statistical Planning and Inference*, **50** (2): 175 – 186

Chebyshev P. (1874). Sur les valeurs limites des integrales. *Journal de Mathematiques Pures Appliques*, **Ser 2** (19): 157 – 160

Chen M.H., Shao Q.M. and Ibrahim J.G. (2001). *Monte Carlo Methods in Bayesian Computation*. Springer Series in Statistics. New York: Springer-Verlag

Chow T.E., Gaines K.F., Hodgson M.E. and Wilson M.D. (2005). Habitat and exposure modelling for ecological risk assessment: A case study for the raccoon on the Savannah River Site. *Ecological Modelling*, **189** (1 – 2): 151 – 167

Codex (2007). Codex Alimentarius Commission 16th procedural manual. Available at http://www.codexalimentarius.net/web/procedural_manual.stm.

Congdon P. (2001). *Bayesian Statistical Modelling*. John Wiley and Sons Ltd

Coolen F.P.A. (2006). On nonparametric predictive inference and objective Bayesianism. *Journal of Logic, Language and Information*, **15** (1 – 2): 21 – 47

Coolen F.P.A. and Coolen-Schrijner P. (2007). Nonparametric predictive comparison of proportions. *Journal of Statistical Planning and Inference*, **137** (1): 23 – 33

Coolen F.P.A. and Yan K.J. (2004). Nonparametric predictive inference with right-censored data. *Journal of Statistical Planning and Inference*, **126** (1): 25 – 54

Coolen-Schrijner P., Coolen F.P.A. and Shaw S.C. (2006). Nonparametric adaptive opportunity-based age replacement strategies. *Journal of the Operational Research Society*, **57** (1): 63 – 81

Cox D.R. and Snell E.J. (1989). *Analysis of Binary Data*. Second Edition, Chapman and Hall, London, UK

Crocker D.R. (2005). Estimating the exposure of birds and mammals to pesticides in long-term risk assessments. *Ecotoxicology*, **14** (8): 833 – 851

Cullen A.C. and Frey H.C. (1999). *Probabilistic Techniques in Exposure Assessment*. Plenum Publishing Corporation, New York

Davison A.C. and Hinkley D.V. (1997). *Bootstrap Methods and their Application*. Cambridge University Press, Cambridge

Dixon W.J. (2007a). The use of Probability Bounds Analysis for Characterising and Propagating Uncertainty in Species Sensitivity Distributions. Technical Report Technical Report Series No. 163, Arthur Rylah Institute for Environmental Research, Melbourne, Australia

Dixon W.J. (2007b). Uncertainty Propagation in Population Level Salinity Risk Models. Technical Report Technical Report Series No. 164, Arthur Rylah Institute for Environmental Research, Melbourne, Australia

Efron B. and Tibshirani R.J. (1993). *An Introduction to the Bootstrap*. Chapman and Hall, New York

EFSA (2005). Opinion of the scientific committee on a request from EFSA related to exposure assessments. *The EFSA Journal*, **249**: 1 – 26

European Commission (2000). Communication from The Commission on the precautionary principle. COM(2000) 1 final. Brussels

European Commission (2002a). Guidance Document on Aquatic Ecotoxicology in the context of Directive 91/414/EEC. SANCO/3268/2001 Rev. 4 (Final). Brussels

European Commission (2002b). Guidance document on risk assessment for birds and mammals under council directive 91/414/EEC. SANCO/4145/2000. Brussels, http://ec.europa.eu/food/plant/protection/evaluation/guidance/wrkdoc19_en.pdf

European Commission (2002c). Guidance document on Terrestrial Ecotoxicology under Directive 91/414/EEC. SANCO/10329/2002 Rev. 2 (Final). Brussels

Evans S.N., Hansen B.B. and Stark P.B. (2003). Minimax expected measure confidence sets for restricted location parameters. Technical report, University of California, Berkeley. Tech Report 617

Fan M., Thongsri T., Axe L. and Tyson T.A. (2005). Using a probabilistic approach in an ecological risk assessment simulation tool: test case for depleted uranium (du). *Chemosphere*, **60** (1): 111 – 125

Ferson S. (1996). What Monte Carlo methods cannot do. *Human and Ecological Risk Assessment*, **2** (4): 990 – 1007

Ferson S. (2002). *RAMAS Risk Calc 4.0 Software. Risk Assessment with Uncertain Numbers*. Lewis Publishers, Boca Raton, Florida

Ferson S. and Hajagos J.G. (2006). Varying correlation coefficients can underestimate uncertainty in probabilistic models. *Reliability Engineering and System Safety*, **91** (10 – 11): 1461 – 1467

Ferson S., Kreinovich V., Ginzburg L.R., Myers D.S. and Sentz K. (2003). Constructing Probability Boxes and Dempster-Shafer structures. Technical Report SAND2002-4015, Sandia National Laboratories, Albuquerque, New Mexico

Ferson S., Kreinovich V., Hajagos J., Oberkampf W. and Ginzburg L. (2007). Experimental Uncertainty Estimation and Statistics for Data Having Interval Uncertainty. Technical Report SAND2007-0939, Sandia National Laboratories, Albuquerque, New Mexico

Ferson S., Nelsen R.B., Hajagos J., Berleant D.J., Zhang J., Tucker W.T., Ginzburg L.R. and Oberkampf W.L. (2004). Dependence in probabilistic modelling, Dempster-Shafer theory and Probability Bounds Analysis. Technical Report SAND2004-3072, Sandia National Laboratories, Albuquerque, New Mexico

Ferson S. and Tucker W.T. (2003). Probability Bounds Analysis in Environmental Risk Assessments. Technical report, Applied Biomathematics, Setauket, New York. Available at www.ramas.com/pbawhite.pdf

Ferson S. and Tucker W.T. (2006). Sensitivity Analysis using probability bounding. *Reliability Engineering and System Safety*, **91** (10 – 11): 1435 – 1442

Fréchet M. (1951). Sur les tableaux de corrélation dont les marges sont données. *Ann. Univ. Lyon, Section A*, **9**: 53 – 77

Frey H.C. (1993). Separating variability and uncertainty in exposure assessment: motivations and method. Proceedings of the 86th Annual Meeting (13-18 June 1993, Denver, CO). Air and Waste Management Association, Pittsburgh, PE

Gelman A., Carlin J.B., Stern H.S. and Rubin D.B. (1995). *Bayesian Data Analysis*. Chapman and Hall, London

Glorennec P. (2006). Analysis and reduction of the uncertainty of the assessment of children's lead exposure around an old mine. *Environmental Research*, **100** (2): 150 – 158

Grist E.P.M., Leung K.M.Y., Wheeler J.R. and Crane M. (2002). Better bootstrap estimation of hazardous concentration thresholds for aquatic assemblages. *Environmental Toxicology and Chemistry*, **21** (7): 1515 – 1524

Haas C.N. (1999). On modelling correlated random variables in risk assessment. *Risk Analysis*, **19** (6): 1205 – 1214

Hart A.D.M., Roelofs W. and Crocker D.R. (2007). Webfram Pesticide Risk Assessment Website. Available at http://www.webfram.com

Havelaar A.H., De Hollander A.E.M., Teunis P.F.M., Evers E.G., Van Kranen H.J., Versteegh J.F.M., Van Koten J.E.M. and Slob W. (2000). Balancing the risks and benefits of drinking water disinfection: Disability adjusted life-years on the scale. *Environmental Health Perspectives*, **108** (4): 315 – 321

Hill B.M. (1968). Posterior distribution of percentiles: Bayes' theorem for sampling from a population. *Journal of the American Statistical Association*, **63** (322): 677 – 691

Hill B.M. (1988). De Finetti's Theorem, Induction, and $A_{(n)}$ or Bayesian nonparametric predictive inference (with discussion). In *Bayesian Statistics 3*. Edited by J. M. Bernardo and M. H. DeGroot and D. V. Lindley and A. F. M. Smith , Oxford University Press

Hill B.M. (1993). Parametric models for a_n: Splitting processes and mixtures. *Journal of the Royal Statistical Society B*, **55** (2): 423 – 433

Hoeffding W. (1940). Masstabinvariante Korrelationstheorie. *Schriften des Mathematischen Instituts und des Instituts für Angewandte Mathematik der Universität Berlin*, **5**: 133 – 144

Kadane J.B. and Wolfson L.J. (1998). Experiences in elicitation. *The Statistician*, **47** (1): 3 – 19

Kass R.E. and Wasserman L. (1996). The selection of prior distributions by formal rules. *Journal of the American Statistical Association*, **91** (435): 1343 – 1370

Kentel E. and Aral M.M. (2005). 2D Monte Carlo versus 2D Fuzzy Monte Carlo health risk assessment. *Stochastic Environmental Research and Risk Assessment*, **19** (1): 86 – 96

Kolmogorov A. (1941). Confidence limits for an unknown distribution function. *The Annals of Mathematical Statistics*, **12** (4): 461 – 463

Krayer von Krauss M.P., Casman E.A. and Small M.J. (2004). Elicitation of expert judgements of uncertainty in the risk assessment of herbicide-tolerant oilseed crops. *Risk Analysis*, **24** (6): 1515 – 1527

Lawless J.F. and Fredette M. (2005). Frequentist prediction intervals and predictive distributions. *Biometrika*, **92** (3): 529 – 542

Lee P.M. (2004). *Bayesian Statistics: An introduction.* Hodder Arnold, London, UK. Third Edition.

Lindenschmidt K.E., Huang S.C. and Baborowski M. (2008). A quasi-2D flood modeling approach to simulate substance transport in polder systems for environment flood risk assessment. *Science of the total environment*, **397** (1-3): 86 – 102

Ma H.W. (2002). Stochastic multimedia risk assessment for a site with contaminated groundwater. *Stochastic Environmental Research and Risk Assessment*, **16** (6): 464 – 478

Madelin R. (2004). The importance of scientific advice in the community decision making process. Opening address to the Inaugural Joint Meeting of the members of the Non-Food Scientific Committees. Directorate General for Health and Consumer Protection, European Commission, Brussels.

Manski C.F. (2003). *Partial Identification of Probability Distributions*. New York: Springer - Verlag

Markov A. (1886). Sur une question de maximum et de minimum proposée par M. Tchebycheff. *Acta Mathematica*, **9**: 57 – 70

Miconnet N., Cornu M., Beaufort A., Rosso L. and Denis J.B. (2005). Uncertainty distribution associated with estimating a proportion in microbial risk assessment. *Risk Analysis*, **25** (1): 39 – 48

Miller L. (1956). Table of percentage points of Kolmogorov statistics. *Journal of the American Statistical Association*, **51** (273): 111 – 121

Moller B. and Beer M. (2008). Engineering computation under uncertainty capabilities of non-traditional models. *Computers & Structures*, **86** (10): 1024 – 1041

Montgomery V.J., Coolen F.P.A. and Hart A.D.M. (In press). Bayesian probability boxes in risk assessment. *Journal of Statistical Theory and Practice*

Mood A.M., Graybill F.A. and Boes D.C. (1974). *Introduction to the Theory of Statistics*. Third Edition, McGraw Hill, New York

Moore R.E. (1966). *Interval Analysis*. Prentice Hall, Englewood Cliffs, New Jersey

Nelsen R.B. (2002). *An Introduction to Copulas*. Lecture Notes in Statistics 139, Springer-Verlag, New York

O'Hagan A. (1998). Eliciting expert beliefs in substantial practical applications. *The Statistician*, **47** (1): 21 – 35

O'Hagan A. and Forster J. (2004). *Kendall's Advanced Theory of Statistics*. Arnold, London, UK, Volume 2B, Second Edition

O'Hagan A. and Stevens J.W. (2001). A framework for cost-effectiveness analysis from clinical trial data. *Health Economics*, **10** (4): 303 – 315

Posthuma L., Suter II G.W. and Traas T.P. (editors) (2002). *Species Sensitivity Distributions in Ecotoxicology*. Lewis Publishers, Boca Raton, Florida

Pouillot R., Miconnet N., Afchain A.L., Delignette-Muller M.L., Beaufort A., Rosso L., Denis J.B. and Cornu M. (2007). Quantitative risk assessment of listeria monocytogenes in French cold-smoked salmon: I. Quantitative exposure assessment. *Risk Analysis*, **27** (3): 683 – 700

Renwick A.G. (2002). Pesticide residue analysis and its relationship to hazard characterisation (adi/arfd) and intake estimations (nedi/nesti). *Pest Management Science*, **58** (10): 1073 – 1082

Rice J.A. (1995). *Mathematical Statistics and Data Analysis*. Wadsworth Inc, Second Edition

Rugen P. and Callahan B. (1996). An overview of Monte Carlo, a fifty year perspective. *Human and Ecological Risk Assessment*, **2** (4): 671 – 680

Saltelli A., Chan K. and Scott E.M. (editors) (2000). *Sensitivity Analysis*. John Wiley and Sons Ltd, Chichester, England

Sklar A. (1959). Fonctions de répartition à n dimensions et leurs marges. *Publications de l'Institut de Statistique de L'Université de Paris*, **8**: 229 – 231

Smirnov N. (1939). On the estimation of the discrepancy between empirical curves of distribution for two independent samples. *Bulletin University of Moscow*, **2**: 3–16

Tanner M.A. and Wong W.H. (1987). The calculation of posterior distributions by data augmentation. *Journal of the American Statistical Association*, **82** (398): 528 – 540

Turkkan N. and Pham-Gia T. (1997). Algorithm AS 308: Highest posterior density credible region and minimum area confidence region: the bivariate case. *Journal of the Royal Statistical Society: Series C (Applied Statistics)*, **46** (1): 131 – 140

Ulam S.M. (1976). *Adventures of a Mathematician*. Charles Scribners Sons, New York

Van Leeuwen C.J. and Hermens J.L.M. (editors) (1995). *Risk Assessment of Chemicals: An introduction*. Kluwer Academic Publishers, Dordrecht

Verdonck F.A.M., Jaworska J., Thas O. and Vanrolleghem P.A. (2001). Determining environmental standards using bootstrapping, Bayesian and maximum likelihood techniques: a comparative study. *Analytica Chimica Acta*, **446**: 429 – 438

Vermeire T., Jager T., Janssen G., Bos P. and Pieters M. (2001). A probabilistic human health risk assessment for environmental exposure to dibutylphthalate. *Human and Ecological Risk Assessment*, **7** (6): 1663 – 1679

Vicari A.S., Mokhtari A., Morales R.A., Jaykus L.A., Frey H.C., Slenning B.D. and Cowen P. (2007). Second-order modeling of variability and uncertainty in microbial hazard characterization. *Journal of food protection*, **70** (2): 363 – 372

Vose D. (2001). *Risk Analysis. A Quantitative Guide*. John Wiley and Sons, Chichester, England, Second Edition

Walker K.D., Catalano P., Hammitt J.K. and Evans J.S. (2003). Use of expert judgment in exposure assessment: Part 2. Calibration of expert judgments about personal exposures to benzene. *Journal of Exposure Analysis and Environmental Epidemiology*, **13**: 1 – 16

Walker K.D., Evans J.S. and Macintosh D. (2001). Use of expert judgment in exposure assessment Part I. Characterization of personal exposure to benzene. *Journal of Exposure Analysis and Environmental Epidemiology*, **11**: 308 – 322

Walley P. (1991). *Statistical Reasoning with Imprecise Probabilities*. Chapman and Hall, London

Whitt W. (1976). Bivariate distributions with given marginals. *The Annals of Statistics*, **4** (6): 1280 – 1289

Williamson R.C. and Downs T. (1990). Probabilistic Arithmetic I: Numerical methods for calculating convolutions and dependency bounds. *Journal of Approximate Reasoning*, **4**: 89 – 158

WinBUGS (1990). Computer Program, http://www.mrc-bsu.cam.ac.uk/bugs/

Zellner A. (editor) (1986). On assessing prior distributions and Bayesian regression analysis with g-prior Distributions. In P.K. Goel and A. Zellner (Eds.), *Bayesian Inference and Decision Techniques.* North Holland, Amsterdam

Zhao Y.C. and Frey H.C. (2004). Quantification of variability and uncertainty for censored data sets and application to air toxic emission factors. *Risk Analysis*, **24** (4): 1019 – 1034